MEASURING PEDESTRIAN GAIT USING LOW RESOLUTION INFRARED PEOPLE COUNTERS

TIMOTHY JOHN CHAMBERLAIN

A THESIS SUBMITTED IN PARTIAL FULFILMENT OF THE REQUIREMENTS OF NAPIER UNIVERSITY FOR THE DEGREE OF DOCTOR OF PHILOSOPHY

SCHOOL OF COMPUTING
NAPIER UNIVERSITY

JUNE
2009

Acknowledgments

I would like to acknowledge the help and support that the School of Computing, Napier University, which has provided funding, and its staff for providing ongoing encouragement and physical resources. In particular the support of my supervisors, Dr A. Armitage, Dr M. Rutter and Dr T. D. Binnie has been substantial. My colleagues and fellow students at Napier have also helped, particularly K. Stewart, S. Clayton, S. Keller, S. Pavitt, and G. Wilkinson. Infrared Integrated Systems Ltd has provided support by allowing me to use their equipment and premises for experiments, in particular the chief software scientist, Dr N. Johnson. They have also provided information enabling access to the trajectory data from the people counter product. I would also like to thank all the people who participated in my experiments, my parents for proof reading this document.

I acknowledge that some of the work presented in this thesis has been presented or published at or in the following places:

[1] T. Chamberlain, S. Clayton, Prof J. Kerridge, Dr A. Armitage, Dr M. Rutter, Dr T. D. Binnie, Dr N. Urquhart, (2007), *Using low cost Infrared Sensors for data capture*, Workshop on calibration of microscopic pedestrian movement simulations, Dec 13-14th, Arsenal Research, Vienna

[2] J. Kerridge, S. Keller, T. Chamberlain and N. Sumpter (2007), Collecting pedestrian trajectory data in real-time, *Pedestrian evacuation and dynamics 2005*, pages 27-39, Springer, Berlin, ISBN 978-3-540-47062-5

[3] T. Chamberlain, A. Armitage, M. Rutter, T.D. Binnie (2006), *Pedestrian sensing with feature extraction*, CD-Rom Proceedings of the ITS world congress, London

[4] T. Chamberlain, A. Armitage, M. Rutter, T.D. Binnie (2006), *Working towards identifiable feature extraction from pedestrians' gait*, Proceedings of 38th Annual UTSG Conference, Trinity College Dublin

[5] J. Kerridge, S. Keller, T. Chamberlain, N. Sumpter, (2005), *Collecting processing and calculating pedestrian flow data in real-time,* Proceedings of 84th Annual Meeting of Transportation Research Board, Washington D.C.

[6] T. Chamberlain, A. Armitage, M. Rutter, T.D. Binnie (2005), *The use of thermal detectors in establishing ground truth in the evaluation of video pedestrian tracking algorithms,* Faculty of Engineering & Computing Postgraduate Research Conference, Napier University

[7] A. Armitage, D. Binnie, T. Chamberlain, M. Nilsson and M. Rutter (2005), *Tracking pedestrians using visible & infrared systems,* Proceedings of 37th Annual UTSG Conference, University of the West of England, Bristol

[8] T. Chamberlain, A. Armitage, M. Rutter, T. D. Binnie, (2004) *Using Low-Resolution Thermal Sensors in Stereo To Measure Pedestrian Movement,* PREP, University of Hertfordshire, poster proceedings p251

Abstract

This thesis describes research conducted into the measurement of pedestrian movement. It starts with an examination of current pedestrian detection and tracking systems, looking at several different technologies including image-processing systems. It highlights, as other authors have, that there is still a substantial gap between the abilities of existing pedestrian measurement and tracking systems and the requirements of users of such systems.

After the review it provides an introduction to human gait and its use as a biometric. It then examines the IRISYS people counter, a low resolution infrared detector, used for this research. The detector's advantages and disadvantages are discussed, a detailed description of the data produced is provided. The thesis then describes in detail a study establishing that human gait information can be measured by the IRISYS people counter. It examines the use of the detectors in stereo to measure the height of the people; however the results are not impressive. During this investigation the presence of oscillations likely to relate to this walking gait is noted in the data.

A second study is carried out confirming that the noted oscillation originates from human gait and further data is gathered to enable the development of measurement algorithms. The magnitude of the walking oscillation noted is examined in detail. It is found to be both individualistic and highly correlated to gender. A gender distribution algorithm is presented and evaluated on data captured in two different locations. These show very promising results. Several different methods are described for processing the information to extract a measure of cadence. The cadence is found to be individualistic and shows interesting correlations to height and leg length.

This thesis advances the field of pedestrian measurement by conducting pedestrian motion studies and developing algorithms for measuring human gait.

Contents

List of figures

List of tables

1 Introduction

Pedestrian measurement and tracking has become a rich and diverse area of research. There are many situations where it is useful to detect, count, measure and track pedestrians. At the time of writing, for most applications, counting and movement analysis relies on human observation or supervised systems. In addition to the time, cost and difficulties encountered extracting pedestrian trajectory information; little individualistic information has been gathered in real-time unconstrained environments. This thesis details studies using ceiling mounted people counters based on a pyroelectric array, which provide a trajectory measurement of people who pass under them. It furthers work published by the author *et al* [1] to examine whether it is possible to extract height, cadence and gender information from the trajectory data available. The device used is the IRISYS people counter.

1.1 Motivation

Measuring pedestrian motion has several important applications. The retail and marketing sectors are increasingly interested as various advantages can be leveraged by accurately studying shop footfall. If a detailed map of customer movement within the environment can be produced, several benefits are available: For example the layout and width of shop isles can be adjusted to optimise customer flow and suitable locations identified for products with the highest profit margins.

The behaviour of pedestrians is relevant to several areas, such as the study of suspicious movement, or of crowd behaviour in building evacuation. The presence of a human observer can change the behaviour of the people being observed, so a non-intrusive measurement system has considerable advantages. The presence of a robust automatic system for tracking pedestrians would not only facilitate this type of research but also reduce the cost of research. As Professor Batty [2] points out there is still a significant gap between the measurement data required by those modelling pedestrian behaviour and what is available.

The security sector has seen an explosion in automated systems in the last two decades. The cost of video surveillance systems has drastically reduced. This, combined with an increased fear of terrorism, has lead to a substantial industry. At the

time of writing, the majority of security systems serve one major purpose: to provide evidence of a crime or incident after the event. Some systems are installed with high visibility to act as a psychological deterrent; some are installed discreetly, so as not to raise suspicions. To date, comparatively little proactive real time analysis has been successfully performed on data from these systems. The availability of pro-active automatic security and surveillance systems is both highly researched and sought after.

The transport sector has become increasingly interested in detecting the presence and motion of pedestrians. This interest is mainly aimed at increasing safety for pedestrians, the most vulnerable transport users. Developing technology for safer pedestrian crossings and automatic braking systems in cars is also receiving increasing attention.

All of these sectors show a significant gap between what technology can currently offer, and what is required. Extracting individualistic measures would enable people to be tracked more reliably. Systems are emerging with the potential to track people. However, significant complications exist when people leave the field of view or cross from one detector or camera to another. Providing information that can aid this matching process or identify the individual without requiring their cooperation would provide significant benefit.

1.2 Research objective

The objective of the research presented in this thesis is to improve the understanding of and progress the field of unobtrusive human motion measurement. Many systems exist to detect the presence and motion of pedestrians. However most do not provide a sufficient quality of information for gait measurement, are not fully automated or are unsuitable for real-time use. Those that are, are generally based on data captured under experimental conditions. This thesis improves the status quo of automatic pedestrian motion measurement by conducting significant studies into the motion of pedestrians and augmenting this by developing new algorithms for processing trajectory data produced by low resolution thermal detectors, the IRISYS people counters (detector).

In particular the work explores the following questions:

- Can individualistic measures be obtained from the detector, based on human gait?
- If so, how individualistic are the measures in relation to other gait measurement research?
- Are correlations present between the cadence measured and the biometrics of height and leg length?
- Is the gait measure highly correlated to gender?

Prior to this research, comparatively little work has focused on the measurement of human gait from a ceiling mounted downward looking view point. Those that have are restricted to clinical gait studies. By developing methods for measuring human gait using the detectors this research aims to establish that it is possible to gather individualistic information about people, from an overhead vantage point with trajectory information derived from low resolution thermal difference images.

1.3 Research approach

Early research by Armitage *et al* [3] and Daamen [4] has shown that IRISYS people counters, a detector based on a 16 by 16 pixel PZT (lead zirconium titanate) array are good at measuring pedestrian flow. The fact that over quarter of million people counters have been produced and sold (*pers. comm.* David Clayson, Managing Director, IRISYS, 2007) is testament to their robust ability to measure pedestrian motion. Three key features about the detectors contribute to their success: Firstly that they are ceiling mounted and have a field of view looking straight down, thus they are not subject to occlusion. Secondly, they image in the 8-14 micron infrared spectrum, a wavelength emitted by people, thus detecting emitted rather than reflected radiation. Finally, they employ a very well developed and mature tracking algorithm to detect and track objects in the field of view.

This research furthers earlier work by building on the robust trajectory data provided by the detectors and constructing a more detailed analysis of pedestrian motion. The focus of the research is to develop algorithms which do not require individual calibration of detectors used but function regardless of detector manufacturing variations. To this end data was collected in three different locations. The first, a significant collaborative study collecting and processing data in real-time, was

collected outside the apex cafeteria at Napier University. The second location was at the entrance to Napier University's Merchiston Library and finally a dataset was collected at the offices of IRISYS (the sensor's manufacturer).

1.4 Contribution to knowledge

This thesis provides a significant contribution to knowledge in the study of human motion measurement, by using trajectory data from the IRISYS people counters to measure and analyse human motion. The first, dataset mentioned above, was collected as part of a significant collaborative study, which was acquired and processed in real time. A description of this study is included in the Pedestrian Evacuation Dynamics 2005 book chapter [1] and peer reviewed TRB conference paper [5], copies included in Appendix E. This study, was then further augmented by data collected at the two additional locations mentioned above.. The latter is presented in the main body of this thesis.

The latter two datasets are further examined to investigate if any human gait information can be obtained. This investigation is intended not only to provide real time trajectory analysis, but also to develop algorithms that can provide additional information about the pedestrian passing. A detailed examination is conducted into stereo use of the trajectory data with a view to measuring the height of people passing, however the results are not impressive. A further study of the trajectory data shows that gait information is available from a single detector. Algorithms for examining this are investigated and a useful gender distribution algorithm is developed. By conducting and reporting this research, a contribution to knowledge in the field of transportation and pedestrian measurement is made. In addition to the main body of this thesis, three peer reviewed papers and five conference presentations are included in Appendix E.

1.5 Layout of the thesis

In addition to this introduction the remainder of this thesis is split into seven chapters. Each is described here.

Chapter 2 describes the main literature and background to pedestrian measurement technologies. It starts by examining the most substantial current and recent research

projects in the area. It then studies the different technologies available for pedestrian detection, tracking and measurement. Finally it introduces the fields of human gait and stereo vision.

Chapter 3 describes the IRISYS people counter in detail. A description of the technology on which the detector is based is presented. It then examines the responsiveness of the pyroelectric material used and the problem of barrel distortion. An experiment is described which measures the extent of the barrel distortion and a method for correcting it is presented.

Chapter 4 examines the use of the IRISYS people counters in stereo. It presents a study into the use of the trajectory data from the detectors for triangulation. This is then examined with respect to the height of the person passing the detectors with a view to producing a height measurement system. The results presented show a notable gait (walking) oscillation.

Chapter 5 describes experiments conducted to study the source of the oscillation noticed during chapter 4. This is developed into a system for measuring footstep location of a person. The chapter describes the experiments conducted, data collected and algorithm used. Examination of the results presented shows a correlation between the magnitude of the oscillation and the gender of the participant.

Chapter 6 further studies the magnitude of this oscillation observed during chapter 5. Experimentation is detailed and significant datasets are presented. The correlation between gender and oscillation magnitude is investigated and a method for determining the distribution of genders passing a detector is proposed. This is further examined using data captured at two locations, where the people being measured were not actively taking part in the experiments but going about their normal daily business.

Chapter 7 presents further analysis of the data collected with a view to measuring the cadence of people as they pass the detectors. Two different methods of accounting for the direction of motion and extracting lateral gait oscillation are presented. Following this three methods for extracting the cadence by processing the data in the Fourier domain are investigated and the results detailed. Results are also presented with

respect to the height and leg lengths of the participants. Chapter, 8 includes a summary of the research conducted, conclusions reached and suggestions for future work in the field.

2 Literature review

Pedestrian measurement and tracking has become a rich and diverse area of research, resulting in substantial effort towards automating motion measurement. While significant advances have been made there is still much room for improvement in those fields involving the measurement of pedestrian motion.

This chapter provides a résumé of pedestrian motion measurement research with the aim of placing this doctoral study in the context of other research. It starts with an introduction to the significant projects in the field and highlights the different sectors that provide motives for this research. Then it provides an overview of the different sensor technologies available and methods used, for the measurement of pedestrian motion. This includes an introduction to the different measurement technologies available: CCTV, thermal sensors, pressure sensitive mats, beam counters, LADAR and traditional human observers. This is then complemented by a detailed review of image processing as it is the area that attracts the most research. The chapter then examines the subject of human gait. First it describes research that categorically establishes human gait can be used as a biometric before reviewing the main research into human gait analysis. This is viewed from the perspective of unobtrusively measuring gait for use as an identifiable feature. Finally the chapter describes the basic principle behind stereo vision and highlights some research using stereo depth perception to aid pedestrian detection and tracking.

2.1 Pedestrian motion research

Several different fields with an interest in the measurement of pedestrian movements were introduced in chapter 1. Such measurement has long received attention from those involved with security and surveillance, most of which focuses on CCTV and image processing. In addition there has been interest from the behaviour or market research communities, town and event planners and the automotive sector. This section introduces the main focus of pedestrian detection and measurement technology, from these areas.

2.1.1 The automotive industry

The automotive sector is mostly concerned with improving road safety by developing sensory equipment that can detect pedestrians and force or aid avoiding-action. For example IBEO in Germany is producing sensors for automatic braking systems that stop a car when an unavoidable collision is detected. The LADAR systems produced by IBEO are described in several conference papers [6-8]. Chan *et al* [9] describe the available technologies well in their interim report on "Experimental Transit Vehicle Platform for Pedestrian Detection". Several different image-based systems have and are being developed such as those reported by Zhenjiang Li *et al* [10] and Leibe *et al* [11].

2.1.2 Behavioural and market research

In the field of behavioural research, detailed pedestrian movement information is difficult to acquire and much sought after. Professor Batty presents a model for understanding and predicting pedestrian motion "Agent-based Pedestrian Modelling" [2]. He highlights that there is a substantial difference between the ability to model and hypothesise about individual decisions when in a crowd, and our ability to collect accurate path information about the trajectories of pedestrians. At the time of writing Footfall Ltd, part of Experian, provides video analysis (performed by human operators), of in-store video footage to establish where customers are most likely to spend their time. Conferences such as PED (Pedestrian Evacuation and Dynamics) disseminate information about pedestrian tracking research to inform building design.

2.1.3 Transport research

The transport research field provides substantial impetus to improve pedestrian tracking for both behavioural and security motivations. Professor Tyler at University College London heads a substantial research lab called PAMELA, which provides a facility to research microscopic pedestrian movements. The transport and planning group at TUDelft in the Netherlands has hosted two major pedestrian measurement and modelling projects at the macroscopic scale. Dammen published her PhD [4] on a substantial part of the study. The PERMEATE project at Napier University examined the use of an early version of the IRISYS people counter product to track pedestrian motion. This project attempted to bridge the gap between the microscopic and

macroscopic pedestrian measurement fields and is well presented by Kerridge *et al* in [12].

2.1.4 Security and surveillance

The security and surveillance sector provides much impetus for pedestrian detection and tracking, with an increasing focus on human gait detection. The work in this sector is almost exclusively based around image processing, due to the prevalence of CCTV. There have been and still are several major research initiatives in the sector several of which are introduced here. The EPSRC funded MEDUSA project [13] aims to process video footage to help provide operator assistance in detecting gun crime. The CAVIAR project [14], lead by Professor Fischer, aimed to determine and classify which vision processing algorithms worked best under different circumstances. The DARPA funded VSAM project [15], provided an automated mechanism for detecting and tracking pedestrians around a campus covered by multiple cameras. A detailed summary of the project is available in the final report [16]. The PASSWORDS [17] project was an EU funded project focusing on similar aims. Collins *et al* describe the motivations for their study and mention some other projects in their paper entitled "Algorithms for Cooperative Multisensor Surveillance" [18].

This sector has a significant interest in measuring human gait as a biometric which is further examined in section 2.4.4 of this thesis.

2.1.5 Summary

This section has introduced the background to some of the past and current pedestrian measurement research projects. It highlights the major motivation for research in the field and provides an introduction to the pedestrian measurement work. The research is predominantly covered by the automotive, market research, transport and security fields. This introductory overview helps place the work presented in this thesis in the context of the work of others. The next section provides a description of the different technologies used to measure pedestrian motion.

2.2 Different pedestrian motion measurement technologies

There are several different technologies available for measuring and tracking pedestrians, each with its advantages and disadvantages. This subsection examines these technologies. It starts with an overview of CCTV and image processing systems

as these attract by far the most interest. In addition to the different systems available there are several different vantage points to mount sensory equipment, each providing different perspectives with different advantages.

2.2.1 CCTV and visible imaging

Video collection is an area that has attracted substantial interest over the last decade. Several factors have influenced the studies that devote ever increasing resources to this area. Firstly, the massive reduction in cost and increase in camera installations mean that there are existing systems for acquiring vast amounts of data. Secondly, recent years have seen several global terrorist attacks that have increased the perceived need for pedestrian detection and tracking technology to improve surveillance and security.

For video data to be used to automatically track pedestrians it must be processed to detect and track pedestrians. This processing is a non-trivial task that has attracted significant attention from the research communities the world over. Section 2.3 further examines this research.

2.2.2 Thermal sensors

As the human body is good at regulating its own temperature, and very few areas of the planet have a temperature similar to humans, an ever-present difference exists. This, combined with the fact that we are detecting emitted, not reflected radiation, makes the measurement of temperature, or infrared images, a good option for detecting pedestrians.

There is currently a wide array of infrared sensors available, each aimed at slightly different markets. The most prominent are based on pyroelectric sensors and they typically have low resolution, often only one pixel. There is an extensive range of medium and high resolution thermal imaging products based on several different underlying technologies. These come with a variety of different advantages and disadvantages, the most notable being cost. Some systems need to stop imaging for a few seconds to re-calibrate for thermal drift. FLIR systems produce some market leading products. These thermal cameras typically produce resolutions of around 320 by 240 pixels and as of December 2008 were often priced above £5000. This type of product is most often used by law enforcement agencies and the military for the

detection and tracking of people at night. However, as their cost reduces, they are receiving increasing interest from the image processing community [19].

There is a plethora of manufacturers producing thermal sensors that successfully detect people. Manufactures include Pyreos, PerkinElmer and Infratec. These are most commonly used as motion detectors in burglar alarms and automatic light switches. A web search for motion detectors will provide many relevant products. IRISYS produce a series of thermal imaging products based on 16 by 16 pixel pyroelectric detectors that often represent a cost effective solution. The IRISYS people counter products are examined further in the next chapter. IBM developed a similar technology which is well described in [20]. To date it has not been developed into a commercially available product.

Okuda *et al* [21] present some interesting work using dual element pyroelectric sensors to measure the position and height of pedestrians. They can successfully discriminate between people with markedly different heights, i.e. adults and children. However they require a lattice of sensors to be mounted in the detection area. Fang *et al* [22] present an interesting system for identifying pedestrians passing sensors. It uses a novel approach involving optics to extract a measure of cadence from a single IR sensor. It is mounted at one side of, and at known distance from, the pedestrian who must be walking in a straight line.

2.2.3 Pressure-sensitive mats & surfaces

Several manufacturers produce pressure-sensitive floor coverings designed to detect pedestrians. Most manufactures produce their products for industrial safety applications; the products are used to switch off mechanical machinery whenever a pedestrian makes contact with the pressure-sensitive surface. Tapeswitch Ltd and Bircher America Inc, among others, produce a wide array of different products. These systems are generally used to prevent automatic doors on trains and buses from trapping passengers as they close.

2.2.4 Manual counting

Manual counting and observing is the longest established method of measuring the movement of pedestrians. It has provided much useful information about the number

of people that visit a particular location; however it has many drawbacks. Firstly, it is expensive as an individual or individuals must be employed to perform the task. Secondly, it is almost impossible to collect much information about the trajectories of the passing people. It is not easy to count a continual flow of people, let alone record features such as their height. Several specialist companies exist to perform manual pedestrian counting tasks such as Footfall Ltd (now part of Experian). Thirdly, the fact that a person is performing the counting or observing, can change the way the subjects being observed behave. All these problems limit the effective use of manual counting / observing in many situations.

2.2.5 Beam counters

Probably the most common automatic people counters, are counters that detect the number of times a light beam is interrupted as people pass through the beam. This type of counter is common as it is cheap and simple to install. However these are not accurate, and not suited to locations where more than one person can pass simultaneously.

2.2.6 LADAR

LADAR (***LA****ser* ***D****etection* ***A****nd* ***R****anging*) systems are essentially the same in principle as Radar; however they use laser light instead of radio waves, giving better angular accuracy. The systems work by emitting pulsed laser light and measuring the time it takes for a reflection to be observed; thus, as the speed of light is known, the distance to the object causing the reflection can be obtained. By using precision mounted mirrors and reflectors a measure of the laser's direction can also be found allowing a 2D or 3D range image to be built up. Ishihara discussed the use of ground-based laser scanners in the detection of pedestrians [23] and appears to have produced some good results.

In general, range information is very useful in tracking pedestrians, as it clearly defines location. The differences between the background and the person are therefore more substantial. However there are problems with the use of LADAR in pedestrian tracking systems. Occlusion of one pedestrian by another, presents problems that are difficult to mitigate. Locating the devices can be complex if they only provide 2D (single scan line) information. LADAR systems such as the one used by Hsu *et al* [24]

are not widely available. 2D systems, such as the one produced by IBEO Automobile Sensor GmbH, at the time of writing cost in the order of 30000 Euros. LADAR sensors are not going to become truly viable in pedestrian tracking or surveillance applications until their cost and availability substantially improve. Unfortunately, a reduction in cost is not likely in the near term due to the high precision needed for positioning the optical reflectors and high speed electronics needed for time-of-flight detection of light.

2.2.7 Sensor mounting positions

Several different technologies have been introduced in section 2.2, many with different typical mounting positions. CCTV cameras are usually mounted side-on, or slightly elevated to give a better view of the scene. This provides a good view of people; however it also introduces the complications of occlusion. When good pedestrian location is available from CCTV there is still the complex problem of extracting the 3D coordinates from the 2D video. Pressure-sensitive mats, generally laid on the floor, give a good view point for sensing the presence of pedestrians; however they do not have the resolution to produce information other than that of presence or absence. The IRISYS people counters look directly down from a ceiling mounting, providing a similarly good vantage point. They do have sufficient resolution to count several people in the field of view at the same time. LADAR is mounted in a variety of positions; as it is still experimental as a result of its price, there is no typical mounting. Ishihara *et al* [23] mounted LADAR at ground level as is usual for light beam detectors.

2.2.8 Summary

This section has introduced the main pedestrian detection and tracking technologies and methods. It has introduced LADAR, CCTV, thermal imaging and manual counting as systems for monitoring the movement of pedestrians. Each is used for a variety of applications, market research, behavioural studies, security and surveillance. The next section examines research for pedestrian detection and tracking from the image processing community.

2.3 Image processing for pedestrian detection

The previous sections of this literature review have provided an overview of the different technologies available for pedestrian detection and highlighted the different

areas that motivate its study. A brief introduction to some of the larger research projects in the area has been presented. In section 2.2.1 the prevalence of CCTV was highlighted, it is however noted that it is not trivial, to process video for pedestrian detection and tracking. This section examines the research in the field of image processing for pedestrian detection. As a topic, it probably attracts the largest research interests of any in the image processing community.

The task is usually split up into several different but related stages, each of which is discussed below. Background subtraction, which "is often one of the first tasks in machine vision" [25], aims to separate the background of the image from the area of interest, the pedestrian. Optical flow detection provides an alternative method for segmenting an image into objects moving at different speeds. Feature extraction looks for pedestrians within images, or attempts to classify objects that have been detected by background subtraction of optical flow as pedestrians. Several algorithms apply a different mechanism for tracking the pedestrians after they have been detected than for detecting them in the first place such as those presented in [11, 26, 27].

In recent years fusing data from additional sensors (IR and LADAR) with visible video has attracted significant interest, this is further discussed in section 2.3.5.

2.3.1 Background subtraction

Background subtraction is a technique for identifying areas of interest in video footage, it. It focuses on production of an image or model of the background and finds pixels that do not conform to that model or image. In its simplest form, background subtraction takes the current video image and subtracts the previous image, displaying all the pixels where the magnitude of the subtraction is greater than a threshold. This will produce an image where only the pixels that have changed are shown. Toyama *et al* [28] describe the process and complications of background subtraction well. They highlight several particularly difficult situations a background model must adapt to. As quoted from [28] these are:

> ***Moved Objects****: A background object can be moved, these objects should not be considered part of the foreground forever after.*
>
> ***Time of Day****: Gradual illumination changes alter the appearance of the background.*

***Light Switch**: Sudden changes in illumination and other scene parameters alter the appearance of the background.*

***Waving trees:** Backgrounds can vacillate* (sic)*, requiring models which can represent disjoint sets of pixel values.*

***Camouflage:** A foreground object's pixel characteristics may be subsumed by the modelled background.*

***Bootstrapping:** A training period absent of foreground objects is not available in some environments.*

***Foreground aperture:** When a homogenously coloured object moves, change in the interior pixels cannot be detected. Thus, the entire object may not appear as foreground.*

***Sleeping person:** A foreground object that becomes motionless cannot be distinguished from a background object that moves and becomes motionless.*

***Walking person:** Walking person, when an object initially in the background moves, both it and the newly revealed parts of the background appear to change.*

***Shadows:** Foreground objects often cast shadows which appear different from the modelled background.*

The task of background subtraction has been furthered by many researchers, for example [25, 29-32]. Several interesting solutions to address some of the issues highlighted by Toyama *et al* are emerging. Stauffer and Grimson [33] present a solution for formulating a mixture model. Lee [30] claims that this model has become standard for the mixture model approach. However the solution does not completely address all the complications; there are still no universal solutions to the complex problem of background subtraction.

Once an image has been split into areas of foreground and background, further processing can be carried out to find pedestrians in the foreground. The most common component at this stage is removal of small objects identified such as 'salt and pepper' noise.

2.3.2 Optical flow

Optical flow techniques are based around the idea of looking for patterns of motion in image data. Horn and Schunk [34] provided an easy to understand description of the basic principles and description of their seminal optical flow algorithm. They specify optical flow as a series of vectors describing the velocity of each pixel location in the image. The calculation of optical flow can be simple, but only if it is possible to make several assumptions about the video sequence, such as affine motion, layering or segmentation. One is however often unable to make these assumptions about video footage. Since the nineteen eighties a substantial amount of work has been carried out in the optical flow field and many improvements have been made, such as those described by Zitnick *et al* [35]. Fermuller *et al* [36] present a substantial paper on the Statistics of optical flow, this references several algorithms from different authors.

2.3.3 Feature detection

Feature detection algorithms work by looking for features, shapes or appearance patterns in images or known foreground regions. Viola and Jones [37] describe an algorithm for finding human faces in static images. They have advanced the algorithm for finding pedestrians from patterns of motion as described in their later work [38]. This work is claimed to be robust and shows much potential for confirming that an area of interest in an image is a pedestrian. However it requires the person's face to be present in the image at a sufficient resolution for detection (rather than the back of the head).

Images that have been split into areas of interest and disinterest by either optical flow or background subtraction are often then classified as human or non-human, as is done by Hariatoglu *et al* [39], Fuentes *et al* [40] and Selinger *et al* [41]. This generally results in the coordinates of a bounding box describing pedestrian(s) location(s) within the image. List and Fischer [42] present an xml schema for describing this information. While significant advances have and are being made, most algorithms tend to be optimised for a particular type of scene. Further research is still required to develop truly universal and unsupervised systems.

2.3.4 Tracking

After images in video sequences have been processed to find pedestrians, often by a combination of background subtraction, optical flow and feature detection, the pedestrian needs to be tracked into the nearby frames. The approach to this task varies dependent upon algorithms and the specialisation of the task in hand. The simplest trackers look for objects in consecutive frames where the location in the second frame is closest to the location in the first. This approach fails where several pedestrians are close by or occluded. Maadi and Maldague [43] present a paper which first subtracts the background, then classifies objects and finally tracks the objects. The tracker employs iterative systems of location predication (for the next frame) and correction based on the location of detected objects in the current frame. Lei *et al* [44] present a more comprehensive system, which uses multiple hypotheses and integrates tracking with detection to improve performance. The main solutions have some form of multiple hypothesis tracking. This introduces resource constraints as to how many hypotheses can be continually tracked and how to decide which hypotheses to discard.

2.3.5 Fusing video with Infrared or LADAR

Fusing video information with data from other sources such as infrared or LADAR is attracting increasing interest. Not only does it provide a useful additional source of information about the scenes, aiding object detection and tracking, but it also allows the systems to be used in environments where only using visible imaging would never work, for example night vision.

Hsu et al [24] present a system for fusing LADAR with video to more easily detect camouflaged objects. The cost of 3D LADAR is still comparatively high according to Siepmann [45] "(>$100,000USD)", however he presents some interesting work which shows potential to reduce the cost of LADAR and increase the frame rate. This could make it more suitable and available for fusing with video in the future. However at present there are military restrictions on 3D LADAR availability.

Fusing visible and infrared images is now also attracting significant attention. Amin *et al* [46] present a system for using both visible and infrared images to count people. The results from the combined system present an improvement over either visible or infrared systems taken individually. Sun *et al* [47] present a method for augmenting

visible and infrared images to make it easier for viewers to find objects of interest. Kong *et al* [48] present a system to aid face detection in varying illuminations by fusing visible and IR images. Their work presented in this area is new and interesting. Several unanswered questions remain about the practicalities of fusing data from different imaging systems, for example the production of optics required capable of focusing the wide range of wavelengths on the relevant sensors.

2.3.6 Summary

The research in image processing for pedestrian detection presents several interesting questions. For example how to model background, how to determine if an object is a pedestrian and how to track the pedestrian, once located. This section has introduced some of the rich and diverse research in image processing, and highlights the main questions in the field. While there are solutions that work well in certain situations there are no complete and autonomous solutions. The problems associated with processing real world CCTV footage to find pedestrians are complex and it is not easy to define how far to develop systems. Should an image processing system be as good as a human operator, or better, is it sufficient to only work well when there is a constant background? The CAVIAR project [14] came about to try and analyse the available algorithms and determine which algorithm is best in different circumstances. This analysis itself is a complex task and several papers have been published on it, for example [49, 50].

CCTV based automatic pedestrian detection and tracking systems still generally require a substantial amount of expertise to set up or operate. The systems used by Phillips *et al* [51] required a human operator to draw bounding boxes round the pedestrians in the footage. The systems described and developed by Collins *et al* [16] require a substantial amount of set-up work. The work of Sarkar *et al* [52] acknowledges the "meticulous" efforts of Stan Janet and Karen Marshall of NIST in creating bounding boxes around pedestrians. While much work is ongoing in the area, it is still the case that the current systems are far from deployable in an unsupervised of-the-shelf system suitable for human motion measurement. This position is supported by Amin *et al* [46].

2.4 Human gait

The current Oxford English dictionary definition of gait is "Manner of walking, bearing or carriage as one walks". This definition allows the topic to include a wide range of research, incorporating biomedical, physical and kinematical studies. This section provides a review of the physics of the human body including their relation to gait, a review of the current state of gait measurement technology, and its use as a biometric.

2.4.1 Physics of the human body

The human body is immensely complex in construction and a full description of its construct is left for text books such as Physics of the human body [52a]. This subsection reviews the main body parts and structure which affect gait. To present this review it is important to define some terminology; much of the difficulty anyone has in understanding experts is in understanding the terminology in use, not the ideas. Herman [52a] presents a good diagram describing the terminology in use in the medical field, shown below.

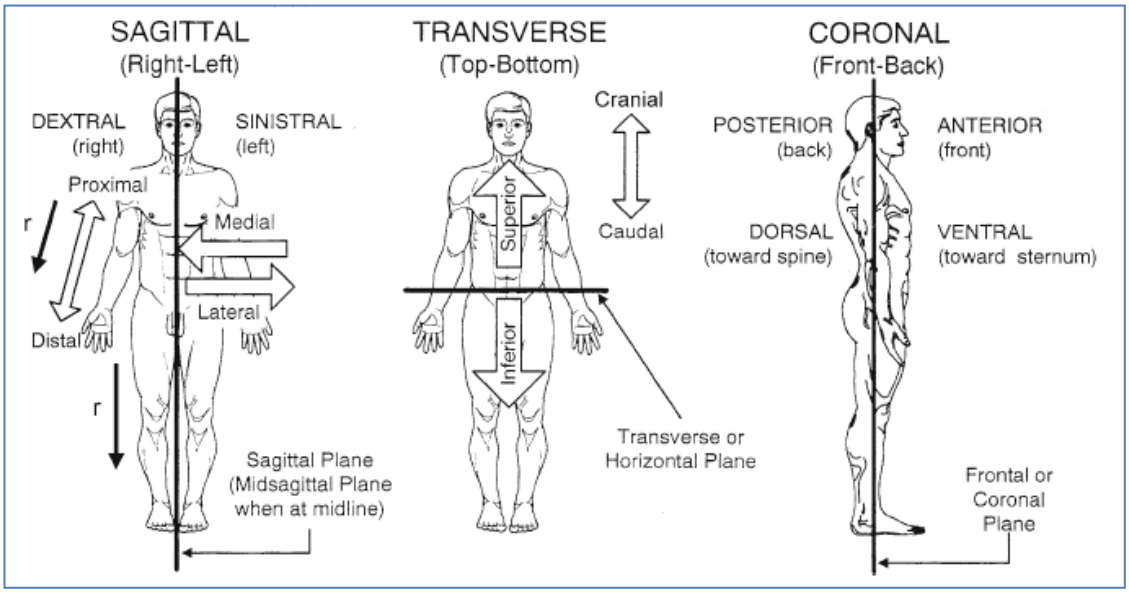

Figure 2-1: Terminology diagram page 2, Herman [52a]

Knowing these terms it is easier to examine existing models of human gait. However it is typically true that medical texts present models that are more complex than is appropriate for developing systems which unobtrusively measure human gait. It is therefore necessary to reduce the degrees of freedom of this representation to a

manageable number. This typically involves representing the human body as a limited collection of hinged parts, each representing limbs.

The simplest model and most relevant to this thesis is that of leg motion considered as a pendulum. There are several phases to walking which involve each foot being lifted off the ground and swung forward to take the body weight so that the other foot can be moved. To conserve energy during walking it is generally accepted that the frequency of swing maintained is that which best utilises gravity and is therefore largely determined by the simple harmonic pendulum motion. Figure 2-2, from Herman [52a] illustrates this.

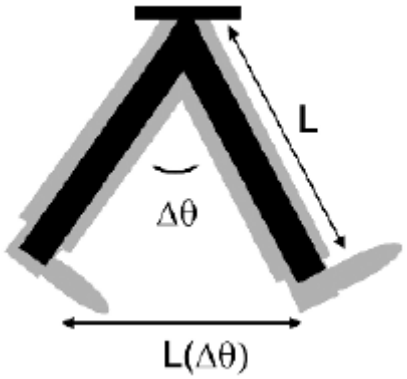

Figure 2-2: Simple pendulum leg model, page 118, Herman [52a]

In this model leg motion can be thought of as a free pendulum such as a ball on string where the period of the gait cycle is determined by Equation 2-1, where: g = 9.8ms^2 (acceleration due to gravity), l is the leg length (in meters) and T is the cadence period.

$$T = \frac{2\pi}{\sqrt{(\frac{g}{l})}}$$

Equation 2-1: Simple harmonic motion gait period

Herman [52a] further expands this model to account for leg articulation, non-uniform distribution of mass within the leg, joint rotation and forced motion. The model he suggests contains more detail than those typically used by researchers who develop systems that unobtrusively measure human gait. Wagg and Nixon [61, 63] present a system which seeks to account for hip joint rotation and model both the upper and the lower leg position in relation to the torso.

Where this model should be expanded is to consider not only the pendulum motion in the coronal plane but also in the sagittal plane, namely the impact walking has on lateral body motion. This motion is of particular relevance to chapters 5 and 6. Figure 2-3 from Oatis [52b] shown below, illustrate the pelvic body motion required to maintain balance while walking.

Figure 48.8: At weight acceptance, the individual shifts laterally to keep the center of mass close to the stance foot, and the pelvis drops on the unsupported side. The stance hip is in adduction.

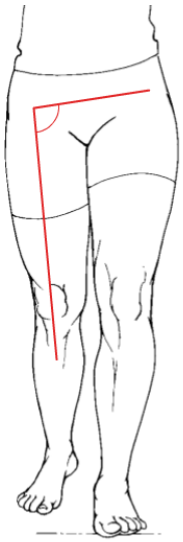

Figure 48.9: During weight acceptance, the hip drops on the unsupported side, which is abducted.

Figure 2-3: Illustration of hip motion, Oatis, page 860 [52b]

During the walking cycle the person must lift one leg and support their full weight on the other; therefore they must move their hip and torso to keep their centre of gravity over the leg supporting their weight. This results in a lateral oscillation at the pelvis and upper body. The nature of this oscillation is complex and affected by several body features including hip width. Mather and Murdoch [86] state that the gait community has long accepted that there is more lateral oscillation of the torso (upper body) in males and less of the pelvis, whereas the opposite is true for females. These differences between the genders reflect different articulation of the leg bones on the pelvis, and differences in the centre of gravity.

Barclay *et al.* [52c] present several measurements including average hip and shoulder widths, summarised overleaf in Table 2-1. These results show that on average males have significantly wider shoulders than females, and to a lesser degree that females have wider hips than males.

Gender	Male (cm)	Female (cm)
Average hip width	38.1	38.8
Average shoulder width	41.8	38.2

Table 2-1: Summary of data from Barclay *et al.* [52c]

The ratio of shoulder to hip width is a factor particularly dependent on gender, as confirmed by Davis and Gao [52d] on a separate data set. Further to this the increased shoulder width in males and increased hip width in females suggests that the centre of gravity is likely to be higher (as a ratio of height) for males than for females. This position is supported by Fullenkamp *et al.* [52e] who present a more detailed set of human dimensions, in their non-gait related study. Given that the position of the centre of gravity in relation to the hip joints is significantly different between genders, it is likely that the lateral gait oscillation will show a strong correlation to gender. This variation in centre of gravity (as a proportion of height) appears to support the accepted hypothesis that males oscillate their upper body more than their hips and the opposite is true for females.

This subsection introduces physics of the human body within the context of gait as far as is relevant to this thesis. It describes the most relevant terminology used in medicine to describe different perspectives of a person and follows on to introduce simple harmonic pendulum motion which dominates the gait cycle. The relationship between this and lateral (sagittal plane) oscillation during the walking period is explored. This is most relevant to chapters 5 and 6 of this thesis where a new measurement system for this lateral oscillation is presented.

2.4.2 Measurement of human gait

The measurement of human gait started in 1836 when Wilhelm and Eduard Webber brought together their skills to study human stride and motion. In the many years since the Webber brothers started their work the measurement of human gait has changed substantially. Johanson [53] describes well the history of this early work.

The introduction of digital video techniques had the biggest impact on the ability to measure human gait. Since its introduction in the 1970s the technology has improved

substantially. However many of the original problems still exist. As the availability of digital video capture and processing power has increased, the range and quantity of research into gait measurement has expanded, examples of which can be found in [54-56]. There are many different systems in existence each with their own advantages and disadvantages.

The best systems for accurately measuring human gait invariably require the cooperation of the subject (person being measured). They also place many constraints on the measurement environment. Systems such as those mentioned by Boyd and Little [56], require the subject to wear reflective pads or lights on their joints. Systems such as the Liberty system made by Polhemus require the subject to locate sensors at various points of their bodies to detect motion and location. Moeslund and Granum [57] provide a good review of more than one hundred and thirty different human motion studies carried out before 2001. In the review they present a general taxonomy of pedestrian tracking systems in which the tasks are split into four processes: initialisation, tracking, pose estimation and recognition.

Initialisation is described as the actions required to ensure a system appropriately accounts for the current scene at commencement of operation. For some systems this involves knowing the parameters of the camera. Many require unobstructed visibility of the scene, and/or expert intervention. It also includes parameter initialisation for models of human outline to ensure they are suitable for both the viewpoint and scene. Tracking, classified as the task of finding coherent relations between people (or limbs) through different frames, is highlighted as a well established research field. Pose estimation, the process of discovering how a human body or individual limbs appear is increasingly attracting attention. Systems are said to vary in complexity and resolution, some only collecting limited information such as centre of mass. Finally, recognition, which is often seen as a form of post processing, is highlighted as a method of determining or classifying the type of action. The review proposes that two different paradigms exist, recognition by reconstruction, and direct recognition.

In their review, Moeslund and Granum [57] conclude that recent advances in technology have significantly increased the study of human motion and gait. They point out that all the solutions reviewed are based on a number of assumptions that

make the problem tractable. They state that the field is at a relatively early stage and imply that a truly general system is a long way from becoming available and that there is significant room for improvement. A significant proportion of the current research uses video footage for measurement. This leads to increased effort in the unobtrusive measurement of gait that is further examined in sub-section 2.4.4.

2.4.3 Human Gait as a biometric

Human gait has long been recognised as a form of biometric identifier. Green and Guan [58] state that, from data published in several sources, there are no average sized people. What is meant by this is that there are no people with average measurements for all of their dimensions; we are all different in some way. As each of our dimensions dictate what our gait will be, we will all have slightly different gait, so it is reasonable to accept that gait can be used as a form of biometric.

Many different human dimensions can be collected for gait analysis, for example leg length, height or more specific data about lower and upper leg length. Abernethy *et al* [59] provide a good description of human anthropometry. The more anthropometric features we can collect about a subject, the better biometric we can achieve. Green and Guan [58] highlight work that shows only 7% of the population are "average in two dimensions".

This subsection has introduced some work, primarily from the biomedical field, which show that human dimensions, and therefore gait, can be used as a biometric identifier. Most automatic systems will only attempt to measure a small number of gait features and are not therefore likely to lead to a finger print like accuracy but they can still provide a significant biometric. How this biometric changes with time is a question that requires further examination. The next sub section examines the measurement of human gait from video.

2.4.4 Measuring human gait from video

In the last decade or so significant effort has been expended to try to unobtrusively measure human gait from video. This sub-section examines some of the major work in the field. In order to measure gait it is necessary to first find the pedestrian(s) in video, however, as examined earlier in this review, there are complex questions and tradeoffs

remaining in that task. For that reason researchers tend to either restrict the scene to: a fronto-parallel view [60], a known background [61], use operators for detection and tracking [51], or indeed all of them. This claim is supported by Sarkar *et al* [52].

Sarkar *et al* [52] present an interesting study and provide a valuable dataset with bounding boxes round each pedestrian in the video. They highlight that several gait studies have been conducted and that it is difficult to compare them. Each dataset and accompanying algorithm has requirements or assumptions that significantly limit the results of other algorithms on the dataset. They attempt to bridge this gap by providing a more substantial dataset and baseline algorithm, with a view to others improving on it. The baseline algorithm they present works by scaling the image of the pedestrian (after production of accurate bounding box) to a known size and then separating the pixels that relate to the pedestrian from the background. The numbers of foreground pixels are then counted. Fewer pixels will relate to the foreground when the person's legs are close together than when further apart; this produces a harmonic relating to the pedestrian's gait.

Collins *et al* [62] present a system for identifying humans, using an algorithm which identifies key poses within the gait cycle. These are then matched to the pedestrian silhouette and the width and height used to measure gait. In fronto-parallel video this provides a gait harmonic. They do not state that they require human assistance to identify and track the pedestrian. However they do note that the algorithm is adversely affected by errors in detection and tracking, for example those caused by shadows not being correctly removed.

Wagg and Nixon [61, 63] present an interesting and substantial study aiming to identify people from video footage by their gait. This project included a significant element of experimentation collecting a database of digital video footage showing subjects walking. They highlight the need to ensure an appropriate camera position and scene view. In the 2004 conference paper the collection of two datasets is described. The first dataset was collected indoors and related to a record of walking motion recorded on a short track, with a controlled background and lighting. The second was collected outdoors where the background was not so tightly controlled and selected to contain a mix of static and moving objects. Both datasets were collected

specifically to facilitate gait recognition. Therefore, a static fronto-parallel (coronal) camera view was used to collect approximately 90 frames of video data for each sequence. The camera used produced 25 frames per second. Collection of the indoor dataset, where a fixed background was provided, is well described in the 2003 sensor review article [63]. This dataset included a single high resolution still photograph of each subject so that the subject's body size could be estimated.

Wagg and Nixon [61] describe in detail the model and system they use to find, measure and represent people in video footage. The first part of their processing algorithm applies a Gaussian filter to remove noise; following this it employs a Sobel edge detector before applying background subtraction. This omits all the static objects, leaving only the edges belonging to moving objects. This combination of objects is then further processed to determine bulk motion, which is used to enable shape position and size estimation for the torso, head, upper and lower legs. When the locations and rotations of each of the above body parts are measured they are then further examined with respect to the pre-created model of human gait. Motion and gait cycle extraction are both adversely affected by rotation of the joints and its effect on the measurement process is reduced by spline interpolation.

After this processing it was noted that there was still significantly more motion information than can be put to use, so the data was further processed to measure features which relate to the individual. These are: lower knee width, gait frequency, ankle width, upper knee width and head x-displacement (anterior distance from head to torso). Each of these parameters was then used to inform a stochastic human ID model that generates their recognition system.

This paper also presents results detailing the F-statistic from analysis of variance for each of the individualistic features described above. This statistic provides a good indication of each measure's ability to discriminate between individuals; those with a higher F-statistic are more discriminative. The results show that the most discriminative feature is the lower knee width, however there is a slight difference in the ranking of gait frequency between the indoor and outdoor data sets. Gait frequency is more important than ankle width in the outdoor datasets suggesting that ankle width is significantly harder to measure when the background is more complex. It is also

true that all measures display a markedly lower F-statistic for the outdoor datasets, indicating that the model-fitting algorithms used perform less well with moving or varied backgrounds.

While, Wagg and Nixon [61] present very promising classification results they note that the algorithm used makes several assumptions and required significant processing power. On the computer they used, a frame rate of around 4 fps was achieved. Their measurement technique was not tested on different clothing, e.g. baggy trousers or skirts, and they note that it is not suited to such clothing. The nature of the algorithms used limits its use to video data where a clear fronto-parallel view of the subject is available and the majority of motion in the scene consists of the subject.

BenAbdelkaert *et al* [64] present a system for identifying individuals based on height and stride. Their parameter extraction system is described in [65] and assumes that the camera is calibrated with respect to the ground plane to allow realistic 3D position estimation. It also relies on the person walking in a straight line. Given these assumptions, they extract the height and three gait parameters: stride length, cadence and velocity. Results presented show 49% correct classification on their dataset. They conclude that their system's success is strongly linked to "the periodic nature of human walking". By this they suggest that cadence is a good discriminator. Bobick and Johnson [66] present a similar technique with similar results and constraints.

This sub-section has reviewed the most relevant work in the field of unobtrusive measurement of human gait from video footage. There is much more research ongoing in the field, such as the work described by Bregler, Su *et al*, Xu *et al* and Yoo *et al* [55, 67-69]. Bregler presents a probabilistic computational framework for learning and recognising human gait using a Hidden Markov Model. Su *et al* present a method for extracting gait features from silhouettes without requiring an explicit human body model. Xu *et al* present a method for applying marginal Fischer Analysis to the problem of dimensionality reduction for human gait reduction, a feature receiving increasing attention in the research community. Yoo, *et al* present work which contributed to the algorithms Wagg and Nixon used.

This review only describes the most relevant research to this doctoral thesis, there are over 150 references mentioned in the review of human motion capture presented by Moeslaun and Granum [57]. Their review also includes the tasks of finding and tracking pedestrians described in section 2.3. Several different datasets have been produced for gait analysis. These data sets consist of data from 6 to 122 people, with a typical number in the region of 20-25.

2.5 Stereo vision

Stereo vision is a topic that has attracted intense theoretical and practical research over time, some of which is described in references [70-73]. Most animals have two eyes and perform some sort of stereo interpretation to gain distance estimations for objects they can see. This task however is a difficult one, presenting many interesting challenges. This section describes the basic theory of stereo vision for depth perception and highlights the currently important topic of stereo correspondence. It also introduces some of the research in using stereo vision to identify and track pedestrians. This section is not an in-depth review but an introduction covering the basic principles and highlighting the status quo in the field of stereo vision. Brown *et al* [74] present a more comprehensive review of the topic.

2.5.1 Stereo depth perception theory

The principle behind the measurement of distance from stereo vision is the parallax effect. When the same object is viewed from two different locations it is possible to use Pythagoras theorem to ascertain the distance to the object. Figure 2-4 shows the concept in the two dimensional plane with the triangulation drawn on.

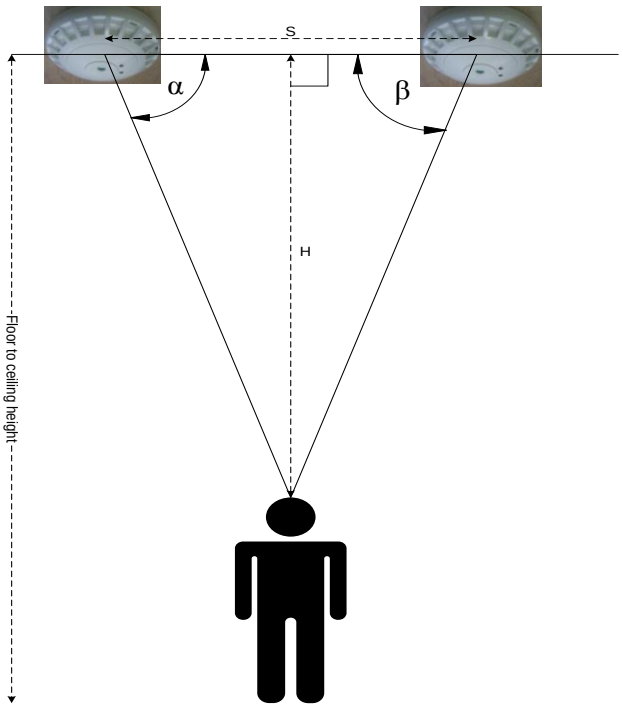

Figure 2-4: Stereo depth perception

This theorem allows the distance 'H' to be calculated from the midpoint between cameras to the top of the object of interest, in this diagram the pedestrian. Several stereo vision systems work out the distance from one of the cameras (called the reference camera) to the object using the same theorem, such as the system developed by Videre design Inc. In order to do this, the angles alpha, beta and distance s in Figure 2-4 must be known. These are found by locating the position of a pixel from the first image in the second. In most stereo vision systems the cameras are mounted at a known distance apart leaving the principal question of stereo correspondence, which is further described below.

2.5.2 Stereo correspondence problem

The theory described in sub-section 2.5.1 works well when it is easy to establish the same point in both images. Without making certain assumptions this is a non-trivial task. In a simple pinpoint image it is easy to establish what the angles are from the x and y coordinates of the pixel(s) in each image. However, this type of image is unusual. Liu *et al* [75] support this position and describe their work on a new technique for concurrent stereo matching. There is a significant body of work on the correspondence problem, for example the research presented by Psarakis *et al.* and Veksler [76, 77] respectively. Psarakis *et al.* propose a correspondence solution with

sub-pixel accuracy. Veksler presents a solution utilising dynamic programming on a tree. Brown *et al* [74, 78] provide two reviews of stereo image processing techniques, one from 1992, and one from 2003. The latter provides a significant focus on correspondence issues.

In the 2003 review Brown *et al* [74] loosely separate correspondence issues into two categories, those with local and those with global constraints. For correspondence methods with local constraints the search is limited to a small number of pixels surrounding the pixel of interest. Those with global constraints restrict the search to either scan lines or the whole image. Several local correspondence matching methods are introduced, for example: block matching, feature matching and gradient methods. Three significant global correspondence approaches are introduced, dynamic programming, intrinsic curves and graph cuts. Correspondence methods with global constraints are highlighted as being more computationally complex and attention is drawn to the significant problems of occlusion.

The review concludes that, while the questions relating to local correspondence are now well understood, those relating to global correspondence are less well understood. They indicate that significant effort is being diverted to the areas of global correspondence and occlusion and that future work should focus on these areas.

2.5.3 Stereo vision for pedestrian detection and tracking

Several researchers have published work utilising stereo depth perception to improve pedestrian detection and tracking in video. This sub-section provides a brief introduction to some of this work. It places the research presented in this thesis in context with the work of others, but does not provide a comprehensive review.

Bertozzi *et al.* [79] present a system for detecting and tracking pedestrians in far infrared images using a fronto-parallel stereo view. They assume that the stereo correspondence problem is only local. Depth perception information is then extracted and fed into the detection process, which allows pedestrians to be successfully detected, even when they partially occlude each other. Munoz-Salinas [80] presents a system for detecting and tracking people using stereo vision to overcome tracking complications found when one person occludes another. Fujimoto *et al* [81] presents a

system for measuring the distance to pedestrians from moving vehicles using stereo vision. They present some interesting tests in their short paper [81] where they successfully detect a pedestrian crossing the road. The pedestrian is crossing in front of the forward looking stereo camera mounted on a moving car. Detection and tracking is achieved at distances below 50m, in good weather. They note that further work is required to make the technology "capable of being used in real-world driving environments".

2.6 Summary

This chapter reviews the main relevant literature to pedestrian detection, tracking and measurement. It starts with a description of the major technologies used to detect and measure pedestrian motion. This includes a short discussion of the different mounting positions typically used for each technology. Typically video based gait analysis is taken from a fronto-parallel view. A top down view is used for the IRISYS people counters, elevated and oblique views for typical CCTV installations. The review then examines the main research fields investigating and funding pedestrian detection and tracking research. This includes an introduction to some of the recent research projects in the area.

The majority of the research into pedestrian measurement takes place in the image processing field. A substantial review of image processing is presented in section 2.3. This review highlights the common problems associated with detecting and tracking pedestrians. It also reviews the standard techniques for solving the common problems, background subtraction, optical flow, object detection and tracking. This includes a description of some of the current research questions in the field.

The review then moves on to the topic of human gait. It first provides a brief history of the measurement of human gait, then it presents credible evidence that gait is an individualistic biometric. After this introduction to gait the review examines the major and current work in the field of measuring human gait as a biometric. This work almost exclusively takes the form of video with image processing to take the measurements. There is significant effort in this field and the work of Wagg *et al* [61, 63], BenAbdelkader *et al* [64, 65], Collins *et al* [62] and Sarkar *et al* [52] present some of the most significant research in this area. It is noted that there are still assumptions

or interactions that limit the real world use of these human gait recognition systems. Generally these are either a restriction on the background or operator interaction for detection and tracking; solving these issues still requires further work.

Finally the review provides an introduction to stereo vision, describing the basic principles and problems. It also introduces some of the algorithms developed that use stereo depth information to augment the detection and tracking of pedestrians.

3 Underlying technology

This chapter discusses the IRISYS (InfraRed Integrated SYStems Ltd) people counter, later referred to as (detector) in detail. The first section provides a description of the detector, its construction and the general theory of operation. The chapter then examines the information available from the detector and the trajectory information produced by the target tracker. This examination demonstrates through data captured that barrel distortion exists. This distortion is investigated and an approximate correction algorithm is presented. It is noted that some of the information presented in this chapter is protected by patent. Agreement was required from IRISYS to gain access to the data used during this research.

3.1 The detector

The detectors are produced by Infrared Integrated Systems Ltd a UK company based in Northamptonshire. They are mainly marketed for counting the number of pedestrians entering and leaving retail locations. The detectors are based on a low resolution thermal difference imager with digital signal processor and algorithm capable of tracking pedestrians within the downward looking field of view. In a typical installation, often above a doorway, two different lines are configured to enable counting of people entering and leaving the location. A full description can be found in the IRC 1004 product information sheet available from www.irisys.co.uk.

The detectors produce much more information than is generally used in a retail environment. A description of the data produced by the detectors and used in this thesis can be found in section 3.2. The remainder of this section describes the detector; starting with an examination of the detector's construction. Then it provides a review of several different aspects of the device, including: the communications systems, normal retailer usage, pyroelectric detector array and a discussion of the digital signal conditioning in the device.

3.1.1 Detector construction

The detector described in this section is protected by patents EP 0 853 237 B1 and US 6,239,433 B1. Figure 3-1 and Figure 3-2 show the detector from the front and rear respectively. Each detector is supplied with a mounting plate to allow easy installation

on a ceiling. The coin shown in Figure 3-1 is a one pound (sterling) coin and is present to provide an indication of the scale of the photographs.

Figure 3-1: IRISYS detector technology

Figure 3-2: IRISYS detector photograph, rear

Each detector contains three main components: a germanium lens at the front, directly behind it a 256 element pyroelectric array, and a printed circuit board containing the digital signal processor and other electronics. Figure 3-3 shows a diagrammatic representation of the detectors, based on observation. The diagram is not an exact representation but provides a good indication of the detector's construction.

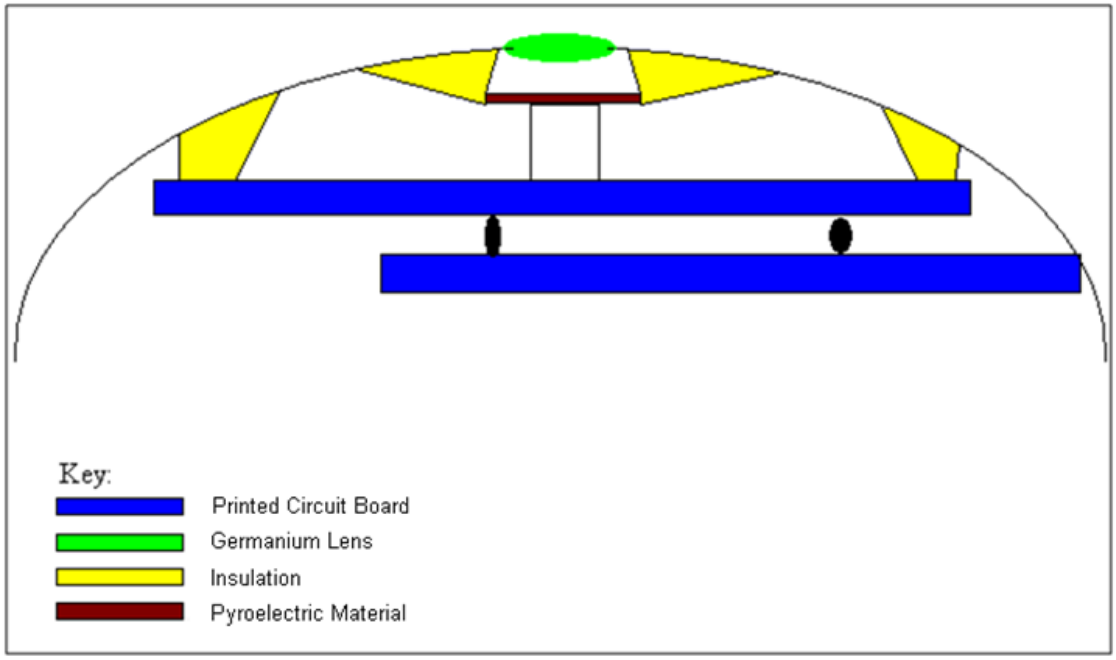

Figure 3-3: IRISYS detector diagram

The main sensing components of the detector are the germanium singlet lens and the pyroelectric array. Germanium is chosen for the lens as it has low absorption of EM radiation in the IR wavelengths of interest (8-12 microns). However it has a high refractive index, making wide angle lenses difficult to make. The affect of this is reduced with an anti-reflective IR coating. The coating also provides a harder surface for the lens than germanium, which reduces the chance of damage during production and transportation. One disadvantage of the lens and detector construction used is that it suffers significantly from aberrations; these are further examined in section 3.4.

3.1.2 Detector communications

The detectors come with three different methods of communication. This section provides an overview of each of them. The simplest is the use of a pair of relays which can be configured to switch when a person is counted in or out. This is generally used to interface the devices with existing systems, such as with the marketing of a variation of product for tailgate detection in automatic security applications.

The second communications protocol used is the CAN (Controller Area Network) bus; this was chosen as it is well suited to long distance two wire communications in noisy environments. It is generally used to connect multiple units together for complex

people counting systems, such as wide doorways where multiple units are required, or for supermarket queue monitoring solutions.

The third and final protocol used is UART; this provides the most comprehensive communications to the device. It is typically used by engineers installing the devices to update configuration setting in the device. It is also used by the author. The UART communications require a line driver to connect to a standard serial port. IRISYS supply two different types. The first, a small device which connects to a socket on the rear of the device, provides a reliable communications connection and is recommended by the author. The second, shown in Figure 3-4, clips onto the outside of the detector. This is more convenient for use by a field engineer who requires to communicate with a ceiling mounted device without removing it from its existing communications network (e.g. CAN). However the contacts do not always connect reliably and can require adjustment.

Figure 3-4: External serial connector line driver unit

3.1.3 Pyroelectric array detector

The 256 element PZT array used is manufactured by IRISYS and consists of a two dimensional sixteen by sixteen array. PZT is a Lead Zirconium Tantalite crystal which has positive charge at one side and negative charge at the other. A layer of crystals can be produced polarised, such that a charge will be generated on surface electrodes when it changes temperature. This change can in turn be measured. A general description of the processes, materials and expected charges from thermal sensors can be found in [82].

The IRISYS arrays are manufactured in a unique way. A wafer of PZT is baked into a thin ceramic wafer and polished flat. On the top of this wafer a metal IR absorber is laid, which is also used as a common ground electrode. On the underside of the PZT wafer a patterned array of 256 electrodes is arranged. Figure 3-5 shows a diagram of this taken from the patent documents.

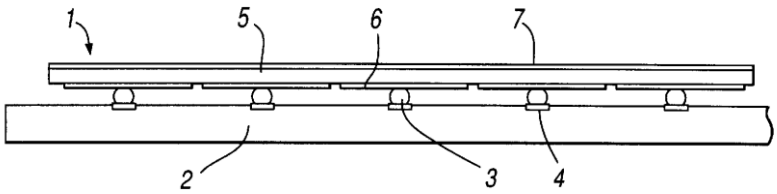

Figure 3-5: IRISYS Detector array (from US Patent no 6,239,433, fig 1 page 2)

These electrodes are then bonded to pads or raised bumps on an application-specific integrated circuit which contains the electronics necessary to read the varying charge generated by the PZT as it changes temperature. The whole assembly is placed in a hermetically sealed package with an IR filter window. The filter window is specially designed to only allow through IR radiation within the frequencies of interest, 8-12 microns (*pers com*. Dr N. Johnson, Chief Software Scientist IRISYS, 5th Dec 2007).

This package provides the main sensing component for the detector. When assembled with optics it produces a thermal difference imager. It is however noted that constructing the array from a single large IR absorber and PZT layer leads to considerable thermal leakage between pixels. If a signal is incident on a single pixel, some of the charge produced will be measureable on the neighbouring pixels as well. This has been confirmed by observation of data produced by several detectors in several different locations.

3.1.4 Digital signal processing

The signals produced by each pixel in the detector are sampled by a 16 bit a-d converter and then further processed. Each channel suffers from DC drift and a digital high pass filter is used to remove this drift. This high pass filter effectively removes any slow change in the signal which is likely to relate to voltage drift in the signal read-out electronics, or change in temperature of the device and its surroundings.

There appear to be two significant processing algorithms operating. The first processes the image data actually obtained from the sensors to remove noise. The second is to detect and track people by matching ellipses to the hot and cold spots noted when people walk under the detectors. Figure 3-6 shows the measured graph of the values received from a mid image pixel in the detector, collected at Napier University. This data was collected by a person walking under the mid pixel of the detector, standing still for approx 10s and then walking out of the field of view.

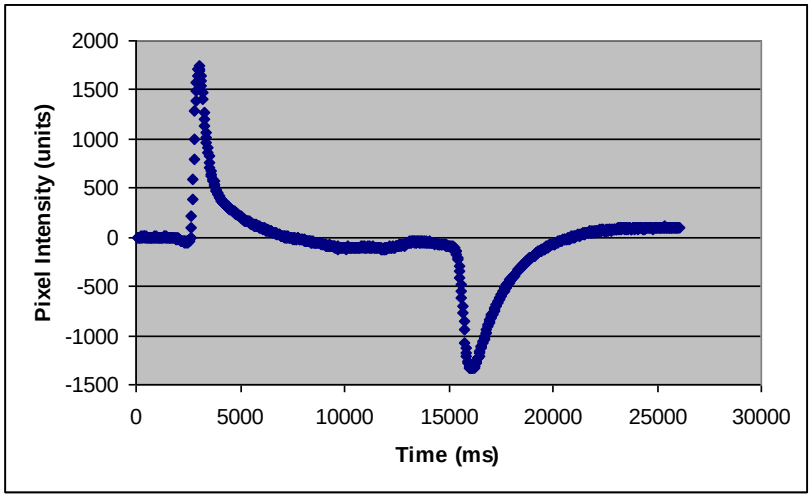

Figure 3-6: Graph of IRISYS pyroelectric element intensity

The upward spike in the signal occurring at around 3s represents the pixel warming up as the hot person moves into its field of view. The downward spike at around 15s represents the pixel cooling down as the person moves out of the field of view. Closer examination of the beginning of this graph shows that there is some other form of signal conditioning occurring. Figure 3-7 shows an enlarged view of some of the first 3s of data displayed in Figure 3-6. It is clear that the intensity drops shortly before it rises which is indicative of a filtering or processing system that takes account of the value measured at the surrounding pixels. The nature of this processing is not available but it is believed to be linked to a complex form of high pass filtering.

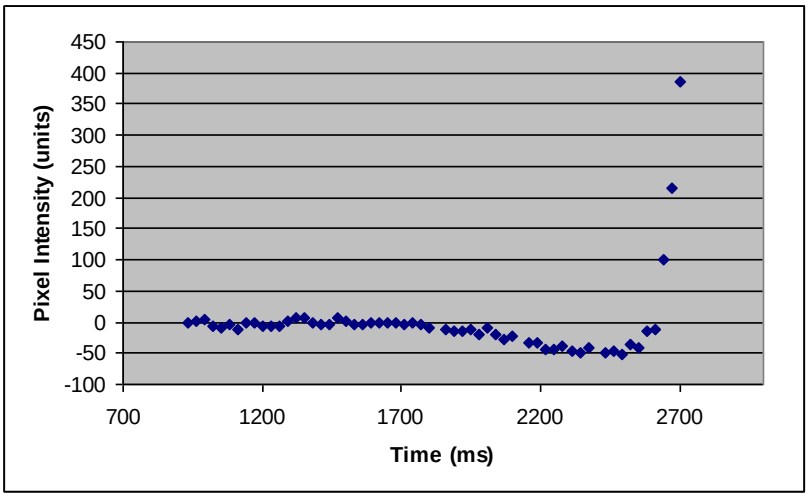

Figure 3-7: Magnified view of Figure 3-6

3.1.5 Elliptical tracker

The start of this section introduced the detectors marketed as the people counters by IRISYS. The previous sub-sections describe how the detectors work and show that they act as a thermal difference imager. In order to count people it is necessary to detect and track people through the field of view. When viewed from above, people look approximately elliptical. Figure 3-8 demonstrates this by showing a person viewed from above with a high resolution IR camera. The pedestrian detection and tracking algorithm applies an elliptical contour tracker to do this. The exact nature of this tracker algorithm is secret and closely guarded by the manufacturers. This sub-section describes it in general terms.

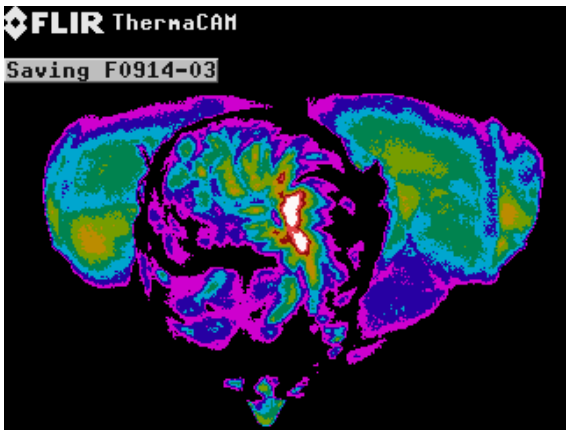

Figure 3-8: Thermal image of pedestrian viewed from above

Figure 3-9 shows image data collected when one person is walking through the detector's field of view while the detector is mounted at 2.5m, the lowest height recommended by the manufactures.

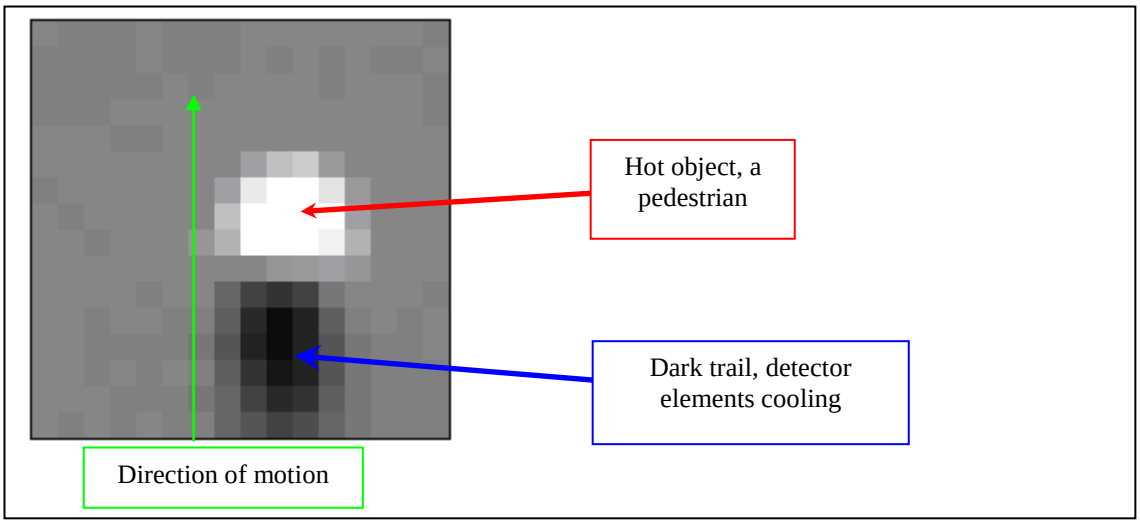

Figure 3-9: IRISYS detector Image, single pedestrian

The grey area represents the background and the bright area indicates the increase in temperature, caused by the pedestrian passing the field of view (marked with the red arrow). The dark area following the pedestrian (marked with the blue arrow) is due to the sensors measuring change in temperature. As the pedestrian leaves the field of view of a pixel its intensity drops, showing that it is cooling down, before returning to its normal background intensity.

This type of image is then processed to look for elliptical shapes applying an unknown algorithm to remove false positive detections. The pixels inside detected elliptical shapes are then used to create a weighted centre of detected thermal signal. This provides a sub-pixel accuracy centroid location. It is believed to be similar to the ACE tracking algorithm presented by Cameron [83]. Once detected, the locations of pedestrians are tracked through the scene until no trace of them can be detected. Figure 3-10 shows a scene viewed by a detector mounted at 3.6m with two pedestrians detected and tracked through the field of view.

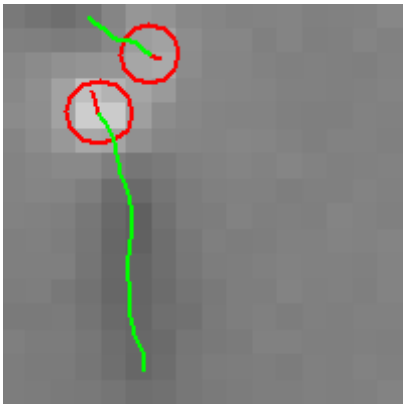

Figure 3-10: Detector image showing two pedestrians detected and tracked

The detectors have a mechanism for noting a connection between two ellipses that appear close together to improve the tracker performance. This is termed a "parent and child" relationship and is maintained from frame to frame. If sufficient distance is reached between the ellipses then the detectors remove this association, similarly, if the distance between them reduces, then the two ellipses become one. This parent-child relationship allows the detector to retain multiple hypotheses about each target when it is difficult to establish if a detected entity is one person or two people walking close to one another.

3.1.6 Normal use as a people counter

The detectors are manufactured and sold as people counters, not as thermal difference imagers. For people counting there is further processing performed on the device to follow the tracks of pedestrians produced by the elliptical tracker. When the devices are installed two different count lines are positioned with respect to the thermal difference image. These lines are used to denote the entrance and exit to/from the field of view in relation to the environment the devices are placed in. A count of the number of people entering and leaving the premises is produced by counting the number of people that cross each line in the prescribed direction. Two example line set-ups are shown in Figure 3-11, which is taken from the product datasheet.

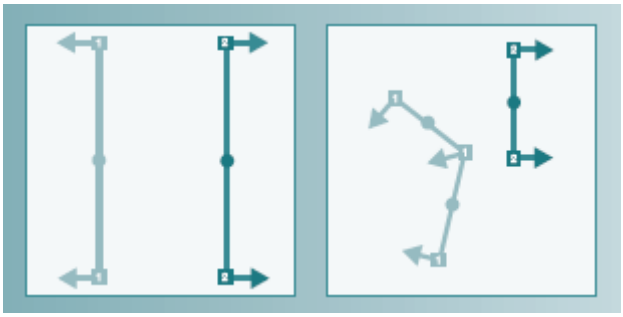

Figure 3-11: Possible count line configurations (image from page 2 IRC 1004 datasheet IRISYS)

This sub-section has introduced the normal usage of the detector; there are several different bespoke uses of the detector in existence. An example of this is a variant used by Tesco Ltd (at the time of writing the UK's largest retailer) to measure the queue lengths at its checkouts. This information is used to maintain a promise made by the retailer to their customers that there will typically be only "one person in-front" at the queue.

3.2 Data produced by the detectors

This section describes the data output by the detectors when using the serial link. There are many different configurations for the sensor and it is possible to reprogram the on-board DSP (digital signal processor). However, reprogramming the DSP is not covered in this thesis. Data produced by the detector is formatted into a bespoke packet structure described by Sumpter in an IRISYS internal document [84] which was kindly made available during this research. A time stamp packet is used to separate data packets into frames, each frame corresponding to a known time. It has been observed that the detector occasionally drops a frame of data. This typically occurs when there are a high number of pedestrians in the field of view. The cause of the detectors dropping these frames is strongly linked to the data rate nearing or breaching the maximum capacity of the serial link, 115K baud.

The remainder of this section describes data from two of the packet types available from the detector: firstly, array data which contains the thermal difference image, and secondly, target data which contains information from the elliptical tracker about people being tracked in the scene.

3.2.1 Array data

As mentioned in section 3.1 the detectors produce a sixteen by sixteen pixel thermal difference image. This information is sent in an array data packet containing a bespoke compression algorithm which can be uncompressed into two hundred and fifty six, signed sixteen bit integers. Each value represents a pixel with zero being the typical background value, negative values representing a cooling pixel, and a positive value presenting a warming pixel. The data can easily be represented as a thermal difference image as is shown in Figure 3-12. The packet format description has not been included due to considerations of confidentiality.

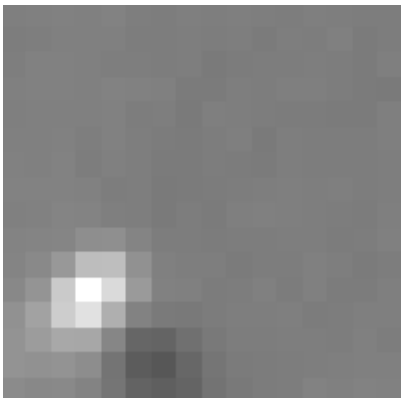

Figure 3-12: Array image

3.2.2 Target data

As mentioned in section 3.1.5 the detectors match ellipses to hot and cold objects, representing pedestrians. This information is termed target data by Sumpter (Software team line manager, IRISYS) in internal communications protocol documentation. It contains a substantial amount of information about each ellipse matched in the field of view. Once the detectors have detected a person (target) they will track it until it leaves the field of view or becomes invisible. There are two causes of targets becoming invisible. Firstly, the pedestrian may stop moving; as the detector only detects change in temperature, they will disappear from the detector's view. Secondly, the person walks out of the detector's field of view. A target packet is transmitted from the detector containing a list of smaller target structures. Each of these structures contains several different bits of information:

- A unique ID, which is maintained as long as the target remains visible.
- Location, x and y coordinates with respect to the origin of the thermal difference image.
- Ellipse dimensions, width, height and angle

- Direction of motion
- Status (also called mode) information about the target.

The status information contains a flag that is set when a target appears to be disappearing without leaving the field of view. This is to help detect the known problem caused when people stop moving (they become invisible in the difference image). As only the x and y coordinates of the target centroid are used in this research, no further explanation of the remainder is provided.

3.3 Trajectory measurements from the IRISYS detectors

The accuracy of the trajectory measurements taken by the detectors is a factor that requires consideration. This section examines what is currently known about the trajectory measurement and presents experiments to further detail the accuracy of the measurement. A significant study confirming the usefulness of these detectors as person trackers is published by Springer [1]. This was written by Kerridge, Keller, the author of this thesis and Sumpter. The book chapter shows very good results can be achieved in tracking and counting pedestrians in both controlled and uncontrolled environments. This section further examines the trajectory information on a more microscopic scale.

Measuring the accuracy of pedestrian detection and tracking systems is known to be a difficult task. List *et al* [50] highlight the problem with respect to the image processing community in their paper "Performance Evaluating the Evaluator". They note that most image processing systems assess accuracy by comparison with a known ground truth generated by a human observer. They also note from their own evaluation a 5% variation in bounding box sizes in the results from two different evaluators examining the same video sequence. The same problems apply to measuring the accuracy of the IRISYS detector.

Trajectory data collected by the detectors is harder to validate than data from video as the spatial resolution is significantly lower and sub-pixel accuracy is required. The complications are compounded by the detector only measuring change in temperature. Participants can be asked to walk along a known path but as previously discussed there is a large amount of variation in human bipedal locomotion. This makes it very hard

to accurately characterise the ability of the detector's tracker to follow a pedestrian at a microscopic scale.

This section looks at two experiments to help understand the ability of the detectors to measure motion accurately. It is not intended to formally characterise the trajectory's accuracy but to establish that it is suitable for further examination. The first examines data collected by asking participants to walk under a detector following known paths. The second examines the results from the detector tracker when it is used to track a small inanimate warm body moving mechanically. The latter examination removes the complications of detecting pedestrian motion and examines more accurately the ability of the detector to reliably produce trajectories at sub pixel accuracy.

3.3.1 Pedestrian walking test

This experiment confirms that correct and repeatable trajectories can be measured from a single person as they walk through the field of view. The path they followed on the way out was separated by 50cm from the path they followed on the return. For this experiment the detectors were mounted at a height of 2.95m. Three different participants each walked along this trajectory repeating their walk three times. Figure 3-13, Figure 3-14 and Figure 3-15 show the measured trajectory plots from each of the participants. Each repetition of a walk is displayed in a different colour to highlight the level of consistency in the trajectory measurements.

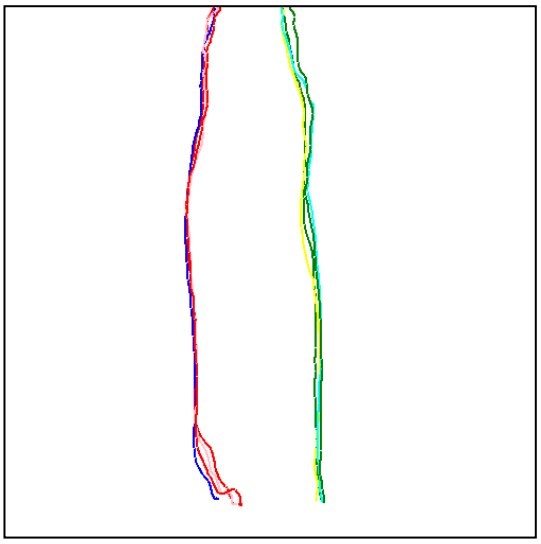

Figure 3-13: Person A walking along two straight lines

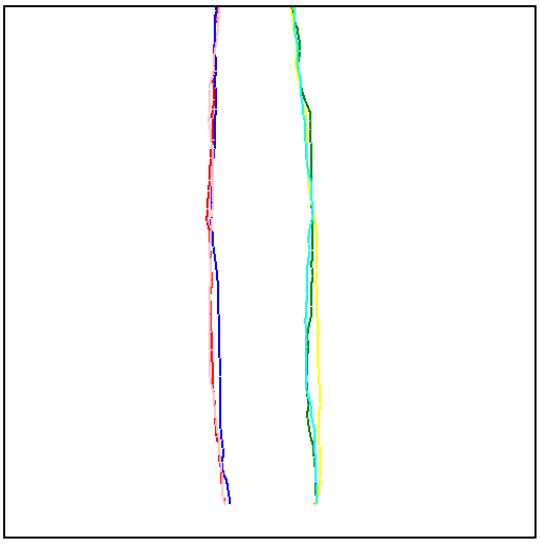

Figure 3-14: Person B walking along two straight lines

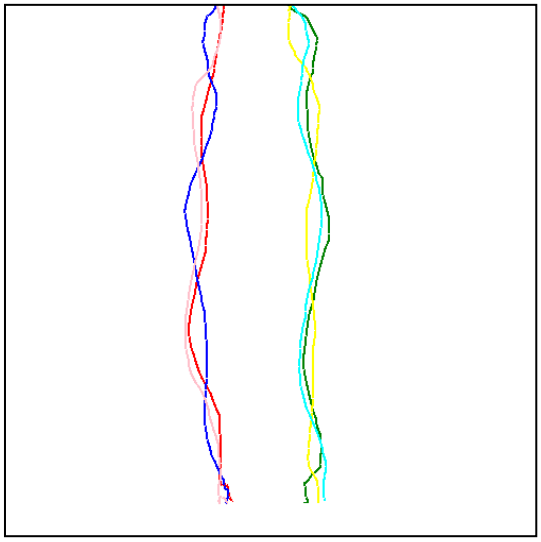

Figure 3-15: Person C walking along two straight lines

It is clear from the above figures that a notable difference is present between the two lines followed by all three participants. This is shown by the difference in location of the red/blue trajectories and the yellow/green trajectories. In Figure 3-15 distinct differences exist in all trajectories plotted. It is also possible to see a similar series of trajectories in Figure 3-13 and Figure 3-14 although the grouping within red/blue and yellow/green are considerably closer together.

This small number of trajectory plots is interesting and demonstrates that, as published by Armitage *et al* [3] and Kerridge *et al* [12], the detectors can track pedestrian motion. The data also confirms that the detectors can successfully discriminate between paths separated by 50cm and implies that much higher tracking accuracy is possible. Figure 3-15 shows that repetitions of a straight line walk collected from a single person can be measured slightly differently. However it is not clear if this is due to difference in the trajectory walked or the measurement technique used.

3.3.2 Sub pixel accuracy experiment

Sub-section 3.3.1 presented a short data capture illustrating the trajectory measurements taken from people as they walk along a known path. This sub-section presents a short experiment examining the ability of the detector to track trajectories at much higher spatial accuracy. This is achieved by using an inanimate thermal emitter moving along a model train track, an accurately repeatable trajectory. By using this experiment we can eliminate the chicken and egg problem of not knowing how

accurate the detectors are and not knowing the location of the pedestrian. The emitter will move along a known straight line, "the track". As the emitter is inanimate and small it also eliminates any uncertainly over which part of a person the detector is tracking.

For this experiment the detector was mounted 1.5m above the ground with a model train track running in a straight line along the ground within the detector's field of view. A height of 1.5m is chosen as it is approximately the height from a typical ceiling mounted detector to a pedestrian's head. At this height the size of each pixel is approximately 8cm squared. The model train carried a small bottle (200ml) of warm water, which acted as an emitter of dimensions smaller than a single pixel. The experiment was then repeated with the model train track moved 5cm to the left of its original position creating a second trajectory for comparison. This set-up establishes if it is possible for the detector to discriminate between trajectories that are separated by less than one pixel distance.

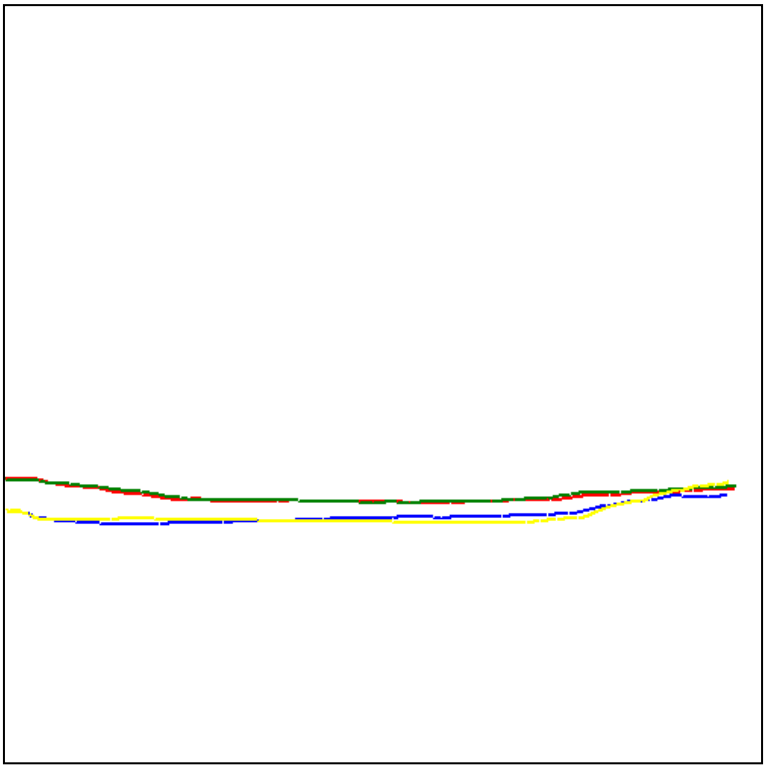

Figure 3-16: Model train trajectories separated by 5cm

Figure 3-16, shows four trajectories collected using the model train set up. Two trajectories are presented from each track location. The yellow and blue are from location one and the red and green are from location two. On the left of the image it is

clear that the trajectories from different track locations are separated. However they appear to converge to the right of the image. The data demonstrates that a detectable difference is present when the trajectories followed are separated by 5cm, which shows that sub pixel tracking of small objects is possible. However it is clear that there are some artefacts affecting the trajectory measurements, particularly at the edges. Examination of this data and the data presented in sub-section 3.3.1 shows that a slight curve in all trajectories measured is present. This curve is believed to relate to barrel distortion which is common in wide angle optical assemblies such as that present in the detectors quoted 60^{o} field of view.

Communications with the manufacturer also confirmed that there are known inaccuracies in trajectories at the edges of the field of view. Several things effect the trajectory measurements at the edges of the field of view, two of which are: the tracker will start to track a person when they are partly occluded, thus the weighted centroid location will contain error, and the detectors use a different algorithm for initialising the tracking of targets from that they use to follow them after initialisation.

3.4 Detector distortion

Observations from early work show that all the detectors suffer from varying degrees of distortion, and that the most notable form of distortion is barrel distortion. This section examines the distortions present and develops a correction algorithm for some of the distortions noted.

All optics suffer from some degree of aberration that make it difficult to properly focus an image on a detector array. This is due to the focal distance of a singlet lens being dependent on both the radii of curvature and the refractive index of the lens material, the latter of which varies with wavelength. The detectors are sensitive to a wide band of IR wavelengths (much wider than the visible spectrum); this makes it very difficult to accurately focus an image on a detector array. This artefact compounds the thermal crosstalk present in a pyroelectric array produced from a single piece of ceramic.

Barrel distortion is also significant in the detectors. It is a well known phenomenon and particularly common in wide-angled optics, Klein and Furtak [85] describe it on page 241. It causes the image passing through the lens to have magnification varying

with distance from the optical axis of the lens. This leads to an image being formed on the detector that is distorted. At the edges of the field of view a single pixel will cover a larger area than at the centre of the optical axis. Figure 3-17 illustrates an expected coverage area for a detector with barrel distortion.

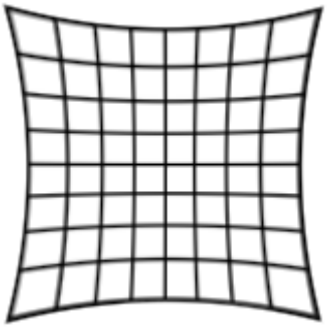

Figure 3-17: Illustration of object area viewed with barrel distortion

The IRISYS detectors are particularly susceptible to this type of distortion, in addition to other aberrations. In order to make use of the data from the detectors for studying motion accurately, corrections must be made to the data to account for barrel distortion. Figure 3-18 shows an illustration of several paths that could be measured by the detectors.

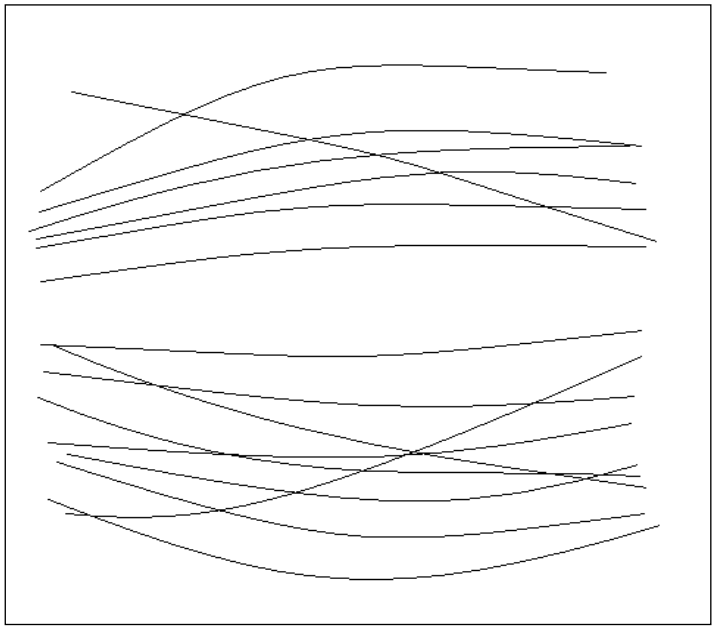

Figure 3-18: Illustration of pedestrian trajectory showing barrel distortion

It is clear from Figure 3-18 that the paths appear curved. However, the subjects this illustration is based on would be mostly walking along a corridor in straight lines. The apparent curvature is mostly the result of barrel distortion.

It is possible to produce a formula that corrects for barrel distortion. This work is derived from that presented by Klein and Furtrak [85]. It is based on three assumptions: Firstly, that the object distance is large (and therefore considered infinite) when compared to the distance between the pyroelectric array and lens, secondly that the magnification increases with the square of the distance from the optical axis. Finally, that the optical axis is centred on the image array.

Equation 3-1 shows a formula that corrects for distortions based on these assumptions. To use this formula it is necessary to find the distortion coefficient, alpha, for the optics in use.

$$y' = y(\alpha(x^2 + y^2) + 1)$$
$$x' = x(\alpha(x^2 + y^2) + 1)$$

Where:
y' = the corrected y location
x' = the corrected x location
α = the lens distortion coefficient

Equation 3-1: barrel distortion correction

The next sub-section presents an experiment to collect data and calculate the most appropriate value for the detectors, as described below.

3.4.1 Barrel distortion experiment

Measurement of the barrel distortion is not as simple for the detectors as it would have been for a visual camera. As the detector is a thermal difference imager any source must continue moving (or appear to continue moving) to be detected. An experimental detector mounting was assembled to collect data, shown in Figure 3-19. This raised the detector approximately 1.5m above the ground, more than 150 times the distance from lens to pyroelectric array.

Figure 3-19: Barrel distortion experiment photograph

A cup of tea was used as the thermal emitter and a cardboard shutter was moved in-between the detector and emitter to create the thermal change necessary to detect the emitter. The complications caused by thermal crosstalk between pixels are minimised by using the elliptical tracker to locate the centre of the object to sub pixel accuracy.

The emitter was placed on the ground and moved until its location measured by the sub-pixel location from the detector was in the centre of a series of pixels. The actual location was then marked on the floor. This was then repeated for five different locations and the distance between the pairs of points was measured. Table 3-1 shows the measurements taken.

Point 1 x,y (pixel coordinates)	Point 2 x,y (pixel coordinates)	Separation distance (cm)
9,9	12,11	39
12,11	14,12	30
9,12	9,14	22
9,12	12,14	43
9,14	12,14	30

Table 3-1: Distance between pixel coordinates

3.4.2 Calculation of alpha

Given the values in Table 3-1 it is possible to use regression to calculate the best fit value for alpha in Equation 3-1. A macro was written to recursively test different values of alpha to find the optimum for the data collected. The test of fitness used first adjusts the x, y coordinates using Equation 3-1. Secondly, Pythagoras Theorem, is used to calculate the distances between all five points measured in adjusted pixel units. This set of distances is then compared to the known separation distances to produce a fitness value. The fitness used is the coefficient of determination from least squares linear regression. The macro repeated the calculations storing the value for alpha with the coefficient of determination closest to one. The value of alpha giving the best result is 0.005662.

3.4.3 Detector distortion conclusions

Figure 3-20 and Figure 3-21 show the blue and yellow trajectory plots from the train experiment results presented earlier in Figure 3-16. The data collected from the model train experiment was collected using a different detector from that used for the barrel distortion experiment. The red plot presents the trajectory before barrel distortion correction and the green presents the trajectory after correction. These results are known to have originated from a target moving in a straight line.

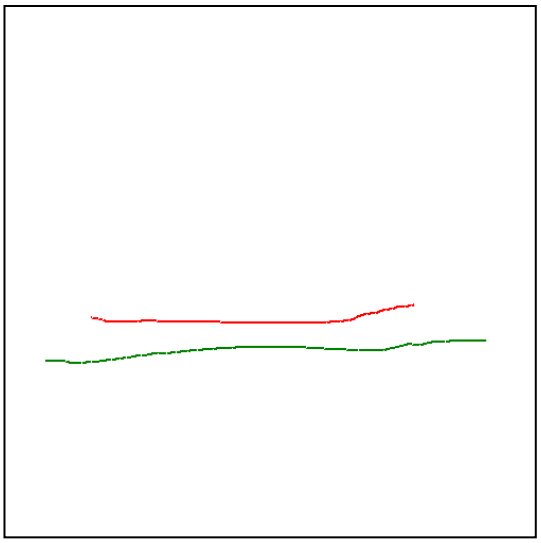

Figure 3-20: Yellow train data before and after distortion correction

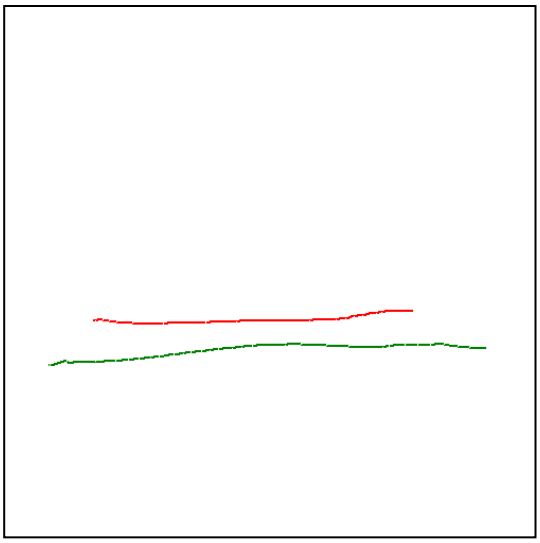

Figure 3-21: Blue train data before and after distortion correction

The plots show that curvature is removed from the trajectories; however the lack of straight line in the corrected trajectories suggests that the distortion correction algorithm is over correcting in this case. It is difficult to produce a general measure of detector distortion without repeating the distortion experiments for each detector in use. The motivation for using the detectors is that they are readily deployable in real world situations. For this reason the usefulness of the distortion correction on a larger scale is confirmed by Expert analysis of live trajectory data. This analysis has been performed by honours project students Graham Wilkinson and Stewart Pavitt of Napier University. They found the correction algorithm to provide a generally good estimation for the distortion present in the data they observed and collected. It is however noted that the best value of alpha varies from detector to detector. As there are several factors affecting distortion between different detectors of the same type, such as differences in lens aberrations and in detector construction, no further examination of the exact distortions is conducted. This experimentation is not intended as a quantitative measurement of distortion but to provide a reasonable approximation for use later on in this thesis and in other work.

3.5 Summary

This chapter examines the IRISYS people counter (detector) product in detail. It presents a significant body of information about the construction of the detector. It then examines the information available from the detector. This examination highlights that there is a robust and unknown tracker algorithm running on the detector which detects and tracks elliptical shapes representing pedestrians as they walk past the detector. The tracker provides a trajectory measurement with sub pixel accuracy. It is believed to have similarities to the ACE algorithm presented by Cameron [83]; however exact details are unavailable.

The ability of the tracker to collect trajectory data is examined with two different experiments. The first demonstrates that it is possible to collect different trajectories from people walking along two lines separated by 50cm. The second demonstrates that a much higher accuracy can be obtained using an inanimate thermal emitter. It is possible to see a clear difference in the trajectories when the paths followed are separated by 5cm. It is clear from the data collected that there is distortion in the trajectories measured by the detectors. This is examined in data from one detector and

an approximation is developed to correct for this distortion. While this approximation is sufficient for most pedestrian tracking applications (for example the studies presented in [1, 5]), it is further addressed in chapters 6 and 7.

It is noted that the distortion varies from one detector to another. The motivation for using the detectors is their ability to produce trajectory measurements with minimal set up and characterisation so no further characterisation is attempted. The next chapter examines the use of the detectors in stereo.

4 Stereo experiments

Several researchers have used stereo vision to aid detection and tracking of pedestrians in visible image processing systems, for example [79-81]. Brown *et al* [74] states that the problems of global stereo correspondence are still not well understood. While the problems of matching a single point in stereo images are well understood if the point can be assumed to be close in both images, they are not when that assumption cannot be made. A significant advantage could be gained by obtaining displacement information for the scene. The IRISYS detectors are downward-facing; therefore displacement information should correspond to the height of the pedestrian. If obtained reliably, this information could readily be used in security or human identification applications.

The IRISYS detectors have several disadvantages and some advantages over visible imagers when considered for stereo use. Section 3.4 highlights and investigates optical distortions and aberrations in the detector. These effects can have an impact on the location of a detected thermal image so it may be hard or impossible to use the stereo parallax effect to measure height. Section 3.1.5 introduces the elliptical tracker used to obtain the trajectory information. The exact implementation of the tracker is unknown and may have an adverse affect on stereo use of the detector trajectory information. The main advantage of using the detectors over standard stereo vision techniques, is the potential solution to global correspondence problems highlighted by Brown *et al* [74]. This problem can be overcome as people are easily noticeable in the field of view and the background is less complicated than in visible imaging.

This chapter investigates the use of ceiling mounted detector trajectory measurements in stereo for measuring the height of passing pedestrians. More specifically, it investigates if any useful measure of height for a passing pedestrian can be obtained using the generalised distortion correction algorithm described in chapter 3. It examines data from detector pairs with different distances of separation to investigate which proves the most appropriate.

4.1 Stereo theory depth perception theory

Stereo imaging and depth perception theory is introduced in section 2.5 of the literature review. The theory of using the differences in location of the objects to gain depth perception is based on the triangulation as shown in Figure 4-1. As the detectors have low resolution it will be necessary to use sub-pixel accuracy information for this. Psarakis *et al* [76] present a paper on stereo correlation with sub-pixel accuracy showing that it is possible to leverage some advantage with sub-pixel location. However, it is far from clear that it will work with the detectors' trajectory data. This section examines the theory necessary to calculate displacement information from the detector trajectories.

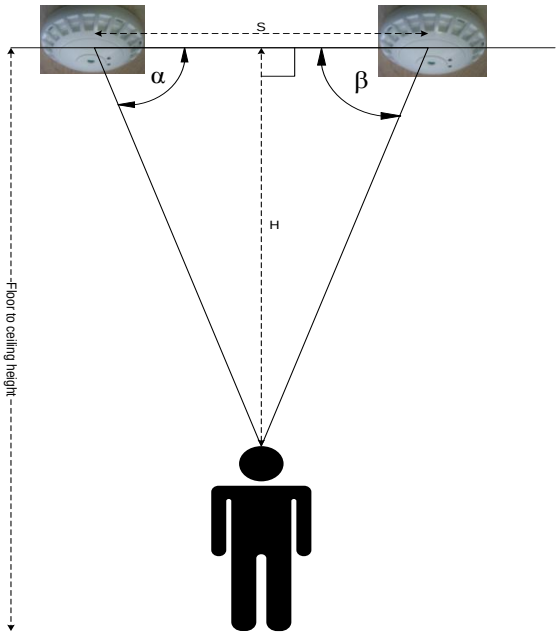

Figure 4-1: Stereo depth perception

The trajectory measurements are presented as Cartesian Coordinates, which require to be converted into angles. This is a simple process, providing we know the field of view for the detector and make some assumptions. According to the manufacturers the detectors are supplied with a 60^{o} field of view. The assumptions we require to make are that: the trajectory measurements are a fair representation of the pedestrian's head, and the Cartesian measurements are taken when the pedestrian passes under a virtual line between the detectors. The first assumption may or may not be true; the exact nature of the tracker algorithm is unknown, therefore it is not possible to confirm that this assumption holds. The results presented later should go some way to answering this question. The second assumption may be addressed by only using the x

coordinate when the pedestrian is under the virtual line between the detectors, as described by the measured y coordinate.

Equation 4-1 describes how to convert the Cartesian x coordinates from the detectors into the left and right angles measured in radians, as required to calculate the distance from the ceiling to the pedestrian. This is based on the aforementioned assumptions and derived from Figure 4-1.

$$\alpha = \pi/2 - \tan^{-1}\left[(x-12.5)/(12.5/\tan(Angle))\right]$$
$$\beta = \pi/2 - \tan^{-1}\left[(12.5-x)/(12.5/\tan(Angle))\right]$$

Equation 4-1: Angle calculation formula

For all the calculations, the x and y coordinates obtained from the detectors are corrected for barrel distortion, shifted and scaled to be in the range of 0 to 25, with the centre point of the detectors' field of view at x=12.5, y=12.5; these are later referred to as adjusted pixel units.

The values of alpha and beta allow calculation of the distance from the detectors using triangulation to resolve stereo parallax effect described in Section 2.5.1 and shown in Equation 4-2: The variable *Angle* denotes the angle of view for the detector in the horizontal plain.

$$h = (\sin\alpha/(\sin(\pi-\alpha-\beta)/d)).\sin\beta$$

Where d is the separation distance of the detectors and h is the distance from the ceiling to the person's head measured in adjusted pixel units.

Equation 4-2: Distance calculation

4.1.1 Stereo correspondence

Stereo correspondence is a well known problem when extracting depth information from stereo vision. According to Brown *et al* [74] the solutions to local correspondence are well understood but those of global correspondence are not. In chapter 3 it is noted that there are substantial optical aberrations and thermal crosstalk in the detector array. Furthermore, it is noted that these aberrations vary from detector to detector. The time-consuming task of quantifying the aberrations of each detector

individually is not warranted. Given that the exact tracker algorithm is unknown it is unclear if doing so would produce sufficient trajectory measurement accuracy to yield useful results. For these reasons the approach chosen is to use a large distance of separation, when compared to those typically used in stereo vision systems. By using a large angle, an error such as that caused by previously noted aberrations will have a proportionally lower effect on the result.

This approach will introduce some additional complications and place a much heavier weighting on the assumption that the measured trajectory follows the head of the participant. Further, it assumes that the weighted centroid of the tracker corresponds to a similar part of the head irrespective of view-point, a major global stereo correspondence problem.

4.2 Experimental set up

The entrance to the Library at Napier University's Merchiston campus was chosen as the experimental location. The entrance is a wide and open hall with a flat carpeted floor and no obstructions limit the movement of people within the measurement area. To help examine what the most appropriate separation distance is, three different detectors are mounted in the ceiling in a straight line. This provides three different stereo pairs, each with different separation distances. The participants were asked to repeat the walks under the detectors several times providing more data so that measurement noise can be reduced by averaging.

Figure 4-2 shows the detectors in the ceiling of the entrance to the university library. Detectors one and two were one hundred and twenty cm apart, detectors two and three were sixty cm apart. This allowed the construction of stereo pairs where the separation was either sixty, one hundred and twenty or one hundred and eighty cm. The detectors were mounted at 3.85 m above the floor.

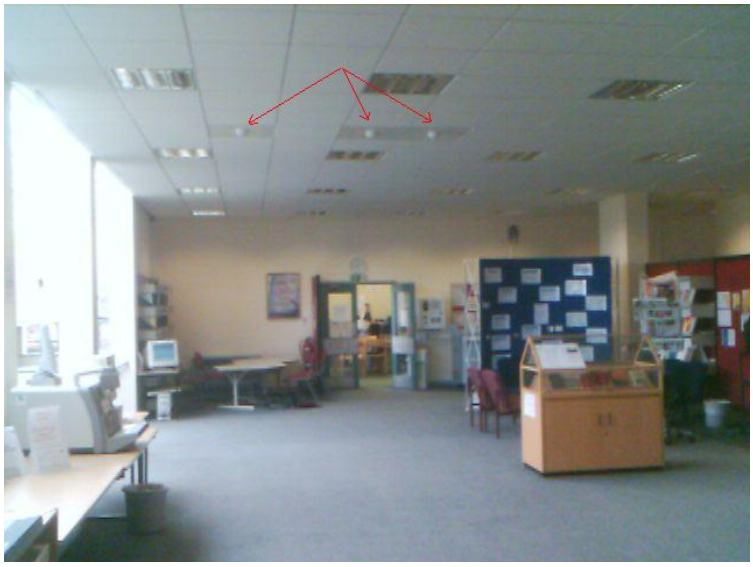

Figure 4-2: Picture of library entrance

Seventeen participants were asked to walk under the detectors. Their heights were also measured with a tape at the same time. None of the participants had any obvious walking abnormalities. This data was complimented by data from another inanimate thermal emitter (a hot water bottle) that was dragged along the floor using a long tether.

4.3 Results

This section presents the results from the experiments. It starts by examining the calculated height with the actual height of the participants. It then examines the distance calculated from the detectors to the participant as they walk through the field of view. Finally, it examines the data from the thermal emitter.

4.3.1 Calculated v actual height of participants

Using the Equation 4-2 and the field of view angle of $\frac{60}{\sqrt{2}} = 43^o$, the distance between the ceiling and each participant was calculated as they walked under the detectors. This was then subtracted from the known height of the detectors (385cm) to produce the calculated height. To reduce noise the Cartesian coordinates (both x and y) were subjected to a low pass filter as described in Equation 3-1.

$$v_i = \frac{v_{i-1}}{4} + \frac{v_i}{2} + \frac{v_{i+1}}{4}$$

Equation 4-3: Low pass filter

Figure 4-3, Figure 4-4 and Figure 4-5 show plots of the calculated height v actual height of the participants, using the detectors separated by 60, 120 and 180cm respectively. To remove any biasing from the participants that provided a larger number of readings, three values are plotted for each: max, min and mean measured (by triangulation) height with respect to actual height.

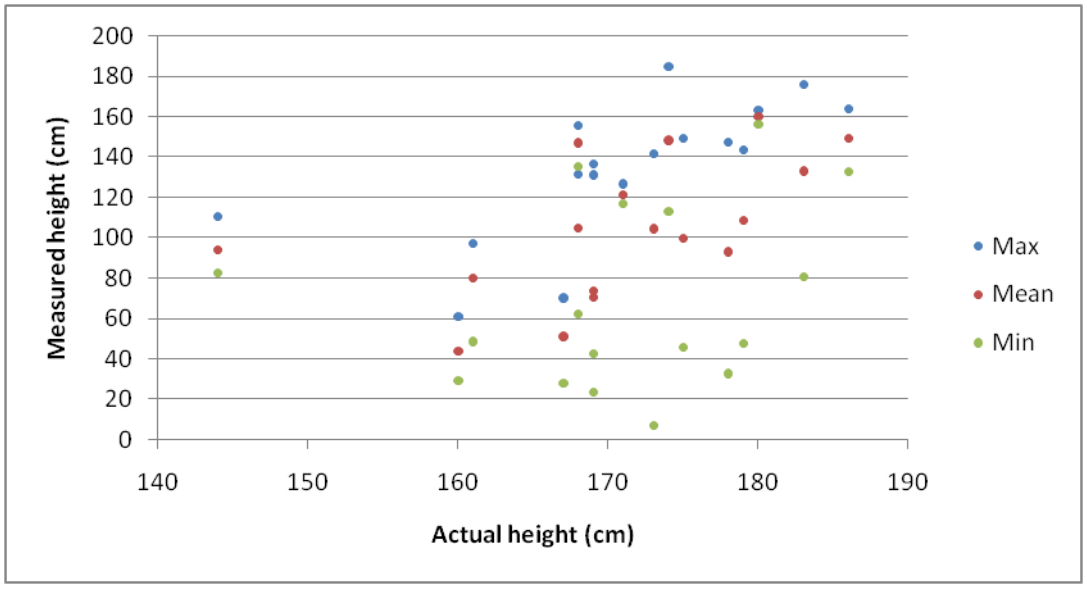

Figure 4-3: Measured v actual, detectors separated by 60cm

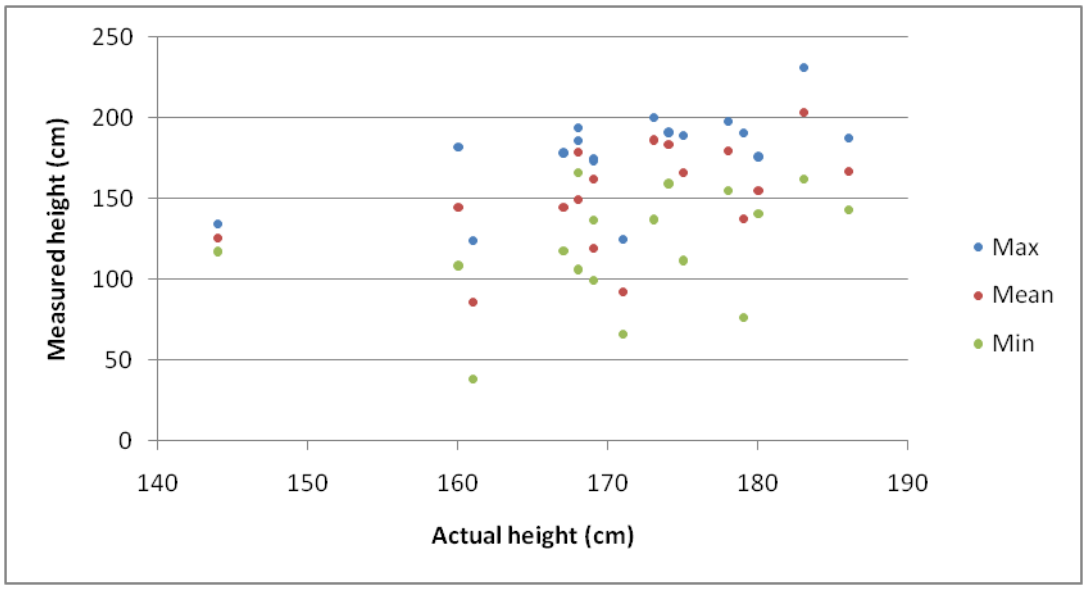

Figure 4-4: Measured v actual, detectors separated by 120cm

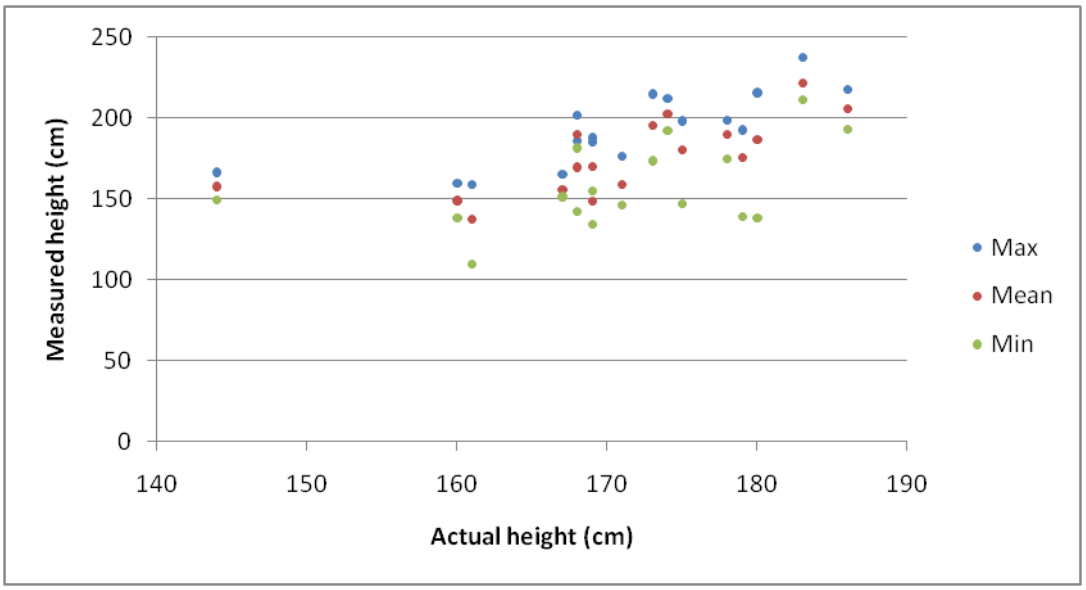

Figure 4-5: Measured v actual, detectors separated by 180cm

Figure 4-3 shows the data from the detector pairs separated by 60cm. This data has a wide spread between max and min values, later referred to as grouping. This indicates that the height measure obtained for an individual is not repeatable and consistent. The grouping improves when data from the detector pairs with larger separation distances is examined. It is clear that the data with the best grouping is from the detector pair separated by 180cm. This indicates that the larger separation distances provide more consistent measurement results.

These results (Figure 4-3, Figure 4-4 Figure 4-5) show that there is a significant variation in the measure obtained. Assuming that the relationship between calculated and actual height is linear, it can be quantified by using least squares linear regression. Figure 4-6 shows the same data plotted in Figure 4-5, but this time plotted with a trend line fitted to the mean readings using the least squares method.

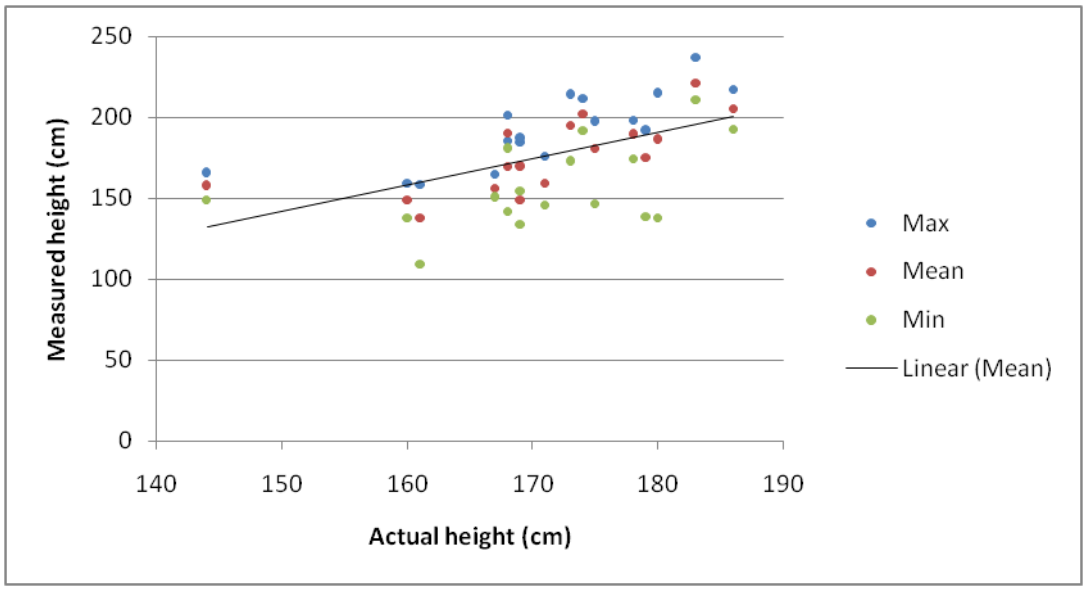

Figure 4-6: Calculated v actual, 180cm separation with trend line

Figure 4-6 shows that there is a general relationship between the calculated heights and the actual heights of the participants. Table 4-1 shows the gradients and coefficients of determination (also known as r^2) for trend lines fitted to all three sets of data using the least squares method.

Detector separation	180cm	120cm	60cm
Gradient	1.634	1.648	1.889
Coefficient of determination	0.501	0.256	0.290

Table 4-1: Trend line data

The data from the detector pairs separated by 180cm is correlated in a statistical sense. However a correlation of 0.501 is not sufficient to suggest that an average measure could be used to determine the height of a person. Given that this result proves disappointing, a further examination of the data collected is conducted in the next sub-section.

4.3.2 Calculated distance v time

This subsection presents the calculated distance from the ceiling to the pedestrian with respect to time. As the participant walks past the detectors the actual distance from the detectors to head varies due to gait and location. Typical recordings from three of the experiment's participants are examined. The data is plotted with respect to time from each of the detector pairs as the participants moved through the detection area. As

each participant walks under the detector the distance from their head to the detector will change, both with location and gait. To help represent the change due to location the expected distance is also plotted. This is calculated from the measured y coordinate and known height of the participant using Equation 4-4 with the angle of 43^{o}.

$$d = h / \cos\left(\pi / 2 - \tan^{-1}\left[abs(y - 12.5) / (12.5 / \tan(Angle))\right]\right)$$

Where d is the expected distance, h is the known height of the pedestrian and y is the measured y coordinate.

Equation 4-4: Expected distance

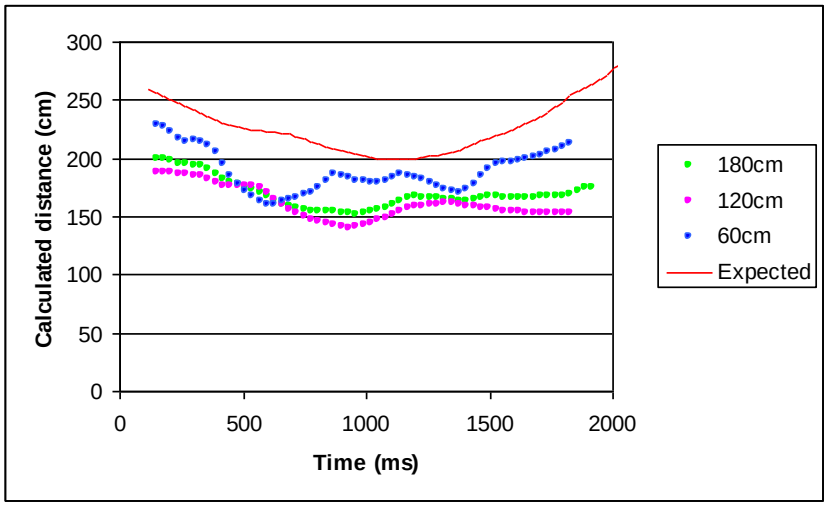

Figure 4-7: Graph of calculated height v time, person 1

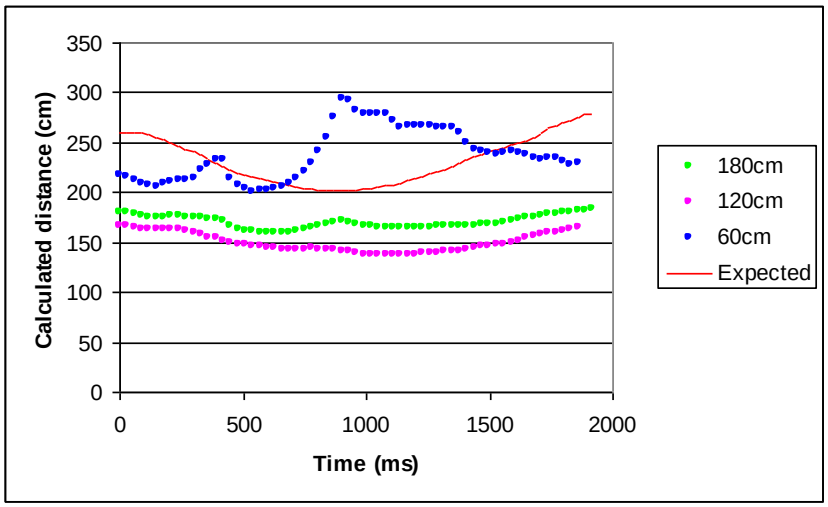

Figure 4-8: Graph of calculated height v time, person 2

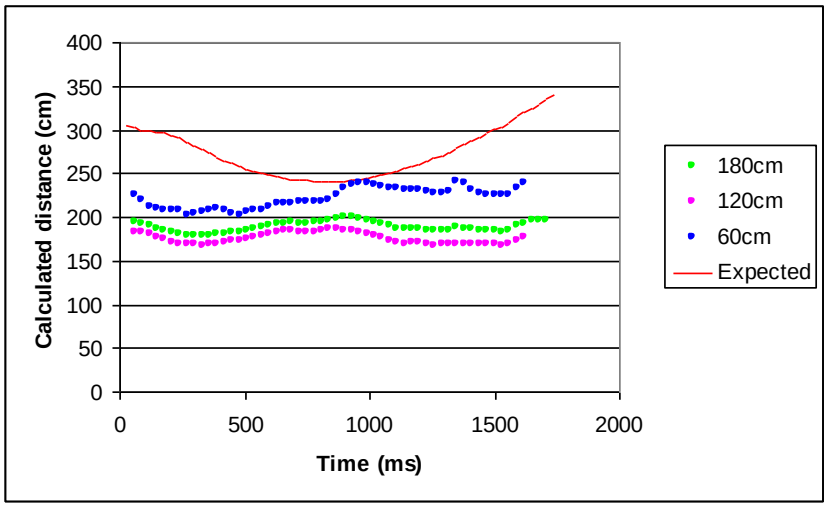

Figure 4-9: Graph of calculated height v time, person 3

The data presented in the above figures show several interesting facts about the data and method used. Firstly, the data from the detectors separated by 60cm shows an oscillation at a frequency consistent with human bipedal locomotion, approximately (1.5Hz). Examination of the remaining data indicates that this is present in most of the data collected. Secondly, the results from the detectors with spacing of 120 and 180 cm, generally produced larger calculated distances than the measurements from the detectors separated by 60cm. Thirdly, the results typically show a curve similar to that found in the expected distance. It is not so prominent in Figure 4-9 as it is in Figure 4-7 or Figure 4-8.

4.3.3 Data from thermal emitter

During the experimentation data was collected using an inanimate thermal emitter (a hot water bottle) moved along the floor at ground level. The possible complications caused by each detector having a different perspective of the participant (an example of a global correspondence issue) are effectively eliminated with this experiment as the hot water bottle is flat. In addition any variations caused by the inherent non-uniformity of human posture are also not present in this data. Figure 4-10 shows a similar plot as presented in Figure 4-7, but with data from the hot water bottle.

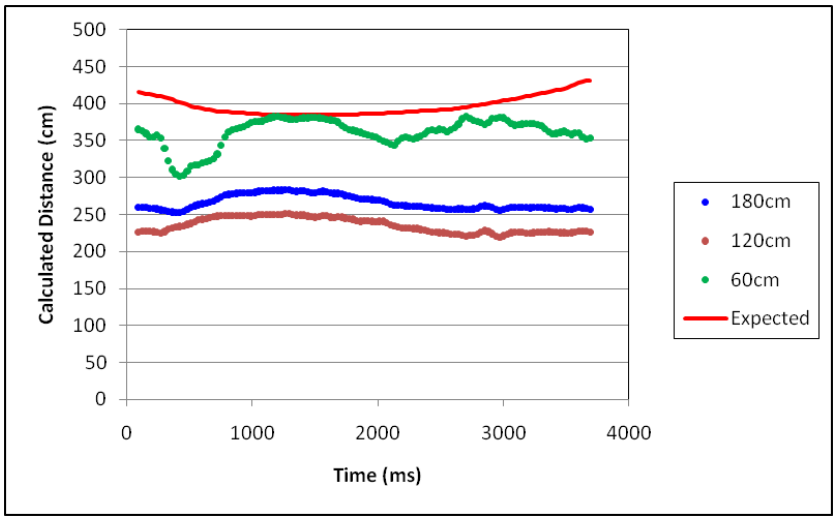

Figure 4-10: Graph of calculated height v time, hot water bottle

As noticed in the data collected from participants, the data from the detector pair separated by 60cm shows less consistency in measurement. There is also a lack of the expected curve in the distance data.

Table 4-2 shows the height measurement calculated from six repetitions of data capture from the hot water bottle. The height measurements were calculated using Equation 4-2 and the standard deviation for the measurements from each detector pair is appended to Table 4-2.

Detector seperation	180cm	120 cm	60cm
Reading 1	329.4	349.2	402.1
Reading 2	353.2	348.2	505.5
Reading 3	314.5	334.1	385.5
Reading 4	335.7	344	453.4
Reading 5	368.5	360.1	570.7
Reading 6	366.7	354.4	588.2
Standard devation	21.7	8.9	85

Table 4-2: Height measurements from hot water bottle

These results show several things about the height measurement method. Firstly it is clear that the distance measurements are not sufficiently consistent to act as a useful height measurement. Given that the hot water bottle used to generate the measurements is essentially a two dimensional inanimate object, the standard deviation of these results provides an indication of the measurement technique's lack of consistency. In theory, the main unknown global correspondence issue in this system

(that of view-point differences for object) should be minimal or non-existent. The high standard deviation for distance measurements from the detectors separated by 60cm indicates that some other unknown factor is strongly influencing the measure in that pair. The standard deviations for the detector pairs separated by 120 and 180 cm are in-keeping with the expectations based on the results presented in the sub-pixel accuracy trajectories presented in section 3.3.2. An error of 5cm at a height of 1.5m as is present in the work described in section 3.3.2 equates to an angular error of 1.9^{o}. As there are two detectors used for triangulation, this error must be doubled to 3.8^{o} which provides a height difference of approx 25cm with a detector separation of 180cm and approx 20cm with a detector separation of 120cm.

4.4 Conclusions

This chapter presents experiments and results examining the use of the detectors' trajectory measurements in stereo pairs for non intrusive pedestrian height measurement. The experiments are designed to replicate as closely as possible a typical installation for the IRISYS people counter so as to maintain the applied focus of this research. The data collected shows unimpressive results for the measurement of height using the target centroid. Several factors are assumed to affect this but the lack of repeatable measurements in the data from the hot water bottle effectively eliminates the technique's use as a system for measuring the height of passing pedestrians.

The data collected from the detectors separated by 180cm presents a correlation between the average height measurement and that of the participants, indicating that height plays a significant part in the measure obtained and that the larger distance of stereo separation has helped. However the data is not strongly correlated and significant variation in multiple measurements obtained from individuals, exist. There are several factors affecting the measurement distance from ceiling to object and significant further work would be required to properly understand the reasons for the technique's failings. The exact nature of optical aberrations for each individual detector would need to be further examined; use of the tracker algorithm in the detectors would require to be changed to a publicly available algorithm so its impact on the measure could be quantified. Both of the aforementioned investigations are out with the scope of this thesis which builds on an established people tracking system

that seeks to develop new algorthiums which can be deployed without significant calibration requirements.

The data presented in section 4.3.1 shows a slight correlation between the calculated height measurement and actual height of the participants. This indicates that there is some height information in the measure but this information is dwarfed by other factors. The data presented in section 4.3.3 highlights that even with an inanimate two dimensional object; the technique is not capable of producing a consistent height measurement. At best the measurements are accurate to within ±10cm. However this result is not replicated on data from people.

The results presented in this chapter have ruled out the use of the detectors' trajectory measurements for accurate stereo depth perception.

5 Stride measurement experiment

During the experiments presented in chapters 3, and 4, an oscillation of walking frequency was noticed in several of the trajectories collected. This oscillation was believed to originate from human gait but the data presented is not conclusive. This chapter further investigates the source of this oscillation and attempts to correlate it to bipedal locomotion of human walking. It describes the experiments conducted, and results collected, to further examine the source of this oscillation. First it describes the experimental design and data collection. Then it describes the background to the analysis performed, the results, and conclusions from the experiments.

5.1 Experiment design and data collection

The experiments were conducted in the same location used for the stereo depth perception experiments, the entrance to the university library. As with the experiments discussed in section 4.2, three detectors were located in the ceiling. This provided three sets of data from each pedestrian walk, allowing some replication of the results. The questions these experiments are designed to answer are:

- What is the source of oscillation noted in previous data?
- Are the detectors sensitive enough to measure the location of the footsteps taken by a pedestrian in the field of view?

5.1.1 Design

For this series of experiments, eight markers were placed on the floor separated by 55cm. The markers were placed in a straight line, starting and finishing outside the detectors' field of view. Figure 5-1 illustrates the experimental set up. This diagram shows all of the detectors and their expected field of view. It also shows eight markers depicting the expected position of the pedestrian's footsteps. The connecting line and arrow describe the participant's direction of motion.

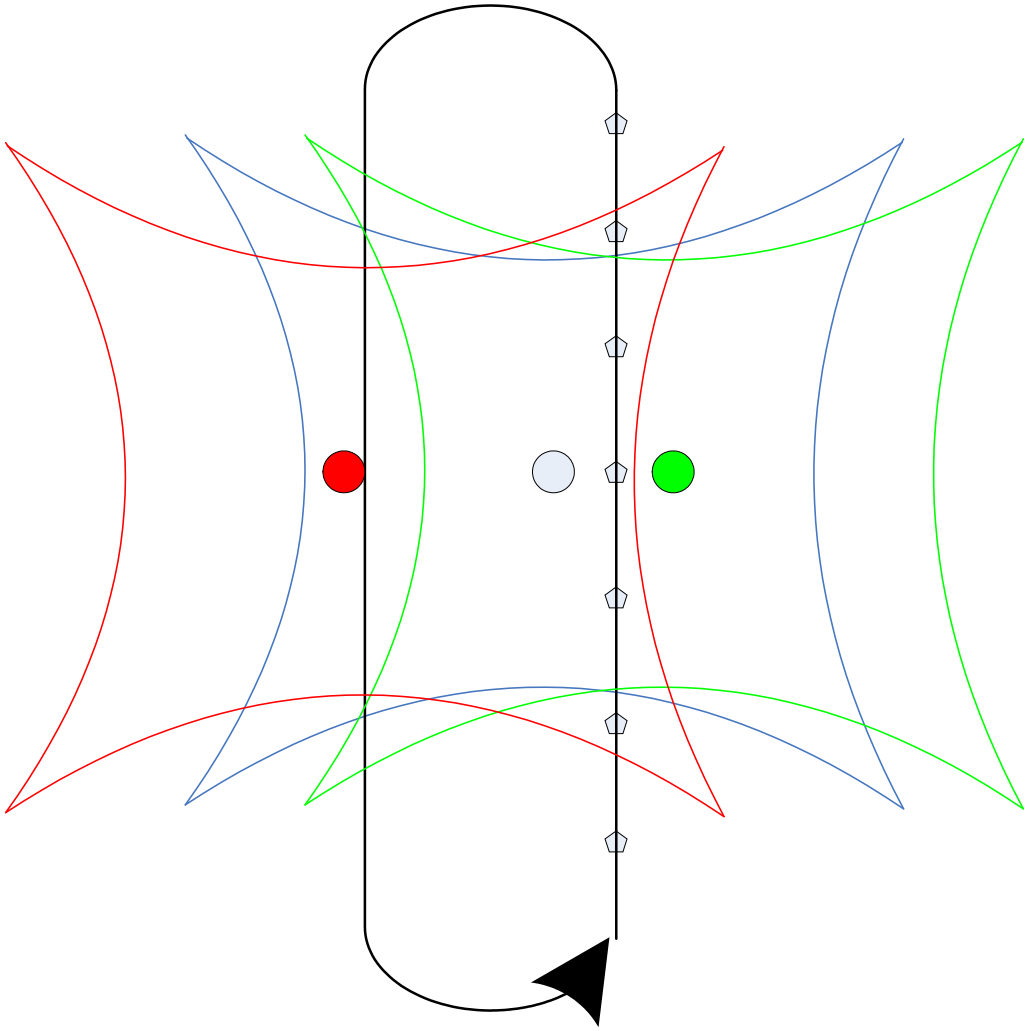

Figure 5-1: Experiment diagram

This setup in many respects emulates the "drunk test" used by some police forces to test coordination of drivers.

5.1.2 Data collection

As with the experiments described in chapter 4 the data was collected and recorded for off-line analysis. Each participant was asked to walk, placing their foot as close to the floor markers as possible. As the participants started walking a note was taken of which foot they placed on the first marker. The experiment was conducted in one day during which seven people took part. All but one of the participants was different from those that took part in the stereo experiments described in chapter 4.

5.2 Accounting for direction of motion

The results collected during this experiment come from an environment where the pedestrian motion is controlled. As this would not be the case in a real world situation,

further analysis is required to put the motion in perspective. This section describes the method used for this research.

When attempting to measure the location of footsteps and analyse the left to right motion of pedestrians with respect to the direction of travel, it is necessary to know the direction of travel. The simplest method of establishing this is to perform linear regression to fit a straight line to the points recorded. After a best fit line has been found, the distance from each point to the line can be calculated, thus providing a relative left to right swing for the subject. Figure 5-2 shows an example trajectory with the best fit line drawn.

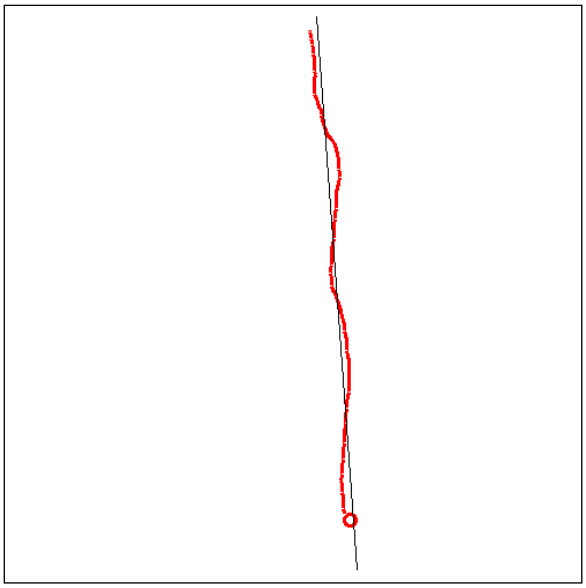

Figure 5-2: Walking trajectory with best fit line

This method works well. However it makes the assumption that the pedestrian is moving in a straight line. In real world situations this is not always the case. However, it can be relied on for all the data collected from the experiments conducted during this and the previous study. Appendix C describes the linear regression method used to establish the best fit line and its parametric description.

5.3 Results

This section presents the results in two different formats. Firstly, the trajectories measured are plotted graphically, showing both multiple recordings from a single participant and single recordings from several participants. Secondly; the left to right

oscillations of the participants are shown after accounting for the direction of travel as described in section 5.3.3.

A low pass filter is mentioned several times in this thesis. This term relates to a filter described by Equation 5-1, where v is the one dimensional array of data and i is the index of the array.

$$v_i = \frac{v_{i-1}}{4} + \frac{v_i}{2} + \frac{v_{i+1}}{4}$$

Equation 5-1: Low pass filter

5.3.1 Single participant

The results presented here show recordings of trajectories taken from four participants. The data from each participant is presented in different figures. Each figure shows several coloured trajectories. Each coloured line represents the measurement from a repetition of the experiment. The circles in the figures represent the start of the trajectory. This information is presented to enable the measurement error noted in section 3.3 to be observed. Before presentation, both the x and y coordinates are processed through a low pass filter.

Figure 5-3 shows four trajectories collected from a male participant, measured from two detectors. They walked placing their feet on the floor markers, starting on the left foot and passed the detectors several times. Figure 5-4 shows trajectories from several passes under a single detector. This was from a male participant, who started on the right foot. The trajectory from each pass is represented by a coloured plot. Both of the figures show clear correlations in the measured trajectories and expected oscillations.

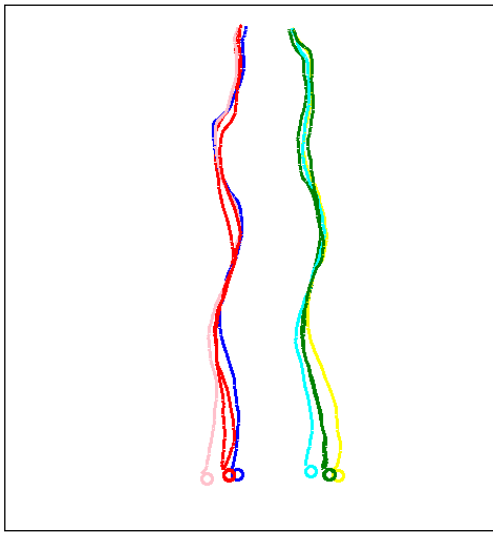

Figure 5-3: Participant A, two detectors

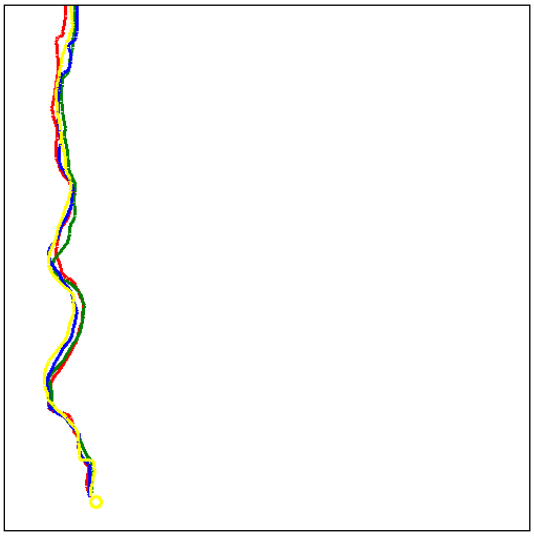

Figure 5-4: Participant B, single detector

Figure 5-4 shows five trajectories that almost identically follow each other. As each trajectory was collected at different times, the result shows that the participant's walk is remarkably similar when controlled by requesting that the participant place their feet on the floor marks. Figure 5-3 shows a similar correlation from four separate walks, it also shows data collected from two different detectors. The track on the left clearly follows the track on the right, thus showing that the detectors are recording the same motion. The vast majority of results confirmed this hypothesis although not all were as clear. Figure 5-5 shows the trajectories from a male participant where the detector to detector correlation is present but less clear. Figure 5-6 shows the trajectories from a female participant, a similar correlation is present but it is harder to see. It should be noted that there is considerably less oscillation in the trajectories of the female participants.

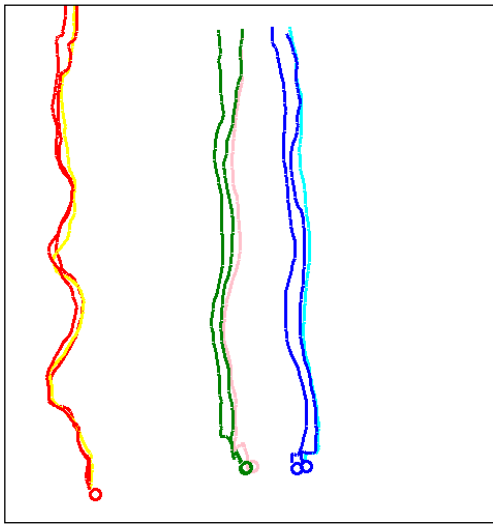

Figure 5-5: Participant C, three detectors

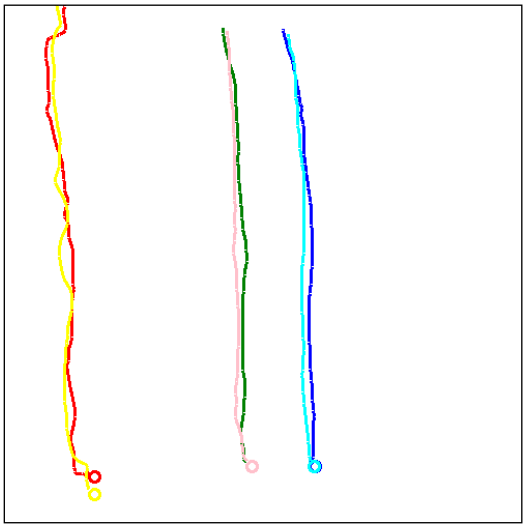

Figure 5-6: Participant D, three detectors

5.3.2 Multiple participants

This subsection presents the trajectories from several participants' walks while following the floor marks. The results are presented in a similar way to the trajectories in section 5.3.1. However each colour in this series represents a different participant.

Figure 5-7 shows the trajectories from three different male participants, Figure 5-8 shows the trajectories from three different female participants.

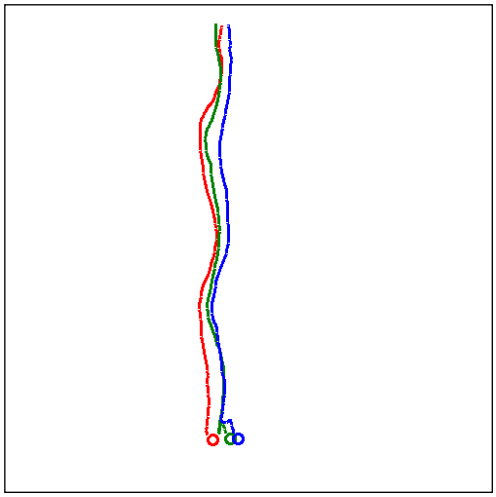

Figure 5-7: Trajectories 3 male participants

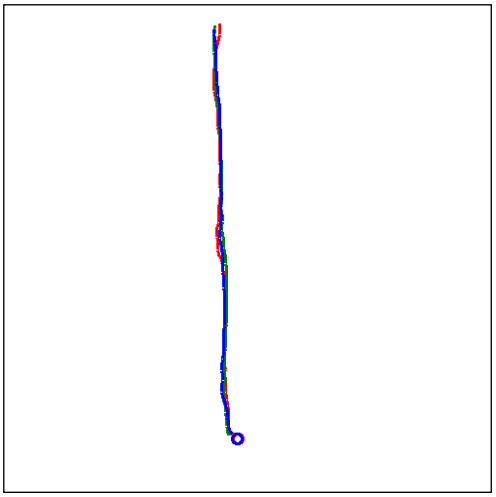

Figure 5-8: Trajectories 3 female participants

It is clear from Figure 5-7 that there is a correlation in the location of the left to right swing from one person to another. Figure 5-8 also shows a strong correlation; however the trajectories are so close, that it is hard to distinguish between them. These results confirm that the source of the previously noted oscillations is gait motion. It also re-affirms the finding from section 5.3.1 that the oscillation noticed in female participants was significantly less than that of male participants.

5.3.3 Left to right swing

This sub-section presents the results when viewed with respect to the participant's direction of motion. The Cartesian coordinates are converted to distances from the best fit line as described in Equation 5-2. These distances are filtered with a low pass filter and then graphically plotted with respect to time.

$$d = \left(\left(x.\cos(\theta) + y.\sin(\theta) \right) - r \right)$$

Equation 5-2: Distance from line

The results ignore the measurements taken from detector zero, shown red in Figure 5-1. When the results from that detector were examined a significant amount of error was found due to the measurements being taken from close to the edge of the detector's field of view. They are also colour-coded to coincide with Figure 5-1 so the data can be related to the detector that collected it.

Figure 5-9 and Figure 5-10 show typical plots from a male participant's walk as recorded by the detectors.

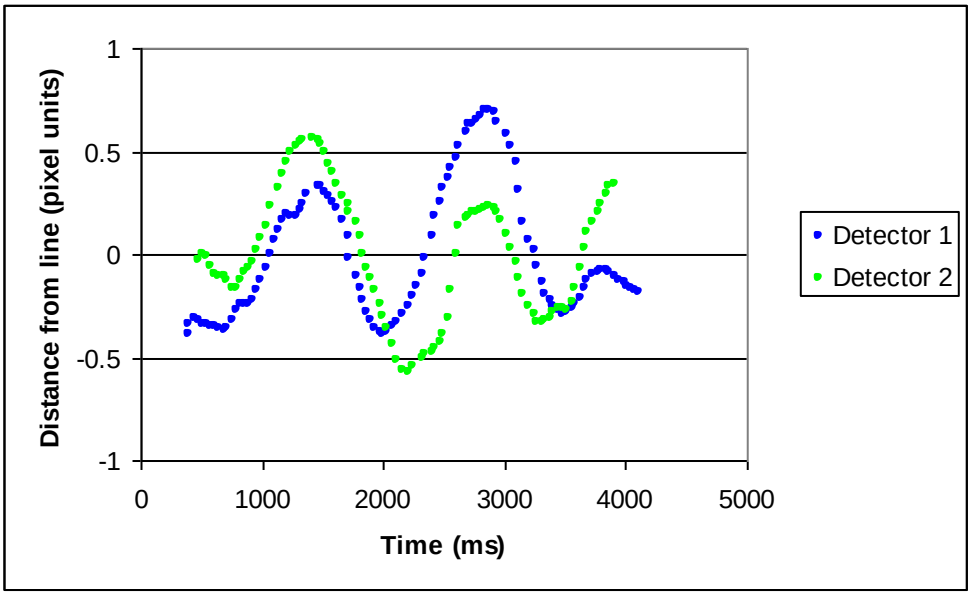

Figure 5-9: Participant A (male), distance v time

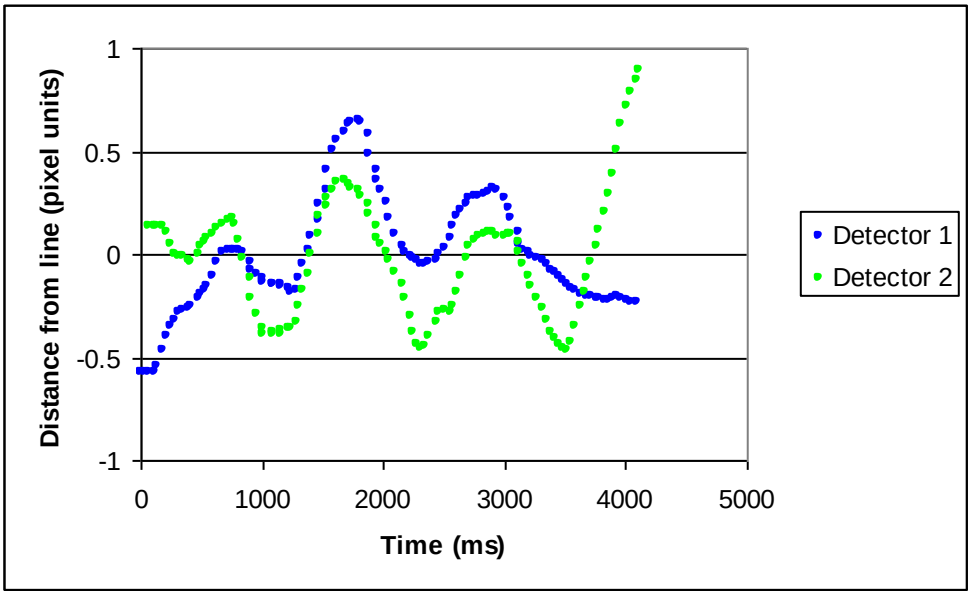

Figure 5-10: Participant B (male), distance v time

Firstly it is clear from the results that there is a distinct left to right oscillation, as found in sections 5.3.1 and 5.3.2. There is also synchronicity with respect to time between the measurements of left to right swing from each detector. As expected, the majority of the data shows reduced synchronicity at the start and end of the plots. This is likely to be caused by the reduction in accuracy of the tracker as people enter and leave the field of view.

Figure 5-11 and Figure 5-12 show typical plots from two different female participants. It should be noted that the scale used in these figures is in the range of -0.5 to 0.5. This is different from the -1 to 1 scale used for the male participants, and enables the oscillation to be more easily seen. The data has connecting lines drawn to help clarify the presentation of results.

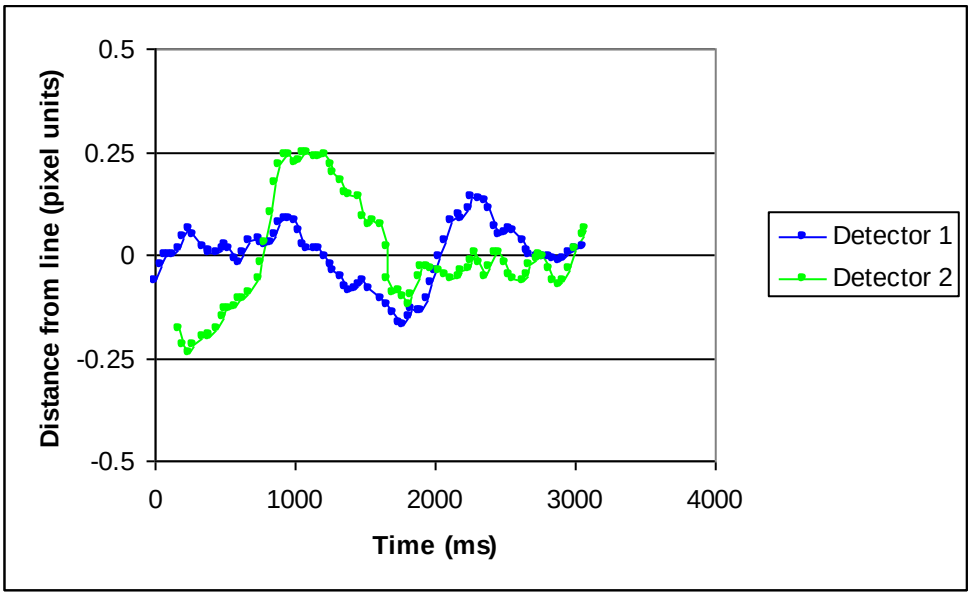

Figure 5-11: Participant D (female), distance v time

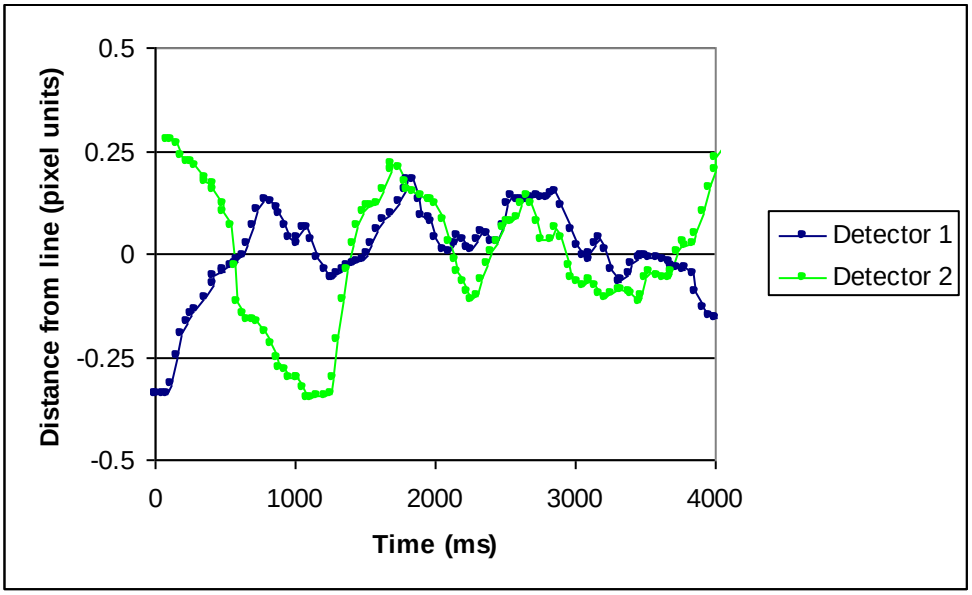

Figure 5-12: Participant E (female), distance v time

The data presented from the female participants shows some synchronicity, however the magnitude of the oscillation is significantly less. The error of measurement is

beginning to introduce some disparity in the synchronicity. Visual inspection of the data presented in Figure 5-12 shows marked synchronicity after 1500ms. However the oscillation just before 1000ms shows a lack of synchronicity.

5.4 Further analysis

This section further examines the results collected during the stride experiments. It starts by quantifying the synchronicity in left to right oscillation measured by two different detectors. After this it examines the magnitude of the oscillations of the different participants. Finally, it counts the number of footsteps each participant took in the field of view.

5.4.1 Quantifying left to right swing synchronisation

Sub-section 5.3.3 presented the left to right swing data for the participants with respect to time. It shows that there is a distinct and clear synchronisation in the measured swing for the male participants. It also shows that the magnitude of the female swing is lower and that the measurement error has an increased effect on this data. This sub-section quantifies the synchronisation by finding correlations in extrema as defined below.

Table 5-1 details the extent of the synchronisation in the data collected during this experiment. It counts the number of major direction changes referred to as extrema that are synchronised and unsynchronised. An extremum is defined as a local maximum or minimum within plus or minus 250ms. An extremum is defined as synchronised if found in data from both detectors within 200ms, provided both changes are in the same direction. These synchronised extrema are later referred to as correlated points. An uncorrelated point is defined as an extremum occurring either, more than 200ms apart, in the opposite direction or in data from only one detector. Counting the number of correlated points was performed automatically by the software developed.

The data at the edge of the detector's field of view is ignored as it is prone to error. All points with an x or y coordinate above 21 or below 4 corrected pixel units, fall into this category. Although it varies from trajectory to trajectory, this generally results in approximately the first and last half second of data being ignored.

Participant	Gender	Walk No	Correlated	Uncorrelated
A	M	1	4	0
A	M	2	4	0
A	M	3	3	0
A	M	4	2	1
A	M	5	3	0
A	M	6	2	2
A	M	7	2	1
A	M	8	3	0
B	M	1	3	1
B	M	2	3	1
B	M	3	3	0
B	M	4	3	1
B	M	5	3	0
B	M	6	3	0
B	M	7	3	0
B	M	8	4	0
C	M	1	4	0
C	M	2	2	2
C	M	3	4	1
C	M	4	3	2
C	M	5	4	0
C	M	6	4	0
D	F	1	1	4
D	F	2	1	0
D	F	3	2	1
D	F	4	3	1
D	F	5	2	0
E	F	1	4	1
E	F	2	5	0
E	F	3	1	0
E	F	4	2	1
F	F	1	3	1
F	F	2	1	0
F	F	3	3	2
F	F	4	1	0
F	F	5	3	2
F	F	6	2	0
G	F	1	4	1
G	F	2	1	1
G	F	3	2	1
G	F	4	2	0

Table 5-1: Left to right swing correlations

The results presented in this table show that 80% of the 140 footsteps measured show correlations. The results also confirm the earlier finding that the extent of the correlation is lower in the female participants than the male. 85% of the male participants' footsteps were correlated whereas only 72% of the female footsteps were correlated.

5.4.2 Quantifying the magnitude of walking oscillations

Sub-section 5.3.2 noted that the magnitude of left to right oscillation was significantly lower in female participants. This sub-section further examines these magnitudes. To quantify the magnitude of the left to right oscillations, the standard deviation from each walk's best fit line is examined. This is referred to as the oscillation magnitude. Table 5-2 shows the average oscillation magnitude from each participant and the standard deviation from the mean for each participant.

Participant	Gender	Average oscillation magnitude	Standard deviation from the mean
A	M	0.319	0.133
B	M	0.430	0.257
C	M	0.301	0.151
D	F	0.234	0.159
E	F	0.260	0.138
F	F	0.269	0.149
G	F	0.192	0.083

Table 5-2: Oscillation magnitudes

These results show the same phenomenon noted in section 5.3.2. The female participants generally had lower oscillation magnitudes than the male participants. Although there are a substantial number of different walks past the detectors there are only seven participants. It is not therefore possible to draw definitive conclusions regarding the measurement of gender from this data. Chapter 6 further develops the oscillation magnitude as a measure and examines its relationship to gender.

5.4.3 Counting footsteps

Sub section 5.4.1 describes a method for extracting the locations of footsteps and correlates them from one sensor to the other. The data shows good correlation in the measurement of extrema as previously defined. These extrema correspond to the time the pedestrian placed their foot on the floor. Table 5-3 shows the number of footsteps and the number of extrema counted each time participant A walked passed the detectors. It shows the direction of travel, the number of footsteps calculated and the number of footsteps counted. The direction of travel indicates whether the participants were placing their feet on the floor markers. In the forward direction they were placing the feet on the markers and they were not in the backward direction. The

counted number of footsteps was manually established by viewing the left to right swing data and counting any major changes in direction.

Sensor No	Walk No	Direction	Calculated no extrema	Counted no footsteps
1	1	f	4	4
2	1	f	5	5
1	2	f	3	5
2	2	f	5	5
1	3	f	4	5
2	3	f	5	5
1	4	f	4	5
2	4	f	3	5
1	5	f	4	5
2	5	f	4	5
1	6	b	1	2
2	6	b	3	4
1	7	b	2	4
2	7	b	7	7

Table 5-3: Participants A footstep counts

As expected, the number of footsteps counted in the left to right swing data is five, in $9/10^{ths}$ of the forward motion walks. As the participant walked by placing their feet on the floor markers, the number of footsteps should be the same in all data in the forward direction. When the data from all participants is examined 48 of the 58 forward direction walks showed five footsteps. Half of the forward direction walks not showing five footsteps came from one female participant. This confirms that the number of footsteps in the detector's field of view can normally be counted using this technique.

The number of extrema calculated using the automated algorithm shows a close similarity to that counted manually, but it is not identical. There are two factors that cause the differences. Firstly, it is possible for a person viewing the data to better distinguish between valid and invalid extrema at the edge of the field of view. The automatic counting algorithm makes no attempt to consider this data. Secondly, the person counting the footsteps can identify major changes of direction that are not extrema. This demonstrates the potential for improving the algorithm for detection of footsteps from the data. Chapter 7 further examines different algorithms for extracting the number of footsteps and cadence from the data.

5.5 Conclusions

The experiments detailed in this chapter set out to establish the answers to two questions. Firstly; what is the source of a previously noticed oscillation? Secondly; is it possible to measure the locations of individual footsteps? The results presented show that the source of the oscillation is the left to right swing of human gait and that it is normally possible to measure the location of a person's footsteps using IRISYS people counters. This is a new discovery that the manufacturers were unaware of (*pers com* David Clayson, Managing Director, IRISYS Aug 2006).

Sections 5.3.1 and 5.3.2 graphically presents typical trajectories measured during the experiments. They show an obvious oscillation in the participant's motion. The change in direction noticed in the data correlate in location to the floor mark that the participants were asked to place their feet on. This applies to both multiple measurements of a single person and to measurements from different people. The footstep locations are similar for both multiple recordings from each participant and recordings from multiple participants. The data demonstrates that there is clear and measurable oscillation and that it originates from gait motion. Chapters 6 and 7 further develop algorithms for measuring and utilising this gait information.

Section 5.3.3 presented a sample of the left to right gait motion with respect to time. It shows the data as measured simultaneously from two detectors. This confirms that it is possible to extract the left to right gait motion from pedestrians. This data is further analysed in section 5.4 to establish the accuracy of the footstep measurement technique. It found that in more than 80% of measurements it was possible to find the location of a pedestrian's footstep. It is further noted that it may be possible to improve the automatic algorithm used for extracting footstep locations.

It was noted that the magnitude of the left to right gait motion from female participants was lower than that from male participants. While the data presented in this chapter is inconclusive, it tends to support the view that the trajectory centroid is heavily weighted towards the head and upper body of the participant. Mather & Murdoch made the following statement: "*Studies of human locomotion have found that male and female walkers differ in terms of lateral body sway, with males tending to swing their shoulders from side to side more, and females tending to swing their hips more than*

their shoulders." [86]. Chapter 6 further examines the oscillation magnitude and tests its relationship to gender.

6 Oscillation magnitude measure

Chapter 5 described the development of an algorithm to measure the magnitude of left to right oscillation as pedestrians pass the detector. This chapter further examines this measure and its potential uses. The results presented in section 5.4.2 suggest that the female participants had noticeably lower left to right oscillation magnitude than the male participants, as might be expected given the assumption that the tracker mostly follows the head and upper body motion. The ability to automatically measure the gender of a pedestrian is of significant interest to market researchers. If the measure is found to be individualistic, it could provide a useful input for human identification system. This chapter investigates whether it is possible to use this information for both gender detection and discrimination between individuals.

Firstly the measure is examined to determine if the gender of an individual can be established and if not, whether the information can be used to help inform a human identification system or establish an accurate measure of proportions of male and females passing the detectors. The experiments conducted, results analysed, and the development and validation of a gender distribution algorithm are presented here.

6.1 Calculating the measure

Calculating the oscillation magnitude measure is a two stage process. First the general direction of travel is ascertained by fitting an equation. Then the standard deviation of distance from the measured trajectory to the fitted equation is calculated.

During chapter 3 barrel distortion found in the detectors was examined and a correction algorithm was proposed. It is noted that this algorithm, while providing a generally good solution, is imperfect as distortion is inconsistent from detector to detector. To limit the effect of this, the algorithm proposed fits a polynomial to the trajectory data allowing an easy representation of the general measured motion of the pedestrian. Given that some trajectories have only three footsteps in the meaningful field of view, a second order polynomial is selected to reduce the chances of over fitting. Before finding the polynomial, linear regression is performed on the data as described in appendix C and the gradient of this line is used to decide whether

Equation 6-1 or Equation 6-2 is best suited to minimise the error of fitting to two dimensional data, with error in both dimensions.

$$y = ax^2 + bx + c$$

Equation 6-1: Rotation of Polynomial 1

$$x = ay^2 + by + c$$

Equation 6-2: Rotation of Polynomial 2

The distance of each point from this polynomial is then calculated (for Equation 6-1 the y distance, for Equation 6-2 the x distance) the root mean square of these values is calculated to provide an oscillation magnitude measure. This provides a good measure of the magnitude of left to right swing of the pedestrian, providing they do not sharply change direction while inside the field of view.

6.2 Experimentation

Two different sets of experimental data were collected to develop and validate the gender detection algorithm. The first was collected at Napier University's Merchiston Library. The second was collected at Infrared Integrated Systems (IRISYS) office in Swan Valley, Northampton. At these two locations, two different sets of data are collected, providing four datasets; firstly, choreographed data where participants were asked to walk under the detector and secondly data capture sessions were arranged in the environment's normal every day usage. The first capture style provides predictable data which can easily be used to develop the algorithm. The second provides valuable real world datasets, to help validate the algorithm developed.

6.2.1 Data collected at Napier University library

The data collection installation at Napier University's Merchiston campus library, described in Section 4.2 (stereo experiments), was used to collect data. In this installation the detectors were mounted at a height of 3.85m. For the first dataset five females and three males were asked to repeatedly walk under the detectors at separate times and measurements were taken. This provided seventy two recordings of males and forty eight of females. This dataset was combined with data collected at the same location, as described during chapters 4 and 5. The resulting dataset contains 166 recordings collected from eleven males and 166 recordings collected from eleven

females. Data collected from ten of the females and nine of the males can be linked to the individual. The genders of the people producing the remaining readings are known but which reading relates to which individual is not. This dataset is later termed choreographed data as all the people were knowingly participating in the experiment.

In addition, data was recorded in the library's normal usage, over thirty minutes. An observer counted the numbers of males and females passing the detectors, and the time of any people passing whom the detectors failed to track. During this time sixty one people passed the detector of whom twenty four were female, thirty six male and one who was not properly tracked. Tracking problems are common to all automatic people tracking equipment. Each person was recorded by two different detectors providing 120 measurements. This dataset is referred to as validation data.

The choreographed and validation datasets were collected using more than one detector. In chapters 3 and 4 it was noted that some difference existed between the detectors. However it is unclear what, if any, effect these differences will have on the oscillation magnitude measure. Section 6.3 of this chapter further examines this point.

6.2.2 Data collected at IRISYS

The data collection at IRISYS took place in a narrow corridor running down the centre of an open plan office. A single detector was located 3.2 meters above the ground, with the corridor running down the centre of the detector's field of view. For collection of the choreographed data, ten different participants, five male and five female, took part. Each participant was asked to repeatedly walk under the detector, providing at least ten measurements from each person. This is later referred to as choreographed data.

To validate the algorithm developed using this data, a full day of data capture was performed in the same location. A video camera was installed with a good view of the measurement location so that gender of each person walking by could be ascertained during analysis. The people passing by were doing so in the course of their normal daily work routine. While there was clear signage indicating that recording was taking place, several people did not notice it. They were therefore unaware that measurements were being taken.

6.3 Factors affecting the oscillation magnitude measure

During chapter 4 some variance between detectors was noted, particularly in connection to barrel distortion. While fitting a polynomial should overcome the majority of barrel distortion present, there may be other factors providing variance from one detector to another. This section investigates what, if any, difference can be found in the oscillation magnitude obtained from each of the three detectors used at Napier University. This is not intended to show that there is no variance in the trajectory measurement between different products from the same detector model, but that oscillation magnitude measure is not affected. It then examines whether the location of the participant within the field of view has an impact on the oscillation magnitude measure.

6.3.1 Examining the differences between detectors

This sub-section, explores if there is significant variance in the oscillation magnitude between detectors. To do this, measurements from five people are analysed using single factor analyses of variance with 95% confidence. This effectively shows whether there is a significant difference between the measures from the individual detectors. The data is taken from the choreographed dataset collected at Napier University. Table 6-1 shows the analysis of variance results of from six of the participants, the data used can be found appendix D.

Gender	Person	Degrees of freedom within groups	Variance detected
M	A	18	No
M	B	24	No
M	C	18	No
F	J	18	No
F	K	27	No
F	R	18	No

Table 6-1: Detector variance results

This table shows that in the data from six people, no variance is attributable to the detector that captured the data. To further support the hypothesis that the measure is not dependent on the detector, single factor analysis of variance was performed on data from all the participants, grouped by detector. This demonstrated that no variance existed between detectors when analysed to 95% confidence. Failing to show that a

significant variance exists does not prove (in a statistical sense) that there is not one; it does however provide a very compelling argument to support the hypothesis. For these reasons, the assertion is made that the measure is not affected by the detector from which it originates.

6.3.2 Examining path taken

This sub-section examines what effect the location of the trajectory, within in the field of view, has on the measure obtained. Figure 6-1 shows trajectories of four passes by person A, all taken near the centre of the field of view. Figure 6-2 shows the trajectories of two different passes near the edge of the field of view. For this analysis, that dataset collected at Napier University is used.

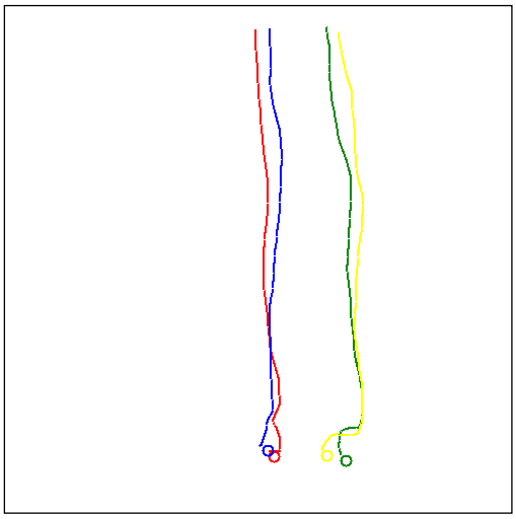

Figure 6-1: Sample trajectories from centre field of view

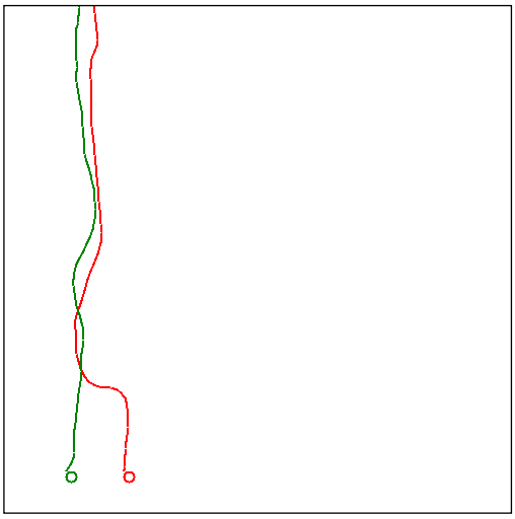

Figure 6-2: Sample trajectories near edge of field of view

When the data is examined it is clear that a significantly larger oscillation is noted at the edge of the field of view. Three factors are believed to contribute to this edge effect. The first of these is barrel distortion, which was investigated in section 3.4 of this thesis. Secondly, when a person is walking at the edge of the field of view some, but not all, of the person is out with the field of view. This could significantly affect the tracker's centroid location and therefore the measure. Thirdly, the view of a person at the edge of the field of view will be different from that in the centre. In the centre, a complete top down view is achieved; at the edge of the field of view much more of the side of the person will be visible. The barrel distortion is unlikely to have a significant effect on the oscillation magnitude measure due to fitting a second order polynomial to

account for direction of motion. However, the differing view point and partial occlusion will almost certainly impact the measure. For these reasons, trajectory measurements where the centre of the trajectory is less than 4 or greater than 21 after correction for barrel distortion are excluded from the trajectory data for calculating the oscillation magnitude measure.

6.3.3 Summary

This section has examined the oscillation magnitude measure with a view to determining if there is any difference in the measurement between detectors. No variation has been found. Based on this is it the author's opinion that the oscillation magnitude measure is not significantly affected by detector variation. A difference has been noted in the measure when the trajectory tracks the edge of the field of view. This confirms the findings in chapter 5 and a system for excluding measures likely to be adversely affected is proposed.

6.4 Choreographed data results

The introduction to this chapter presents two major questions. Firstly, can the oscillation magnitude be used to determine the gender of people passing under the detector? Secondly, can this measure be used to determine the distribution of male and females that pass under the detector? This section examines the results from the choreographed data, with a view to answering the above questions.

6.4.1 Data collected at Napier University

The full results from the choreographed experiment are shown in Table 13-1 in appendix D. Table 6-2 shows a summary of the data collected from the nineteen participants.

Groups	*Count*	*Sum*	*Average*	*Variance*
Person A (male)	14	1.438	0.103	0.007
Person B (male)	14	1.211	0.087	0.022
Person C (male)	14	1.279	0.091	0.006
Person D (male)	14	1.039	0.074	0.006
Person E (male)	14	1.476	0.105	0.005
Person F (male)	14	1.336	0.095	0.005
Person G (male)	14	2.876	0.205	0.043
Person H (male)	14	1.217	0.087	0.009
Person I (male)	14	2.338	0.167	0.016
Person J (female)	14	0.506	0.036	0.001
Person K (female)	14	0.658	0.047	0.002
Person L (female)	14	0.685	0.049	0.003
Person M (female)	14	0.603	0.043	0.001
Person N (female)	14	0.544	0.039	0.001
Person O (female)	14	0.447	0.032	0.001
Person P (female)	14	0.426	0.030	0.001
Person Q (female)	14	0.549	0.039	0.002
Person R (female)	14	0.971	0.069	0.005
Person S (female)	14	1.039	0.074	0.011

Table 6-2: Summary of Oscillation magnitudes from Napier Data

It is possible to establish whether the oscillation magnitude measure is linked to the individual by performing single factor analysis of variance. The results presented in Table 6-3 shows the results from this analysis when performed to a confidence interval of 0.01 (99%).

Source of Variation	*SS*	*df*	*MS*	*F*	*P-value*	*F crit*
Between Groups	0.5384	18	0.0299	3.8915	0.0000	2.0080
Within Groups	1.8984	247	0.0077			
Total	2.4368	265				

Table 6-3: Analysis of variance, Napier data oscillation magnitudes

This result establishes that the measure stems from an individualistic factor and can therefore contribute to the identification of an individual. However the variances shown in Table 6-2 and Table 6-3 demonstrate that there is significant overlap between individuals. The value of SS within groups is higher than between groups, indicating that the variance in the measure of oscillation magnitude from a single person is higher than the variance of the mean between groups. Therefore while the oscillation magnitude can contribute to identification, it alone will not be sufficient to identify an individual.

To clarify the relationship between the measure and gender, the data is split into two groups, male and female. On examination of this data we can see that a noticeable difference exists in the means of each gender. Table 6-4 shows the results of a two sample t-test assuming unequal variance with a confidence interval of 0.01.

t-Test: Two-Sample Assuming Unequal Variances		
	Male	*Female*
Mean	0.115	0.049
Variance	0.013	0.003
Observations	166	166
Hypothesized Mean Difference	0	
df	243	
t Stat	6.631	
P(T<=t) one-tail	0.000	
t Critical one-tail	2.342	
P(T<=t) two-tail	0.000	
t Critical two-tail	2.596	

Table 6-4: Gender t-test results, Napier Data, oscillation magnitude

The value of t Stat is larger than that of t Critical thus demonstrating to 99% certainty that the difference in the mean readings from male and females is not random. The corollary of this is that the oscillation magnitude provides a significant indication of the gender of the participant. Figure 6-3 shows a histogram of the data from the Napier dataset, containing 166 reading for both males and females.

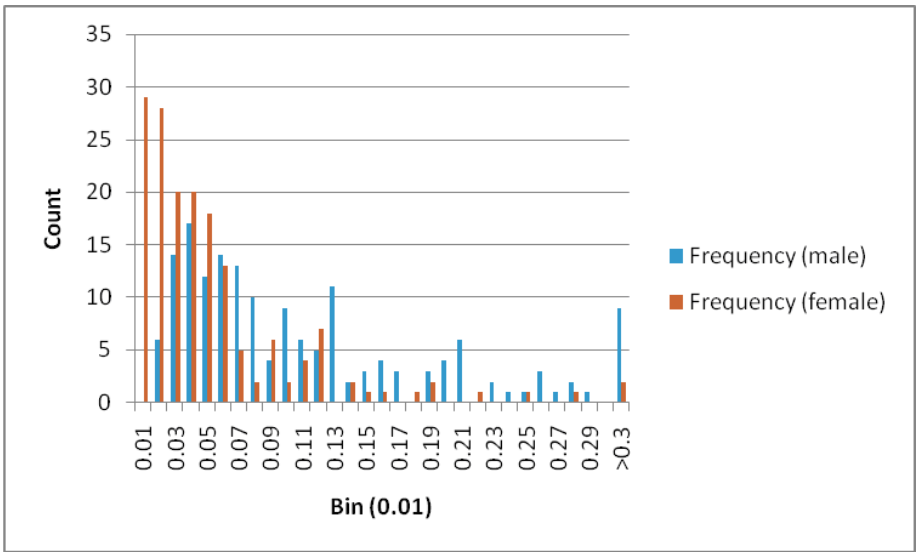

Figure 6-3: Histogram of Napier gender data

6.4.2 Data collected at IRISYS

The full results from this experiment are shown in appendix D. Table 6-5 shows a summary of this data. It should be noted that none of the participants in this data set took part in the experiments at Napier University. This data does not include any measures considered to be erroneous, as described in section 6.3, as none of the measurements taken in this location were near the edge of the field of view.

SUMMARY				
Groups	*Count*	*Sum*	*Average*	*Variance*
Person A (male)	10	0.7607	0.0761	0.000310
Person B (male)	10	0.3140	0.0314	0.000113
Person C (male)	10	0.2674	0.0267	0.000119
Person D (male)	10	0.3452	0.0345	0.000675
Person E (male)	10	0.2912	0.0291	0.000510
Person F (female)	10	0.2438	0.0244	0.000109
Person G (female)	10	0.1296	0.0130	0.000052
Person H (female)	10	0.1051	0.0105	0.000048
Person I (female)	10	0.3399	0.0340	0.000125
Person J (female)	10	0.0824	0.0082	0.000013

Table 6-5: Average of IRISYS results

It is possible to show whether the oscillation magnitude is linked to the individual in this data by performing single factor analysis of variance. The results presented in Table 6-6 show to a 99% confidence that the results found stem from an individualistic factor.

Source of Variation	*SS*	*df*	*MS*	*F*	*P-value*	*F crit*
Between Groups	0.0333	9	0.0037	17.8598	0.0000	2.6109
Within Groups	0.0187	90	0.0002			
Total	0.0520	99				

Table 6-6: Analysis of variance for IRISYS results

The variances shown in Table 6-5 and Table 6-6 demonstrate that there is significant overlap in the data between individuals as is found in the results from the Napier dataset. This shows that, while the measure is influenced by the individual, it is not possible to identify the individual solely by this measure. By splitting the data into two different groups, male and female, we can see that a more significant difference

exists in the means of each group. Table 6-7 shows the results of a two sample t-test assuming unequal variance with a confidence of 99%.

	Male	*Female*
Mean	0.0396	0.0180
Variance	0.0007	0.0002
Observations	50	50
Hypothesized Mean Difference	0	
df	71.0	
t Stat	5.3095	
P(T<=t) one-tail	0	
t Critical one-tail	2.3800	
P(T<=t) two-tail	0	
t Critical two-tail	2.6469	

Table 6-7: Gender T-Test results, IRISYS Data

This analysis proves that we can be 99% sure that the difference in the means between males and females, is not random. Figure 6-4 shows a histogram of the data from male and female participants.

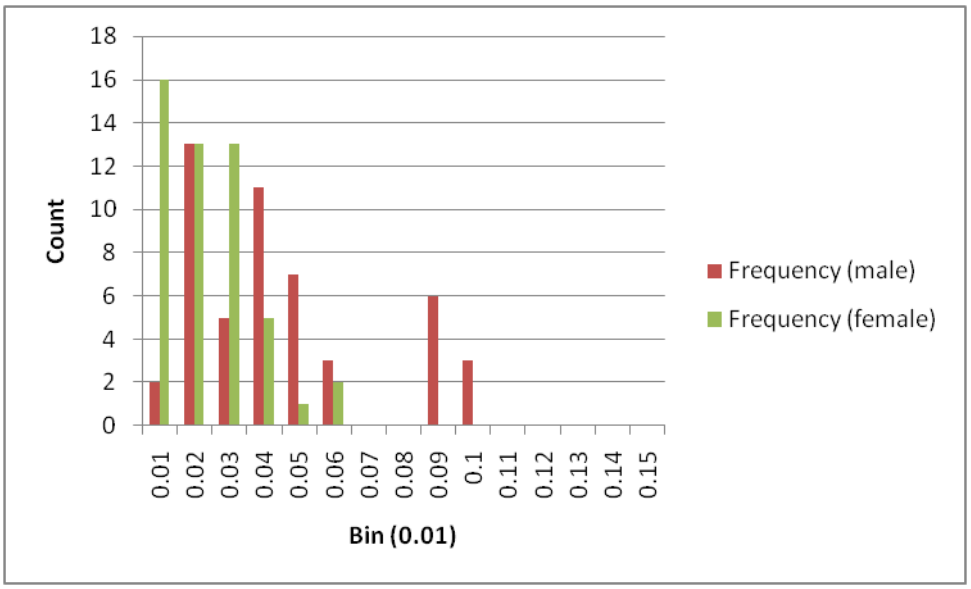

Figure 6-4: Oscillation magnitude gender histogram IRISYS Data

This histogram shows graphically the difference in the measure between the genders. This is slightly easier to see when the histogram data is filtered (using Equation 4-3) and plotted as a line graph as shown in Figure 6-5. It should be noted that the filtering applied assumes that there is a finite linear distribution of noise in the measure.

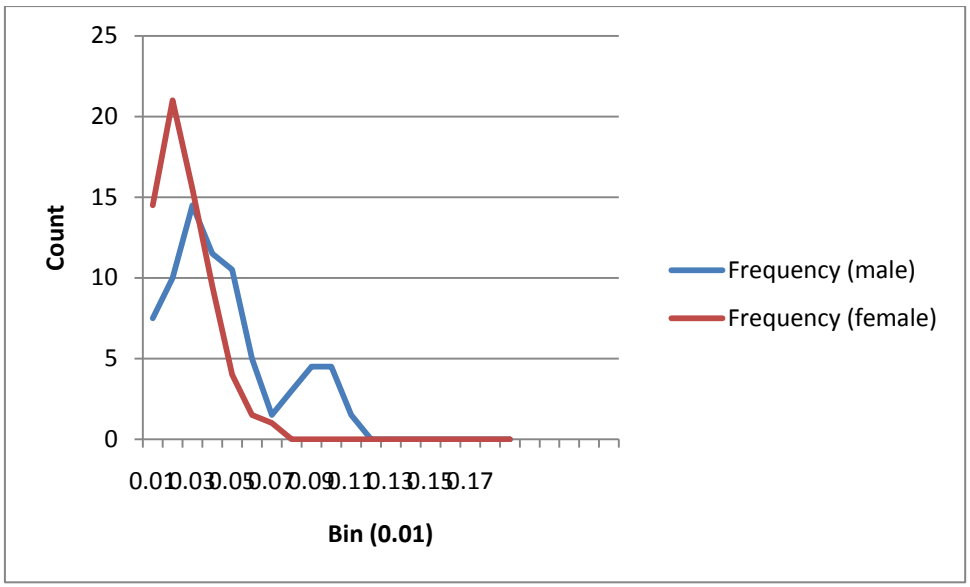

Figure 6-5: Filtered line graph representation of Histogram IRISYS Data

The results presented in this sub-section confirm those in the Napier Data. It is noted that the absolute values in this dataset differ from those in the Napier dataset. The author believes that the different mounting heights of the detector largely account for this difference.

6.4.3 Summary

This section has presented the results and analyses from the two different choreographed datasets, the first collected at Napier University, the second collected at IRISYS. Based on these results it is clear that the oscillation magnitude measure developed is strongly influenced by the individual to which it relates. There is however significant overlap and variance in the measure. This effectively rules out the use of this measure as a sole identifiable feature; however it could be used as an input to a stochastic human gait ID model such as that proposed by Wagg and Nixon [61]. A significant difference in the absolute measures from the two different experimental locations is noted; this is believed to originate for the varying mounting height. As there is only data from two different mounting heights it is not possible to accurately quantify the relationship between the mounting height and the measure of oscillation magnitude.

The results of the t-tests on both the IRISYS and Napier Data show with 99% certainty that gender plays a significant part in the measure. Therefore it is fair to conclude that

a measurable quantity, highly correlated to gender exists, in this data. There is overlap in the measure, so it is not possible to establish the gender of an individual pedestrian. There is however sufficient information to establish the distribution of genders in a population, purely from the oscillation magnitude measure. The next section proceeds to test this point, and to investigate the accuracy of the measure's ability to correctly determine the distribution of genders in validation datasets.

6.5 Gender validation results

The choreographed results have shown that the oscillation magnitude measure developed is influenced slightly by the individual and strongly by the gender of the participant. In theory, establishing the distribution of genders in any population should be simple. The mean oscillation magnitude from any population should lie between the means for males and females. Further, the ratio between the two means for the male and female should be equivalent to the ratios of each gender in the population. Equation 6-3 shows this calculation.

$$male\% = 100\left(\frac{o - mf}{mm - mf}\right)$$

Where o = mean oscillation magnitude from population
mm = mean measure from male only data
mf = mean measure from female only data

Equation 6-3: Gender distribution equation

This is based on the assumption that the people taking part in this experiment are a fair representation of any population being examined; i.e. that should the data collection exercise be repeated with a different group of individuals the same mean measure would be found for each gender. It is also assumed; that the fact the subjects were taking part in the experiment did not affect the oscillation magnitude measure obtained an assumption also made by Nixon *et al* [63]. Establishing the first assumption is beyond the scope of this thesis. This section examines the data collected from the validation exercises with a view to clarifying the second assumption and further validating the measure's usefulness in determining gender distributions.

6.5.1 Napier data gender distribution validation results

Section 6.2.1 described the data collection process at Napier University. The second set of validation data was collected as people used the library during the course of their normal activity. While there was clear signage indicating that data was being

collected, most people did not notice it. Therefore they were not generally aware the measurements were being taken.

The space in the library where the measurements took place is a large open entrance lobby, shown previously in Figure 4-2. While people were generally walking past the measurement area, there was no obstruction limiting the direction or motion of the people. They could enter and leave the area from any edge of the field of view. Most however travelled into or out of the library from top edge to bottom edge or vice-versa, walking broadly in a straight line.

Fourteen of the one hundred and twenty measurements were considered to contain insufficient data as they related to trajectories that broadly followed the edge of the field of view. These were removed from the data leaving 106 useful measurements. Table 6-8 shows the mean of the oscillation magnitude measure from the validation dataset and the percentage of males this corresponds to as calculated using Equation 6-3 and the mean for males and females from Table 6-4. The full sets of results are included in appendix D.

Mean	%Males
0.127	118.471

Table 6-8: Napier validation dataset result

It is clear from this result that the mean measurement is greater than that expected for only male participants and the gender distribution algorithm is not yielding a correct result in this dataset. Further examination of the data shows that there several readings where the oscillation magnitude measure is significantly higher than would normally be expected from the data. This is due to the trajectory taken by the person not being well modelled by the second order polynomial fitted, to account for the direction of motion. It is not possible to control the trajectory an individual passing the sensor takes in the Napier library entrance; therefore it is necessary to eliminate any readings where the result is likely to be misleading. This is achieved by removing any readings where the oscillation magnitude measure is greater than three standard deviations above the mean for male participants in the choreographed dataset, shown in Table 6-9.

Stdev	0.114
Mean	0.115
Mean+3*Stdev	0.458

Table 6-9: Napier male choreographed dataset summary

By applying this selection criteria 8 of the 106 readings (7.5%) were deemed to be erroneous and were removed, leaving a recalculated result shown in Table 6-10.

Mean	%Males
0.094	68

Table 6-10: gender distribution results

Given that the actual number of males was 60% and that 22 of the 120 readings were discounted, this result, showing 68% males, demonstrated good potential for use of the oscillation magnitude measure as a system for discerning distribution of genders in the population. The next section further examines the gender distribution algorithm on the IRISYS validation dataset.

6.5.2 IRISYS gender distribution validation results

Section 6.2.2 introduced the data captured at IRISYS to validate the results. This was captured by placing the detector over a corridor in an open plan office. The corridor was approximately one metre wide. A video camera recorded people passing so their gender could be established when the data was analysed. Many of the people walking past did not notice that they were being recorded. Some of these people had taken part in the choreographed experiments at the same location but they accounted for the minority of the data collected. The corridor at the time of recording was used by approximately 30 different people; some contributed to multiple readings some only passed once.

Figure 6-4 shows a histogram of the oscillation magnitude readings from the validation data capture at IRISYS, the full dataset is shown in appendix D. By viewing the video footage of the data it is possible to ascertain the gender of each individual. There were 62 measurements taken, fifty nine from males and three from females. The pattern shown in this data is very similar to the values found from the males in the IRISYS choreographed dataset.

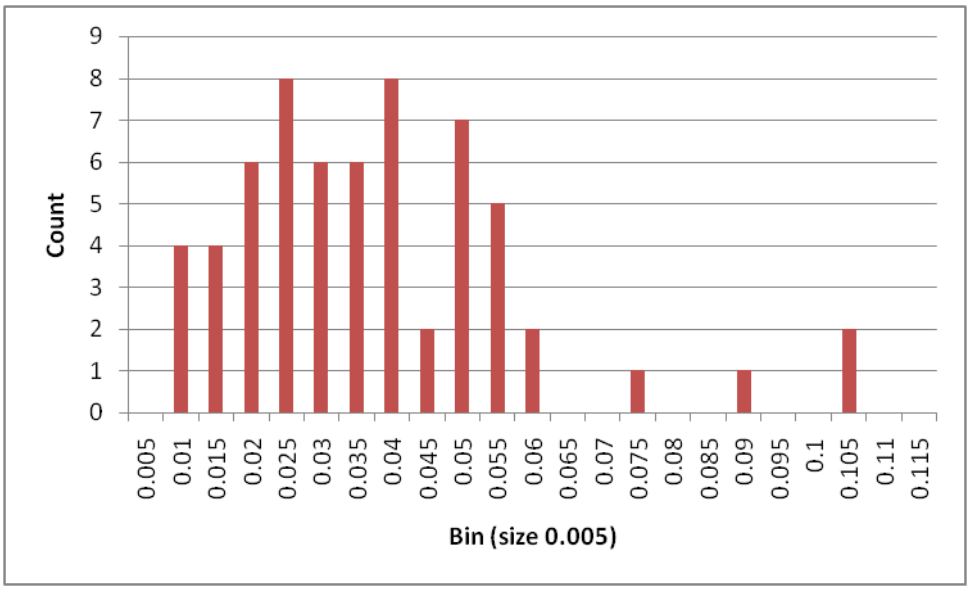

Figure 6-6: Histogram of IRISYS Validation data

The histogram shows that the distribution follows the expected result, based on the choreographed data collection. It is noted that this data does not exhibit any extreme (greater 3 standard deviations above the male mean) readings as were found in the validation data collected at Napier. This is likely to be influenced by the layout of the corridor where that data collection took place. The corridor was narrow at approximately one meter wide, which constrains the trajectory to a straight line. Table 6-11 shows the mean measure obtained and results from the gender distribution Equation 6-3. The values for all male and all female used in the gender distribution equation are taken from Table 6-7.

Mean	% Male
0.035	80

Table 6-11: Gender distribution results IRISYS

This result shows that in the dataset of 62 people the gender distribution has been measured as 80% where as the actual proportion of males in the data is 95%. This result indicates that there is some merit in the algorithm, it is however possible that the fitting of a second order polynomial over fits the trajectory data, reducing the quality of the measure. To understand this better, the analysis is repeated constraining the value of a=0 (the squared term) in Equation 6-1 or Equation 6-2. The IRISYS dataset was captured at a considerably lower height than the Napier dataset; therefore fewer data points are available for each trajectory. This, combined with the knowledge that

the data capture area was narrow, straight and running close to the centre of the detectors optical axis, suggests that better results might be obtained if a straight line is fitted instead of a second order polynomial. Table 6-7 shows the mean results from all measurement in the choreographed dataset, calculated by fitting the straight line to the data. This consisted of all 100 readings, 50 for male and 50 for female. As with the analysis described in section 6.4.2 a student t-test was conducted on the data to a confidence interval of 99% confirming that the difference in the means is statistically significant.

Femal	Male
0.030	0.051

Table 6-12: Mean results IRISYS choreographed data straight line fit

Table 6-13 shows the mean straight line measurement and the proportion of males and females in the dataset calculated using Equation 6-3 and the gender mean values from Table 6-12.

Mean	%Male
0.048	87

Table 6-13: Straight line fit validation dataset results IRISYS dataset

This shows a very impressive results considering that the data actually consisted of 59 males out of 62 people. The improvement in the result presented in Table 6-13 over the results presented in Table 6-11 suggest that fitting a second order polynomial is in this instance over fits the data. The same is not the case with the Napier dataset. Fitting a straight line is better when the data collection is constrained to people walking in a narrow corridor, following a path known to have minimal optical distortion (near the centre of the optical axis and not crossing the field of view diagonally) and with a low mounting height.

6.6 Conclusions

This chapter has presented a study into the extraction of a measure of oscillation magnitude measure based on the findings of chapter 5 and its relationship to the gender of the person from whom it originated. It presents the experiments conducted, both at Napier University and IRISYS. Each experiment consisted of gathering two different datasets, a choreographed set and a validation data set. The choreographed datasets were generated by arranging for a group of individuals to repeatedly walk under the

detector so a known set of measurements could be taken. The validation datasets were collected when the measurement area was being used in its normal every day use. At Napier an observer noted the gender of the people passing by. At IRISYS the data capture also recorded video so the gender of the individual could be determined during analysis.

The choreographed datasets are analysed using both analysis of variance and Student t-test. While the absolute values from Napier and IRISYS differ, both show the same trends, namely that the oscillation magnitude is both individualistic and highly correlated to the participant's gender. The difference in absolute measures is believed to originate primarily from differing mounting heights of the detectors.

Analysis of variance of both choreographed datasets show to 99% certainty that the measure is linked to the individual. There is significant variance and overlap in the measure which means that the measure cannot be solely relied on as a form of identification. However, it could be used to inform a stochastic human ID model, such as a hidden Markov model. Wagg and Nixon [61] produced several different identifying features from their video based human gait analyses; in addition they performed analysis of variance and found that both cadence and parameters relating to head displacement from body were most significant. To provide an indication of how significant each measure is likely to be Wagg and Nixon present two tables in their paper showing the F- Statistic for each measure extracted. The F statistic from analysis of variance conducted on the Napier choreographed dataset is 3.89 and the IRISYS data is 17.85. These are significantly lower than the worst of the measures used by Wagg and Nixon which was 34.92 from the outdoor dataset. From this analysis the results suggest that the measures extracted by Wagg and Nixon were more individualistically discriminative that the oscillation magnitude developed in this research, however the imager perspectives were significantly different.

Analysis of the choreographed data sets, using an un-paired t-test assuming unequal variance, shows to 99% certainty that the difference in the means from each gender is not random. Given the accepted position [86] that the lateral oscillation of the upper body in human locomotion is typically smaller in women than in men, this research establishes that a measure of upper body oscillation can be obtained from the IRISYS

detector trajectory data. Further, this research establishes that it is possible to automatically obtain a measure that is both individualistic and highly correlated to gender. Given the statistical significance of the differences in the mean readings for males and females, determining the distributions of gender in a population, is possible. A gender distribution algorithm is developed and tested on two datasets, with promising results.

This chapter has examined the oscillation magnitude measure and found that it can be used as in input to a human gait model. Further, a gender distribution algorithm has been developed based on the choreographed dataset.

7 Cadence measurement algorithms

The results presented in chapters 5 and 6 shows that some human gait information is available from the IRISYS detectors. Many other researchers have examined stride and cadence looking for individualistic features, including Winter [87], BenAbdelkader *et al* [88] and Wagg & Nixon [61]. As others have presented successful results using cadence measures, this chapter examines whether useful cadence measures can be obtained from the trajectory information.

BenAbdelkader *et al* [65] present a system for estimating three stride parameters from video footage: velocity, cadence and stride length. According to Winter [87] the stride length of a person is dependent on several factors such as stature, age, weight, gender and walking speed. Winter noted that the walking stride distance of an individual is directly proportional to their speed. This essentially indicates that out of the three features BenAbdelkader detected, only cadence is significant for human identification.

This chapter first investigates the algorithms used to account for direction of motion. Following on from this it examines the measurement of cadence using a discrete Fourier transform of the lateral motion data extracted from the trajectory, after accounting for direction of motion. Three different measures are extracted from the Fourier view of the data, the most significant harmonic (cadence), a filtered average cadence and finally an average of all harmonics present.

7.1 Accounting for direction of motion

The work presented in chapter 5 provided a method for extracting the location of footsteps using extrema, after accounting for direction of motion, by fitting a straight line to the trajectory data. This was found to be successful in 80% of footsteps from a limited and controlled dataset; the regression used to fit the straight line is described in appendix C. Chapter 3 investigated barrel distortion found in detectors and noted that the distortion varied from detector to detector. In Chapter 6 a second order polynomial is fitted to trajectory data to account for direction of motion, thus eliminating any problems caused by inaccurate barrel distortion correction, as described in section 6.1. This section examines the two different methods of accounting for direction of motion with a view to selecting the most relevant for extracting a stride measurement.

Figure 7-1 shows a trajectory plot from the Napier dataset; the red line depicts the trajectory data from a subject before correcting for barrel distortion (as described in chapter 3) and the green line, after correction for barrel distortion.

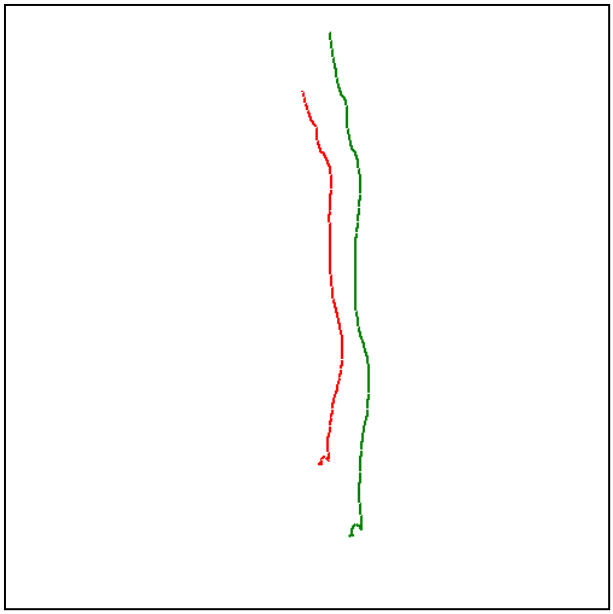

Figure 7-1: Trajectory plot

To the human eye it appears that the green line is a good correction for barrel distortion. However there is still slight uncorrected distortion. The barrel distortion correction algorithm presented in chapter 3, was aimed at a general solution suitable for measuring pedestrian motion such as is presented in [1] but not for detailed analysis of the Napier dataset. Figure 7-2 shows plots of the lateral distances from both the straight line and second order polynomial, plotted in the time domain, from this same trajectory.

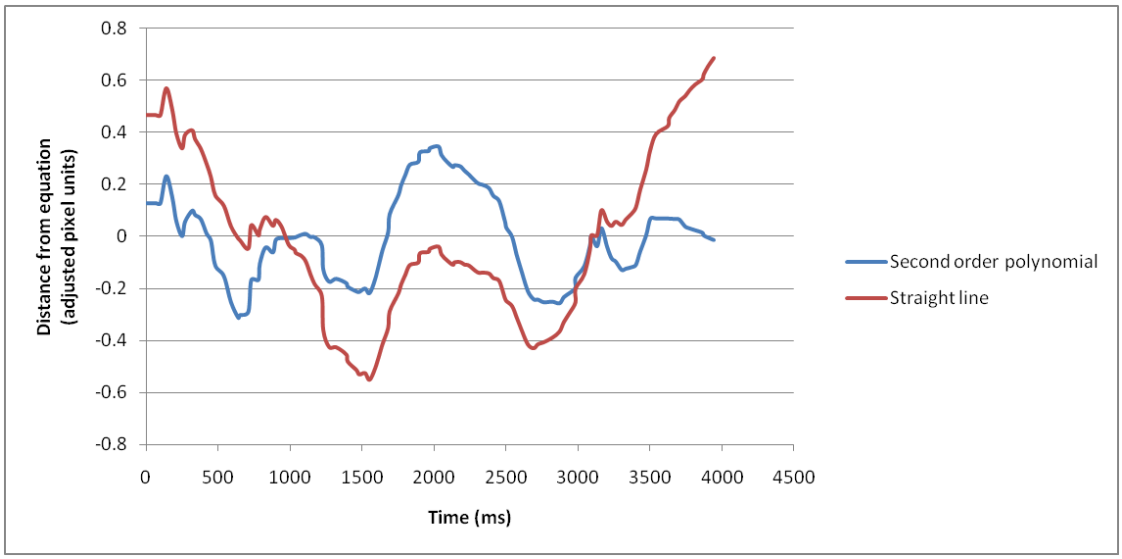

Figure 7-2: lateral distance from direction of motion fit

Figure 7-2 shows that the distance from the second order polynomial, better presents the lateral gait oscillation this research attempts to measure than the distance from the straight line. The results of the IRISYS gender validation dataset presented in section 6.5.2 found that, for the purpose of ascertaining gender distribution, fitting a second order polynomial produces a less accurate result due to over-fitting the data. Further analysis of the IRISYS data set demonstrates that as the mounting height decrease, the number of data points also decrease. This in part explains why the advantage gained by fitting a second order polynomial on the Napier data set is not present in the IRISYS dataset.

The remainder of the chapter describes a method for extracting cadence using a discreet Fourier transform and examines this data with respect to the individual and their biometrics.

7.2 Measuring cadence in the Fourier domain

This analysis extracts the most significant harmonic from the data available using a discrete Fourier transform on the time series lateral motion data extracted as described in section 7.1 (such the blue plot shown in Figure 7-2). Before converting the data into the Fourier domain two different process steps are taken. First an algorithm processes the data checking if any frames of data are missing. Missing frames are rare but they do occasionally occur. Where they are found linear interpolation is used to ensure that the time series data represents discreet samples. Secondly, a window is applied to the

data to limit edge or out of phase effects in the Fourier domain. The windowing used is a Hann window as described Blackman *et al*. [89].

7.2.1 Results

This sub-section presents a summary of the results of the cadence measure as described above. The values of cadence are expressed as the period of cadence, in milliseconds. This is taken as the point with the highest magnitude in the Fourier domain. Table 7-1 summarises the cadence measurement results from the Napier dataset. The full table of results is included in appendix D, Table 14-1. It is noted that only data from 17 of the participants is examined as biometric data is not available for the other 4 participants.

Groups	*Count*	*Sum*	*Average*	*Variance*
Person A	14	6233	445	11833
Person B	14	8531	609	32938
Person C	14	6504	465	12094
Person D	14	8398	600	10385
Person E	14	7518	537	23853
Person F	14	7248	518	18340
Person G	14	7809	558	44684
Person H	14	7939	567	30285
Person I	14	9549	682	37488
Person J	14	8691	621	51760
Person K	14	9306	665	42470
Person L	14	9254	661	39324
Person M	14	8279	591	18751
Person N	14	7960	569	24663
Person O	14	8293	592	43009
Person P	14	8929	638	51033
Person Q	14	8722	623	13622

Table 7-1: Cadence results summary, Napier dataset

Single factor analysis of variance is performed on the data assuming unequal variance with a confidence interval of 0.05. Table 7-2 presents a summary of this analysis.

Source of Variation	*SS*	*df*	*MS*	*F*	*P-value*	*F crit*
Between Groups	982489	16	61406	2.0609	0.0110	1.6894
Within Groups	6584921	221	29796			
Total	7567410	237				

Table 7-2: ANOVA cadence result, Napier dataset

As the value of F is greater than the value of F-critical, this analysis establishes to better than 95% certainty that the cadence measure extracted is individualistic. However it is clear that there is significant measurement variance in the data. The F statistic of 2.06 is very low, indicating that the cadence measure extracted in this research has lower discriminating ability than the oscillation magnitude measure described in chapter 6.

Further analysis of the Fourier domain data was conducted to improve this result. Firstly, a measure calculated using a weighted sum of magnitudes in the Fourier domain for cadence periods greater than 333ms and less than 1500ms. This is later referred to as *filtered Fourier cadence.* The lower time period is selected as it is a good measure of the fastest step rate the author could maintain for 10 seconds. The larger of the two figures is taken as a round number (approx 50ms), slightly above the slow gait figure used by West and Scafetta [90]. A set of points, D (magnitude and harmonic index) is constructed in this range. The range is chosen as a wide but reasonable estimate of likely walking harmonics. Equation 7-1 shows the filtering calculation applied to this set. Inspiration for its derivation is obtained from the sub-pixel accuracy centroid calculations used by Cameron *et al* and Li *et al* [83, 91]. The second method, later referred to as *weighted Fourier cadence,* uses the same equation. However the set D consists of all magnitude data in the Fourier domain.

$$f = \frac{S \times 33}{\left(\frac{\sum_{i=0}^{n} D_i \times index}{\sum_{i=0}^{n} D_i} \right)}$$

f	is cadence harmonic in milliseconds
D	is the set of magnitudes in the Fourier domain
n	is the number of elements in D
index	is the harmonic index in the Fourier domain
S	is the number of sample in the Fourier domain

Equation 7-1: Harmonic filtering equation

The results of both the filtered and weighted Fourier cadence can be found in Appendix D, Table 14-3 and Table 14-4 respectively. The results and single factor analysis of variance performed to a confidence of 95% show a similar response to that for the Fourier peak cadence measure, namely that the measure is individualistic. Table 7-3 shows the F-statistics of the three different methods of extracting the cadence measure from the Fourier domain.

	F-Statistic
Peak Fourier Cadence	2.06
Weighted Fourier Cadence	2.62
Filterd Fourier Cadence	1.88

Table 7-3: Cadence F- Statistics

This presents a surprising result in that the weighted cadence measure, which includes all the high frequency noise, shows a larger F Statistic than either of the other two measures. This indicates that the weighted Fourier cadence measure is better at discriminating individuals than either the peak or the filtered measure. This result in turn poses interesting questions: Is the weighted measure a better indication of cadence than the Fourier peak or is it merely better at discriminating individuals, and can the same affect be found in video data? Perhaps these are interesting topics for future study.

7.2.2 Summary

This section has presented three methods for extracting a measure of cadence from participants. Analysis of the results shows to 95% certainty that the measure is individualistic. However all three have a low F statistic which indicates that its ability to aid the identification of individuals is low. Wagg, Nixon *et al* [61, 63] produced a significantly higher F statistic for the cadence measure they extracted from video footage indicating a significantly higher level of accuracy (approximately 100 times more discriminative). However they had several advantages over the trajectory data from the IRISYS detectors. They were viewing participants from a fronto-parallel view, which provides an image of leg motion. While this provides a significant advantage for gait extraction, it requires participants to walk in single file, a disadvantage the system presented here does not have.

7.3 Relating cadence to biometric features

This section examines the cadence measure described in section 7.1 with respect to height, inside and outside leg length of the participants from the Napier dataset. The peak cadence measure is used as it is unclear if the more discriminative weighted measure actually relates to cadence; the less discriminative filtered measure is considered less likely to accurately represent cadence. As there is significant noise in cadence measure the average peak cadence measure is taken from 14 different passes

of the detector for each participant. Figure 7-3, Figure 7-4 and Figure 7-5 respectively show plots of this cadence measure in relation to height, inside and outside leg length. Each plot has a linear trend line plotted using least squares regression; the equation and coefficients of determination (r^2) for the trend lines are also shown. Table 14-2 in Appendix D shows the actual results.

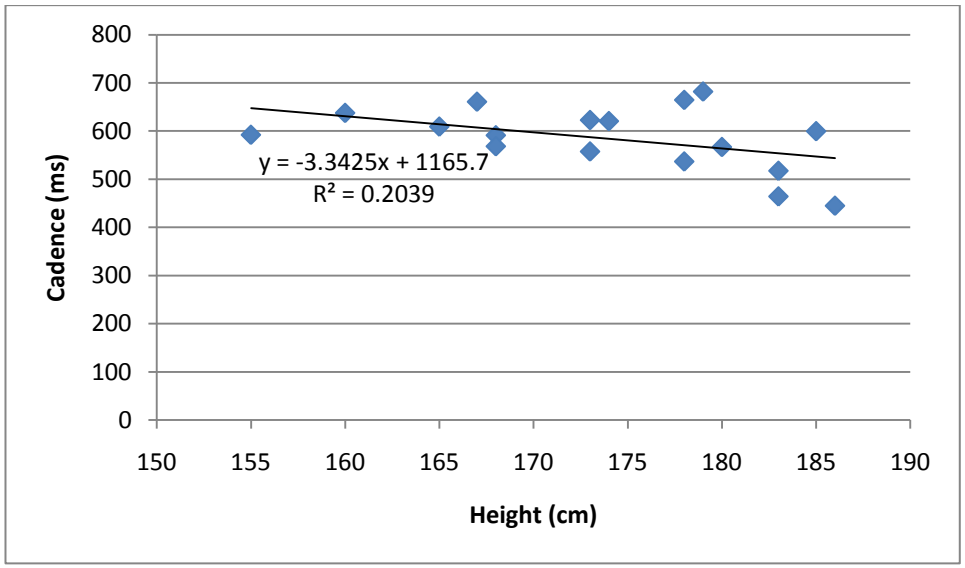

Figure 7-3: Cadence v Height

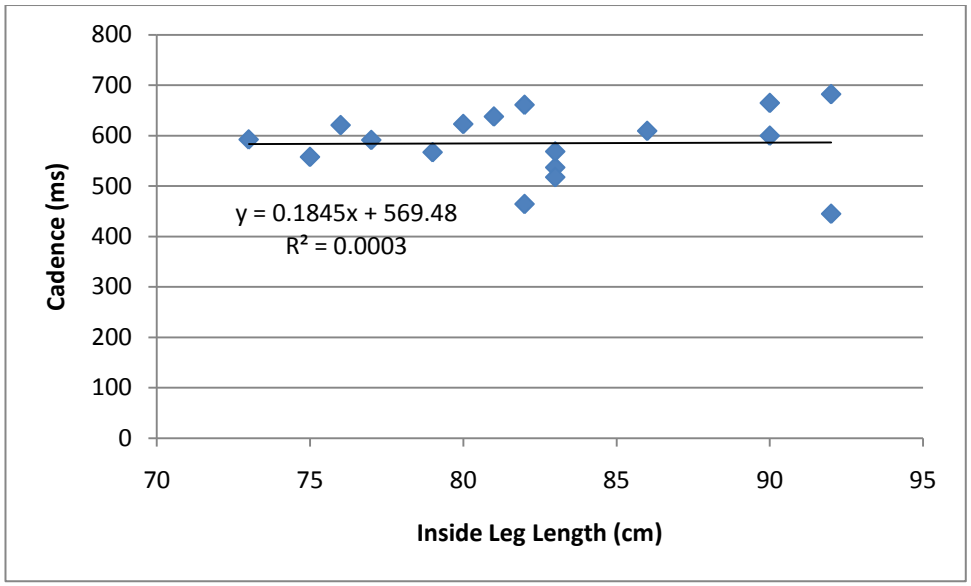

Figure 7-4: Cadence v Inside Leg Length

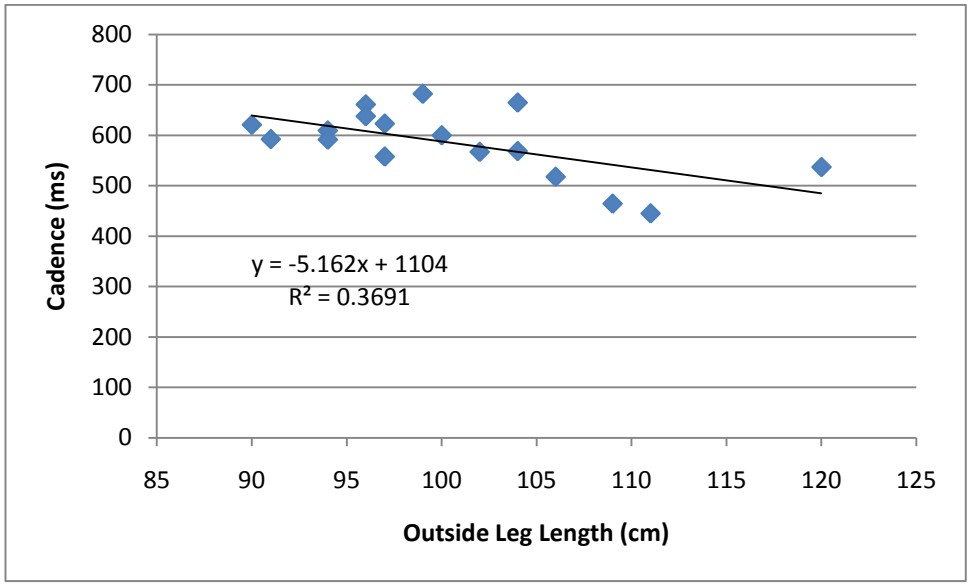

Figure 7-5: Cadence v outside leg length

The results presented here show some interesting features, although it is noted that the correlations are very loose. The slopes of the regression line are opposite for the outside and inside leg lengths, implying that the hip size (difference between inside and outside leg lengths) has more of an impact on the measure than any other feature. Figure 7-6 shows a plot of this.

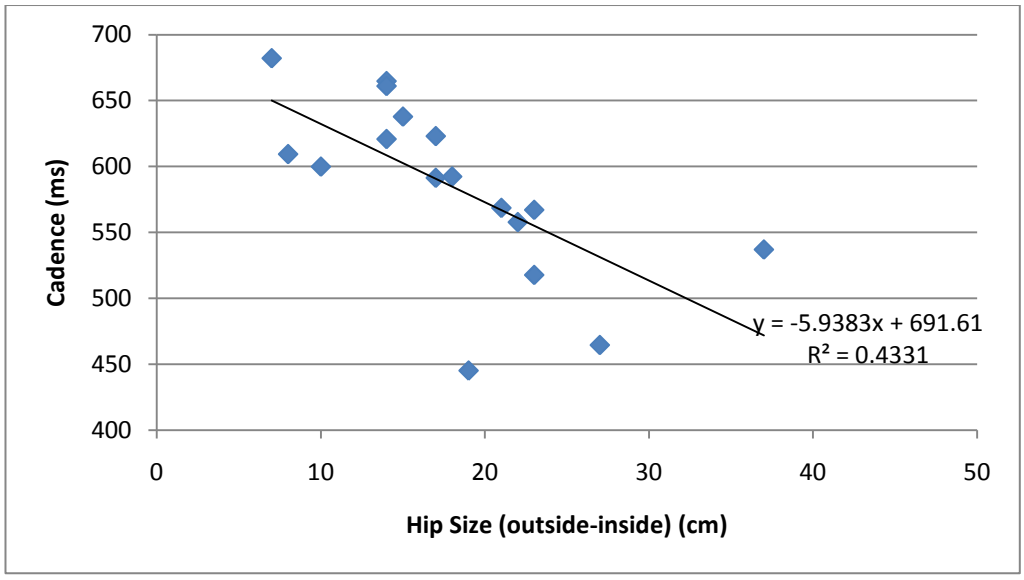

Figure 7-6: Cadence v hip size results

Given the looseness of the correlations it is not possible to draw definitive conclusions about this relationship. This poses an interesting topic suitable for further analysis, perhaps within the field of clinical gait analysis.

7.4 Summary

This chapter has examined the measurement of cadence using a discrete Fourier transform on distance from a second order polynomial equation fit to trajectory data. This provides a measure of lateral gait oscillation of the participant as they pass under the measurement area. Three methods are examined for extracting a measure from the Fourier domain. The first extracts the dominant frequency, that with the largest magnitude, and is considered to be the most likely to represent cadence. The second takes a weighting of all frequencies present within the range expected for walking gait; this attempts to filter out high frequency noise from the data. The third takes a weighted measure for all frequencies present.

The results presented show that, taking a weighted sum of all frequencies in the Fourier domain, provides a measure that is more individualistic than the most significant harmonic. This is not to suggest that this is a more accurate measure of cadence than the harmonic with the highest magnitude.

The contribution of the cadence measures described to discriminate between individuals is shown to be minimal, as indicated by the significantly lower F-statistic than that reported by Wagg and Nixon [61] in their measure of cadence. Most other researchers use different camera viewpoints (fronto-parallel). This enables leg motion to be visible, thus simplifying the gait measurement task, but it introduces the complication of occlusion. Significantly higher special resolution and lower crosstalk found in visible imagers makes it significantly easier to make accurate location (and therefore cadence) measurements. However infrared images are considerably better for separating people from background and therefore more suited for use in off-the-shelf people tracking products.

8 Conclusions

The research reported in this thesis develops the state of the art in pedestrian measurement techniques using the IRISYS people counters trajectory data. The IRISYS people counters are based around a relatively inexpensive infrared detector array, with tracker algorithm producing trajectory measurements. This chapter summarises the research conducted and conclusions reached. It reflects on the work conducted and compares it to the work of others. Finally, some future work is suggested, highlighting some potentially interesting questions.

8.1 Summary

In the first chapter of this thesis, the principal sectors showing interest in the measurement of pedestrian motion are introduced. The second chapter describes the main research, literature and background to the field. It then examines different pedestrian measurement and detection technologies. A significant gap is noticed between what is currently required and what is currently available. A brief introduction is then provided to the fields of stereo vision and human gait. The third chapter describes the detector in detail. It then presents an experiment investigating the barrel distortion found in the detector and proposes a general solution. The solution is deemed acceptable for general trajectory measurements, such as the studies presented in [1, 5]; however it is noted that there is variation between detectors.

Four principal studies are then presented. The first develops and demonstrates that pedestrian trajectory data can be collected and processed in real-time using the IRISYS detectors, details of which are included in Appendix E. The second, an original study, attempts to build on the first and uses detectors in stereo pairs to test if the trajectory data produced is sufficient for stereo triangulation height measurement of pedestrians. During this study an interesting phenomenon was noticed, that an oscillation exists which is consistent with cadence. This in turn led to the second study, an examination of the cause of this oscillation. This second study demonstrates that the location of an individual's footstep can generally be found in the data. It also shows that there is a link between the magnitude of lateral walking oscillation and gender of the participant. A further study is conducted to clarify the link between this oscillation magnitude and

gender. The final study investigates the development of a measure of walking cadence.

8.1.1 Use of IRISYS people counters in stereo

Chapter 4 describes the experiments conducted examining the use of the IRISYS people counters in stereo. It presents a study testing if the trajectory data can be used to measure the height of pedestrians using triangulation without requiring the detailed calibration of each sensor. Other researchers e.g. Psarakis *et al* [76] have used stereo imaging with sub-pixel accuracy; however at the start of the study it was unclear if the trajectory data provided by the IRISYS detector would be suitable.

It was noted during the research that there was an oscillation that appeared to originate from walking gait. The results show that it is not possible to use the trajectory data alone for accurate triangulation. It may however, be possible to use the image data for stereo triangulation. It is the author's opinion that should further study be conducted, it would be better to use an imager or detector with higher resolution and better spatial characterisation than the IRISYS detectors.

8.1.2 Stride measurement

Chapter 5 described an experiment to investigate the source of oscillations noted in the stereo experiment's dataset. This was done by placing markers on the floor under the detectors and asking 7 different people to walk under the detectors several times placing their feet on the floor markers. The data collected demonstrates that it is possible to see a similar oscillation in the data from all participants. It also shows that the results were consistent when the data from repeated walks was examined. This demonstrates that the oscillation noted during the stereo experiments originates from human gait and is not an artefact of the measurement technique.

The chapter then examined the left to right swing with respect to time. This highlighted some interesting facts. Firstly a significant synchronisation was found in the measurements of extrema in data collected simultaneously from two different detectors. This adds weight to the fact that an oscillation exists in the measurement that is related to human motion. Secondly, the number of changes in left to right direction can generally be counted automatically. As the measurement relates to gait

motion, these correspond indirectly but consistently to the location and time of the pedestrian's footsteps.

The result establishes that measurable gait information is present in the data collected; however, it is unclear what impact the constraints placed on the participant's motion during the experimentation have on the gait measurements. This in turn lead to two further studies collecting data without constraining the pedestrian's motion, the first exploring the magnitude of oscillation relationship to gender, and the second measuring and examining cadence.

8.1.3 Oscillation magnitude

Chapter 6 investigates the observation made during chapter 5, that the oscillation magnitude present in the trajectory data is linked to gender. During chapter 5 the motion of participants was constrained to placing their feet on floor markers. This constraint is removed from the data collected and analysed for oscillation magnitude to ensure that the result is unbiased. The participants were all asked to walk as normally as possible from a point on one side of the measurement area to a point on the other side; the data collected is later referred to as choreographed.

A second set of data was collected at the offices of IRISYS in a narrow corridor. While this certainly does not constrain the measurements to the same extent as asking participants to place their feet on locations marked on the floor, it does ensure that they walk in a straight line. At both of the data capture locations two data sets are acquired; the second consists of unsupervised capture of trajectory data from subjects moving through the measurement area during their normal daily activities.

A method of extracting the magnitude of lateral oscillation by fitting a second order polynomial to the data is proposed. Analysis of variance performed on the oscillation measure from the choreographed data shows that the measure is linked to the individual. However the F-Statistic, a measure of the relationship of variation within and between groups, is not as high as that presented by Wagg and Nixon [61] in their fronto-parralel video gait analysis. This indicates that the technique is not likely to be as good at discriminating individuals. However, while the IRISYS trajectory data largely represents lateral upper body oscillation, Wagg and Nixon were examining

oscillation primarily of leg motion. It is not surprising that an order of magnitude difference exists in the F statistic. During typical walking, the difference in separation between legs parallel and legs apart is likely to be of the order 50cm; the lateral upper body oscillation of a male is likely to be of the order 5cm.

The oscillation magnitude is also analysed with respect to gender and in both datasets there is shown to be a significant difference in the means for male and female participants. This establishes in principle that the measure can be used to determine the distribution of genders in a population. This in turn is investigated with the validation data captured from both locations. The results from the IRISYS capture produce a distribution that is 8% away from the actual distribution.

The data collected at Napier University was found to include 22 readings out of 120 where people changed direction within the field of view. For these it was not therefore possible to extract a useful measure of the oscillation magnitude. It is likely that this would adversely affect the results of a gender distribution algorithm, though, assuming that this is a good indication of the proportion of people who will change direction within the field of view, the algorithm would have an error bar of ±18%. The results presented are still fairly promising with the distribution 10% away from the actual result. As the size of any datasets analysed by the gender distribution algorithm increase, the probability of the error being as high as 18% reduce significantly. With larger samples it is likely that the proportions of males and females who generate unusable readings more accurately represent the proportions of males and females in the dataset, thus eliminating the cause of error.

The work presented has shown that meaningful information relating to the individual can be found from the oscillation magnitude. It has shown that there is a strong link between this measure and the gender of the person. A method for establishing gender distribution from people passing the detectors has been proposed and produces meaningful results.

8.1.4 Cadence measurement algorithms

Following from the discovery detailed in chapter 5 that stride can normally be measured. The findings of Winter [87] show that the stride length of an individual is

proportional to their speed so an investigation into the measurement of cadence is presented. Chapter 7 starts by accounting for the direction of motion. During the study of the oscillation magnitude in chapter 6 it is noted that, fitting a second order polynomial to the IRISYS dataset, appears to over-model the actual trajectory. A further investigation is then carried out on the Napier dataset, using three different methods to extract cadence from the Fourier domain.

These algorithms attempt to replicate the successes of other authors eg [61, 63, 64] in measuring cadence, using IRISYS trajectory data instead of video footage. in video footage on data from the IRISYS detectors. The first algorithm examines the most significant harmonic in the Fourier domain and is expected to be the best indicator of cadence. The second algorithm examines a weighted sum of all harmonics within the periods expected for walking gait. The third and final algorithm examines a weighted sum of all different harmonics. The last proves to be the most individualistic measure, the one with the highest F statistic. However, it is likely that the first is a better indication of actual walking cadence. Analysis of variance shows to 95% confidence that all three measures are individualistic, however the F statistics, are low. This indicates that the variance within groups is significant and that it is likely to limit the measure to a minor component in a human ID system.

The results presented are disappointing, considering that, in the data examined in chapter 5, 80% of footsteps could be measured, and that most of those that could not, were linked to a small number of individuals. However, several issues contribute to this difference: the data examined in chapter 5 is acquired from people who are not walking in their normal manner and they are placing their feet on marked locations. This is compounded by the fact that a typical trajectory contains only 4 footsteps. Therefore, only two complete gait cycles are available to contribute to the measure, an insufficient number to obtain a consistent measure of cadence.

8.2 Reflection

The research presented in this thesis and Appendix has advanced the state of the art in measuring pedestrian motion. The peer-reviewed papers presented in Appendix E demonstrate that significant pedestrian trajectory measurement can be obtained using the IRISYS people counters. Further advances are made by a detailed study of the

trajectory data providing an understanding of what can and cannot be achieved from the data. This includes the development of a gender distribution algorithm which allows the proportions of male and female passing under the detector to be determined.

8.2.1 Research questions answered

The research presented in this thesis set out to improve the automatic unobtrusive measurement of human gait by examining the data from the IRISYS people counter. This thesis has presented a substantial study into the trajectory information available and examined it with respect to the biometrics of participants. It has found several interesting correlations and presented methods for obtaining measures of cadence and oscillation magnitude. Analysis of variance establishes that the measures both of cadence and oscillation magnitude are individualistic. However, their use in Human Identification is limited to a small potential contribution from a probabilistic or stochastic model, such as a hidden Markov model. The derivation of such a model is not warranted solely from the trajectory data produced by the detector but would benefit from it, if other non-perfect human identification features were also available.

Further examination of the oscillation magnitude shows a high correlation with gender. The assertion is made that the measure extracted, largely relates to upper body lateral gait oscillation, which has long been accepted by the biomechanics field [86] as having a strong link to gender. This research has shown that an indication of gender distributions can be obtained. The application of this theory is demonstrated on data captured in two different locations, with considerable success. It is noted that the height at which the sensors are mounted has an impact on the datasets acquired, and the algorithm developed is only intended for use with the equipment mounted at the heights specified.

8.2.2 Comparison of results with the work of others

The task of measuring and processing pedestrian trajectories in real-time in unsupervised environments is a significant one. The collaborative work presented in the author's papers [1, 5] copies included in appendix E is an advance over work previously reported in the field. Most pedestrian trajectory measurement systems are based on processing CCTV or visible video footage. The studies of Philips *et al.* [51] and Kukla *et al.* [92] required human assistance to find and track the pedestrian in the

video sequence. Some studies, such as that carried out by Wagg and Nixon [61], did not require human intervention. However, their success rate dropped significantly when used outside the laboratory environment. Their motion detection method would almost certainly suffer further when applied to real world data without constraints, such as camera housings not being washed, or participants wearing different clothing. While new systems are emerging which show potential, such as those considered by Greene-Roesel *et al* [93], at the time of writing none have rivalled the work presented in this thesis. This work is furthered by a much more detailed examination of the trajectory data available from the IRISYS people counters.

Obtaining identifiable biometrics based on human gait is a significant and emerging field in itself. Most attention has been given to extracting gait features from video footage, due to its availability. This is however fraught with difficulty; the task of just finding the pedestrian in video footage still poses a challenge. The people counter used during this study is ideally suited to installations where little or no maintenance is required. Currently hundreds of thousands of them are commercially deployed as people counters. Most are installed in indoor retail environments; there is however an outdoor model.

Lee and Grimson [54] present a study of gait analysis for recognition and classification using video. Their work is also subject to data collection requirements similar to those imposed by Wagg and Nixon. Again Lee and Grimson found that good classification results (better than 80% correct) can be obtained in a laboratory environment. They highlighted that much better results can be found if an average gait measure is taken over a longer time frame. The results presented in this thesis relating to Human Identification are clearly not on a par with side-on video gait analysis such as presented by Lee [30], but they were not ever likely to be; overhead gait analysis has significantly less information to utilise, but avoids the problems associated with a fronto-parallel view and image processing. In addition to this, other authors attempting gait analysis for human identification see refs. [54, 61, 64, 65] typically observe the subjects for longer than is practical with the IRISYS people counters (> 4s). The model presented by West and Scafetta [90], suggests that even longer may be necessary; however this almost certainly depends on the data collection environment and circumstance.

Very little published work exists describing the study of human gait from above. It is a field that has not previously attracted much attention, due to side-on video being much more easily available and containing more gait information. Most of the studies that have, are detailed studies of kinematics in the biomedical field which captured data from multiple view points to better understand bipedal locomotion. This study demonstrates that it is possible to measure human gait from above using a very low resolution device (16 x 16 pixels) and the gait information collected can significantly aid the determination of gender.

8.2.3 Critical reflection of research

During chapter 4, studies on the use of the detectors in stereo are conducted. Data is collected and an algorithm is produced to measure the height of the pedestrian. The chapter concludes that it is not possible to accurately measure the height of the participants using the technique presented. Furthermore, the detector in its current form is probably not suitable for accurate stereo depth perception. While it is clear from the results that it is not possible to measure an individual's height accurately, it may be possible to gain an individualistic measure. The chapter examines the coefficients of correlation for trend lines fitted to the data when plotted with respect to height.

The oscillation noticed during the stereo chapter is further examined in chapter 5. By taking multiple recordings of the same walk it is possible to correlate the extrema found in the data. This provides a very compelling argument to support the hypothesis that the location of footsteps can normally be measured using this technology. The magnitude of the left to right oscillation is examined with respect to gender and the individual. This measure is found to be both individualistic and highly correlated to gender. A gender distribution algorithm is developed, based on data collected from participants, but it is dependent on the participants being truly representative of the population. However, this is an assumption that generally has to be made in any similar human gait analysis work. It is noted that this algorithm is best suited to locations where people passing the detectors do not generally change direction within the field of view, which is approx 3m by 3m.

Chapter 7 further investigates the trajectory data and presents methods for extracting cadence. The results presented show results with little ability to discriminate between individuals. It is felt likely that a combination of the size of field of view and downward looking view point of the IRISYS people counters limit the ability to produce a good measure of cadence. It is not possible from this research to say if the measures of cadence extracted well represent the actual cadence of the participants, however it certainly is correlated to it. This point requires further clarification if the cadence measure developed were to be used for studies of biomechanics where accurate results are required.

8.3 Future work

During the course of the research several interesting discoveries have been made. Measures have been developed for oscillation magnitude and cadence. Both are shown to be individualistic, however they are not sufficiently discriminatory to identify an individual. This section suggests future work based on this research that could improve the measures obtained. It suggests work to further develop the gender distribution algorithm established in this thesis, to an algorithm invariant to detector mounting height. Secondly, it suggests alternative approaches for capturing data, throughout the duration of this research; several companies have been actively attempting to reduce the cost of thermal imagining components and systems.

8.3.1 Developing a mounting height invariant gender distribution algorithm

Chapter 6 investigates the oscillation magnitude measure. It presents research that established a measure of gender can be extracted from the trajectory data produced by the IRISYS people counters. Section 6.5 describes an algorithm for measuring the distribution of genders passing the detectors based on this measure. The algorithm works relatively well in both locations in which it is trialled. However it is noted that the algorithm requires to be tuned to the mounting height of the detectors. This dependence could almost certainly be modelled by collecting data at several different mounting heights. The relationship between mounting height and absolute values for mean measurement of males and females could then be established and an equation fitted to model it. Should this be done it is recommended that further validation exercises be conducted to confirm the algorithm function.

8.3.2 Using high resolution thermal or visible video from above

This thesis demonstrates that it is possible to extract individualistic measures for people using the ceiling-mounted IRISYS people counters. The results show that there is significant noise in the data and it is therefore not possible to rely solely on this data for identification of individuals. It would be interesting to examine further, similar gait detection techniques on trajectory data collected from downward looking devices which cover larger areas. The algorithm for measuring cadence presented in chapter 7 should work better if longer trajectories (>4s), based on the upper body motion are analysed. This could be developed from either visible imaging devices or thermal imaging devices. In the author's opinion, thermal cameras would be likely to provide a more robust tracking solution. However visible video cameras are cheaper and typically have higher spatial resolution. If available, it would be worthwhile to attempt a similar analysis of high resolution aerial or satellite footage.

8.4 Summary

The research presented in this thesis has developed the state of the art in pedestrian measurement technology. It has described considerable research demonstrating how detailed pedestrian trajectory data can be acquired in real-time. In addition to this it has developed new algorithms for measuring human gait from the IRISYS people counters. In turn this demonstrates that it is possible to extract individualistic measures relating to walking gait from a thermal detector where each pixel covers a square with approximately 25cm sides. A measure of the lateral walking oscillation is developed and results establishing that it has a very high correlation to gender are presented.

9 References

[1] J. Kerridge, S. Keller, T. J. Chamberlain, and N. Sumpter *Collecting, Processing and Calculating Pedestrian Flow Data in Real-time,* in *Pedestrian evacuation and dynamics 2005*. 2007, Springer: Berlin. p. 27-39.

[2] M. Batty, *Agent-based pedestrian modelling*. 2003, Centre for advanced spatial analysis, University College London,. p. 26.

[3] A. Armitage, D. Binnie, J. Kerridge, and L. Lei. *Measuring Pedestrian Trajectories with Low Cost Infrared Detectors: Preliminary Results*. in *Pedestrian and Evacuation Dynamics* 2003. Greenwich: CMS Press London.

[4] W. Daamen, *Modelling passenger flows in public transport facilities*, PhD *Department Transport & Planning*. 2004, TUDelft

[5] J. Kerridge, S. Keller, T. J. Chamberlain, and N. Sumpter *Collecting, Processing and Calculating Pedestrian Flow Data in Real-time,* in *Transportation Research Board 84th Annual Meeting*. 2005: Washington DC.

[6] K. Fürstenberg, J. Hipp, and V. Willhoeft. *New laser scanner for driver assistance*. in *EAEC*. 2001. Bratislava, Slovakia.

[7] K. Fürstenberg, J. Hipp, and A. Liebram. *A Laser Scanner for detailed traffic data collection and traffic control*. in *7th World Congress on Intelligent Transport Systems*. 2000. Torino, Italy.

[8] U. Lages. *Laser Scanner for Obstacle Detection*. in *6th International Conference Advanced Microsystems for Automotive Applications, Berlin*. 2002. Berlin, Germany.

[9] C.-Y. Chan and F. P. Bu, *Literature review of pedestrian detection technologies*. 2005, Institute of transport studies University of California: Berkeley.

[10] Z. J. Li, K. F. Wang, L. Li and F. Y. Wang. *A Review on Vision-Based Pedestrian Detection for Intelligent Vehicles*. in *IEEE International Conference on Vehicular Electronics and Safety*, 2006.

[11] B. Leibe, K. Schindler, N. Cornelis, and L. Van Gool, *Coupled Object Detection and Tracking from Static Cameras and Moving Vehicles.* IEEE Transactions on Pattern Analysis and Machine Intelligence, 2008. **30**(10): p. 1683-1698.

[12] J. Kerridge, A. Armitage, D. Binnie, and L. Lei, *Monitoring the Movement of Pedestrians Using Low-cost Infrared Detectors: Initial Findings.* Transportation Research Record, 2004. **ISSN 0361-1981**.

[13] J.-C. Nebel. *MEDUSA: Multi Environment Deployable Universal Software Application*. [www] [cited 2006 21 March]; Available from: http://www.kingston.ac.uk/~ku33185/MEDUSA.html.

[14] R. Fischer. *CAVIAR: Context Aware Vision using Image-based Active Recognition:*[www] [cited 2006 21 March]; Available from: http://homepages.inf.ed.ac.uk/rbf/CAVIAR/

[15] R. T. Collins. *VSAM: Visual Surveillance And Monitoring* [www] [cited 2006 21st March]; Available from: http://www.cs.cmu.edu/~vsam/vsamhome.html.

[16] R. T. Collins, A. J. Lipton, and T. Kanade, *A system for Surveillance and Monitoring, VSAM Project Final Report*. 2000, Robotics Institute, Carnegie Mellon University.

[17] *PASSWORDS: Parallel and real time Advanced Surveillance System With Operator assistance for Revealing Dangerous Situations*. [www] [cited 2006 21st March]; Available from: http://spt.dibe.unige.it/ISIP/Projects/passwords.html.

[18] R. T. Collins, A. J. Lipton, H. Fujiyoshi, and T. Kanade, *Algorithms for cooperative Multisensor Surveillance.* Proceedings of the IEEE, 2001. **89**(10): p. 1456 - 1477.

[19] C. Dai, Y. Zheng, and X. Li, *Pedestrian detection and tracking in infrared imagery using shape and appearance.* Computer Vision and Image Understanding, 2007. **106**(2-3): p. 288-299.

[20] P. C. D. Hobbs. ***A $10 Thermal Infrared Imager*** in *SPIE Sensors and Controls for Intelligent Manufacturing II*. 2001.

[21] S. Okuda, S. Kaneda, and H. Haga, *Human position/ height detection using analogue type pyroelectric sensors,* in *LNCS* 2005, Springer: Nagasaki, Japan. p. 306-315.

[22] J.-S. Fang, Q. Hao, D. J. Brady, M. Shankar, B. D. Guenther, N. P. Pitsianis, and K. Y. Hsu, *Path-dependent human identification using a pyroelectric infrared sensor and Fresnel lens arrays.* Optics Express, 2006. **14**(2): p. 609.

[23] N. Ishihara, H. Zhao, and R. Shibasaki. *Tracking passenger movement with ground-based laser scanner*. in *22nd Asian conference on remote sensing*. 2001. Singapore.

[24] S. H. Hsu, G Jones, P Usowicz, S. Samarasekera, and R. Kumar. *Automatic registration and visualization of occluded targets using ladar data*. in *Laser Radar Technology and Applications VIII*. 2003. Orlando, FL, USA: SPIE.

[25] M. Heikkila and M. Pietikainen, *A Texture-Based Method for Modelling the Background and Detecting Moving Objects.* IEEE Transactions on pattern analysis and machine intelligence, 2006. **28**(4): p. 657-662.

[26] Hee-Deok Yang and Seong-Whan Lee. *Multiple pedestrian detection and tracking based on weighted temporal texture features*. in *Proceedings of the 17th International Conference on Pattern Recognition,* 2004.

[27] P. Kelly, N. E. O'Connor, and A. F. Smeaton, *Robust pedestrian detection and tracking in crowded scenes.* Image and Vision Computing. **In Press, Corrected Proof**.

[28] K. Toyama, J. Krumm, B. Brumitt, and B. Meyers. *Wallflower: Principles and practice of background maintenance*. in *International Conference on Computer Vision*. 1999. Kerkyra, Corfu, Greece.

[29] M. Harville, G. Gordon, and J. Woodfill. *Foreground Segmentation Using Adaptive Mixture Models in Color and Depth*. in *IEEE Workshop on Detection and Recognition of Events in Video*. 2001. Vancouver, Canada.

[30] D.-S. Lee, *Effective Gaussian Mixture Learning for Video Background Subtraction.* IEEE Transactions on pattern analysis and machine intelligence, 2005. **27**(5): p. 827-832.

[31] K. Kim, D. Harwood, and L. Davis, *Background updating for visual surveillance.* Lecture notes in computer science 2005 (Special issue 3804): p. 337-346.

[32] K. Kim, T. H. Chalidabhongse, D. Harwood, and L. Davis, *Real-time foreground-background segmentation using codebook model.* Real-time imaging, 2005. **11**(3): p. 167.

[33] C. Stauffer and W. E. L. Grimson. *Adaptive background mixture models for real-time tracking*. in *Computer Vision and Pattern Recognition*. 1999. Fort Collins, Colorado.

[34] K. P. Horn and B. G. Schunck, *Determining Optical Flow.* Artificial Intelligence, 1981. **17**: p. 185-203.

[35] C. L. Zitnick, N. Jojic, and S. B. Kang. *Consistent Segmentation for optical flow estimation*. in *International conference on computer vision*. 2005. Beijing: IEEE.

[36] C. Fermüller, D. Shulman, and Y. Aloimonos, *The Statistics of Optical Flow.* Computer Vision and Image Understanding, 2001. **82**(1): p. 1-32.

[37] P. Viola and M. Jones. *Rapid object detection using a boosted cascade of simple features*. in *Computer Vision and Pattern Recognition*. 2001. Kauai, Hawaii: IEEE Computer Society.

[38] P. Viola, M. J. Jones, and D. Snow. *Detecting pedestrians using patterns of motion and appearance*. in *IEEE International Conference on Computer Vision*. 2003. Nice, France.

[39] I. Hariatoglu, D. Harwood, and L. Davis. *Ghost: A Human Body Labeling System Using Silhouettes*. in *14th International Conference on Pattern Recognition*. 1998. Brisbane Australia.

[40] L. M. Fuentes and S. A. Vaelastin. *People tracking in surveillance applications*. in *2nd IEEE Workshop on PETS*. 2001. Kauai, Hawaii, USA.

[41] A. Selinger and L. Wixson. *Classifying moving objects as rigid or non-rigid without correspondences*. in *DARPA Image Understanding Workshop*. 1998. Monterey, CA, USA.

[42] T. List and R. B. Fisher. *Computer vision markup language* in *International conference on pattern recognition* 2004. Cambridge

[43] A. El Maadi and X. Maldague, *Outdoor infrared video surveillance: A novel dynamic technique for the subtraction of a changing background of IR images.* Infrared Physics & Technology, 2007. **49**(3): p. 261-265.

[44] B. Lei and L.-Q. Xu, *Real-time outdoor video surveillance with robust foreground extraction and object tracking via multi-state transition management.* Pattern Recognition Letters, 2006. **27**(15): p. 1816-1825.

[45] J. P. Siepmann. *Fusion of current technologies with real-time 3D MEMS ladar for novel security and defense applications*. in *Laser Radar Technology and Applications XI-SIPE*. 2006: The International Society for Optical Engineering.

[46] I. J. Amin, A. J. Taylor, F. Junejo, A. Al-Habaibeh, and R. M. Parkin, *Automated people counting by using low-resolution infrared and visual cameras.* Journal of International Measurement Confederation, 2008. **41**: p. 589-599.

[47] F. Sun, S.T. Li and B. Yang *A new color image fusion method for visible and infrared images*. in *IEEE International Conference on Robotics and Biomimetics, ROBIO* 2007.

[48] S. G. Kong, J. Heo, F. Boughorbel, Y. Zheng, B. R. Abidi, A. Koschan, M. Yi, and M. A. Abidi, *Multiscale Fusion of Visible and Thermal IR Images for Illumination-Invariant Face Recognition.* Int. J. Comput. Vision, 2007. **71**(2): p. 215-233.

[49] J.C. Nascimento and J. S. Marques, *Performance evaluation of object detection algorithms for video surveillance.* IEEE Transactions on Multimedia, 2006. **8**(4): p. 761-774.

[50] T. List, J. Bins, J. Vazquez, and R. B. Fisher. *Performance evaluating the evaluator*. in *2nd Joint IEEE International Workshop on Visual Surveillance and Performance Evaluation of Tracking and Surveillance* 2005.

[51] J. Phillips, S. Sarkar, I. Robledo, P. Grother, and K. Bowyer. *Baseline Results for the Challenge Problem of Human ID Using Gait Analysis*. in *Fifth IEEE International Conference on Automatic Face and Gesture Recognition*. 2002. Washington D.C.

[52] S. Sarkar, P. Phillips, J , Z. Liu, I. Vega, R, P. Grother, and K. Bowyer, W, *The Human ID Gait Challenge Problem: Data Sets, Performance, and Analysis.* Transactions on pattern analysis and machine intelligence 2005. **27**(2): p. 162-177.

[52a] I.P. Herman, *Physics of the Human Body*, 2007, Springer: New York, ISBN: 987-3-540-29603-4

[52b] C.A. Oatis, *Kinesiology: The Mechanics And Pathomechanics Of Human Movement*, 2008, Lippincott Williams and Wilkins, ISBN: 978-0-781-75513-9

[52c] C.D. Barclay, J.E. Cutting and L.T. Kozlowski, *Temporal and spatial factors in gait perception that influence gender recognition*, Perception & Psychophysics, 1978, (23) p145-152

[52d] J. W. Davis, H. Gao, *An expressive three-mode principal components model for gender recognition*, Journal of Vision, 2003, 4(5) p. 362-377

[52e] A. M. Fullenkamp, K. M. Robinette and H. A. M. Daanen, *Gender Differences in NATO Anthropometry and the Implication for Protective Equipment*, Technical Report, United States Air Force, 2008

[53] M. E. Johanson, *Gait Laboratory: Structure and Data Gathering*, in *Gait Laboratory: Structure and Data Gathering in Human walking*. 1994, Williams and Wilkins: Baltimore. p. 201-224.

[54] W. E. L. Grimson and L. Lee. *Gait Analysis for Recognition and Classification*. in *Fifth IEEE International Conference on Automatic Face and Gesture Recognition*. 2002

[55] C. Bregler. *Learning and recognizing human dynamics in video sequences*. in *IEEE Conference on Computer Vision and Pattern Recognition*. 1997. San Juan, Puerto Rico

[56] J. E. Boyd and J. J. Little. *Global versus Structured Interpretation of Motion: Moving Light Displays*. in *IEEE Workshop on Motion of Non-Ridged and Articulated Objects*. 1997. San Juan, Puerto Rico

[57] T. B. Moeslund and E. Granum, *A Survey of Computer Vision-Based Human Motion Capture.* Computer Vision and Image Understanding, 2001. **18**: p. 231-268.

[58] R. Green and L. Guan, *Quantifying and Recognizing Human Movement Patterns from Monocular Video Images - Part II: Applications to Biometrics.* IEEE Transactions on Circuits and Systems for Video Technology, 2003 (Special Issue on Image and Video-Based Biometrics).

[59] B. Abernethy, S. J. Hanrahan, V. Kippers, L. T. Mackinnon, and M. G. Pandy, *The Biophysical Foundations of Human Movement*. Second Edition 2005: Palgrave Macmillan, Australia.

[60] L. Wang, T. L. Tan, H. Z. Ning and W. M. Hu, *Silhouette analysis-based gait recognition for human identification.* IEEE Transactions on Pattern Analysis and Machine Intelligence, 2003. **25**(12): p. 1505-1518.

[61] D. Wagg and M. Nixon. *On Automated Model-Based Extraction and Analysis of Gait*. in *IEEE International Conference on Automatic Face and Gesture Recognition*. 2004. Seoul, Korea

[62] R. T. Collins, R. Gross, and J. Shi. *Silhouette-based Human Identification from body Shape and Gait*. in *5th International Conference on Automatic Face and Gesture Recognition*. 2002. Washington, D.C.

[63] M. S. Nixon, J. N. Cater, M. G. Grant, L. Gordon, and J. B. Hayfron-Acquah, *Automatic recognition by gait: progress and prospects* Sensor Review, 2003. **23**(4): p. 323-331.

[64] C. BenAbdelkader, R. Cutler, and L. Davis. *Person Identification using Automatic Height and Stride Estimation*. in *IEEE International Conference on Pattern Recognition*. 2002. Québec, Canada.

[65] C. BenAbdelkarder, R. Cutler, and L. Davis. *View-invariant Estimation of Height and Stride for Gait Recognition*. in *Workshop on Biometric Authentication ECCV* 2002. Copenhagen, Denmark.

[66] A. Bobick and A. Johnson. *Gait recognition using static, activity-specific parameters* in *IEEE Conference on Computer Vision and Patern Recognition* 2001. Hawaii

[67] D. Xu, S. Yan, D. Tao, S. Lin and H.J. Zhang, *Marginal Fisher Analysis and Its Variants for Human Gait Recognition and Content- Based Image Retrieval.* IEEE Transactions on Image Processing, 2007. **16**(11): p. 2811-2821.

[68] H. Su and F. G. Huang *Human gait recognition based on motion analysis*. in *Proceedings of IEEE International Conference on Machine Learning and Cybernetics,* 2005.

[69] J. H. Yoo, M. S. Nixon, and C. J. Harris. *Model-driven statistical analysis of human gait motion*. in *Proceedings of International Conference on Image Processing* 2002.

[70] F. Dornaika and R. Chung. *Stereo correspondence from motion correspondence,* in *IEEE Computer Society Conference on Computer Vision and Pattern Recognition,* 1999

[71] W. S. Kim, A. I. Ansar, R. D. Steele, and R. C. Steinke. *Performance analysis and validation of a stereo vision system*. in *IEEE International Conference on Systems, Man and Cybernetics,* 2005.

[72] V. Kolmogorov, A. Criminisi, A. Blake, G. Cross, and C. Rother, *Probabilistic fusion of stereo with color and contrast for bilayer segmentation.* IEEE Transactions on Pattern Analysis and Machine Intelligence, 2006. **28**(9): p. 1480-1492.

[73] S. Peleg, Y. Pritch, and M. Ben-Ezra. *Cameras for stereo panoramic imaging*. in *Proceedings of IEEE Conference on Computer Vision and Pattern Recognition,* 2000.

[74] M. Z. Brown, D. Burschka, and G. D. Hager, *Advances in computational stereo.* IEEE Transactions on Pattern Analysis and Machine Intelligence, 2003. **25**(8): p. 993-1008.

[75] J. Liu, P. Delmas, G. Gimel'farb, and J. Morris. *Stereo reconstruction using an image noise model* in *IEEE Conference on Digital Imaging Computing: Techniques and Applications*. 2005. Queensland

[76] E. Z. Psarakis and G. D. Evangelidis. *An enhanced correlation-based method for stereo correspondence with sub-pixel accuracy*. in *IEEE International conference on computer vision*. 2005. Beijing

[77] O. Veksler. *Stereo Correspondence by Dynamic Programming on a Tree*. in *IEEE Conference on Computer Vision and Pattern Recognition*. 2005. San Diego

[78] L. G. Brown, *A survey of Image Registration Techniques.* ACM Computing Surveys 1992. **24**(4).

[79] M. Bertozzi, A. Broggi, C. Caraffi, M. Del Rose, M. Felisa, and G. Vezzoni, *Pedestrian detection by means of far-infrared stereo vision.* Computer Vision and Image Understanding, 2007. **106**(2-3): p. 194-204.

[80] R. Muñoz-Salinas, *A Bayesian plan-view map based approach for multiple-person detection and tracking.* Pattern Recognition, 2008. **41**(12): p. 3665-3676.

[81] K. Fujimoto, H. Muro, N. Shimomura, T. Oki, K. Maeda, Y. Kishi, and M. Hagino, *A study on pedestrian detection technology using stereo images.* JSAE Review, 2002. **23**(3): p. 383-385.

[82] J. W. Gardner, *Microsensors Principles and applications* 1994, Chichester: Wiley. 331.

[83] K. Cameron. *ACE: Automated centroid ectractor for real time target tracking*. in *Electron conventions*. 1990. LA, USA.

[84] N. Sumpter, *New people counter communications protocol*. 2003, IRISYS ltd.

[85] M. V. Klein and T. E. Furtrak, *Optics*. Second ed. 1986, Washington: John Wiley & Sons.

[86] G. Mather and L. Murdoch. *Gender Discrimination in Biological Motion Displays Based on Dynamic Cues* in *Biological Sciences* 1994: Royal Society.

[87] D. Winter, *The biomechanics and motor control of human gait*. 1987: University of Waterloo Press.

[88] C. BenAbdelkader, R. Cutler, and L. Davis. *View-invariant Estimation of Height and Stride for Gait Recognition*. in *Workshop on Biometric Authentication ECCV* 2002. Copenhagen, Denmark.

[89] R. Blackman and J.W. Turkey, *Particular Pairs of Windows.* The Measurement of Power Spectra from the Point of View of Communications Engineering, 1959. **87**: p. 95--101.

[90] B. J. West and N. Scafetta, *Nonlinear dynamical model of human gait.* Physical Review E, 2003. **67**(5): p. 051917.

[91] Z.Y. Li and K.S. Zhen. *A new filtering method for precision target tracking*. in *National aerospace and electronics*. 1992. Proceedings of the IEEE National Aerospace Engineering conference.

[92] R. Kukla, J. Kerridge, A. Willis, and J. Hine, *PEDFLOW: Development of an Autonomous Agent Model of Pedestrian Flow.* Transportation Research Record, 2001. **1774**: p. 11-17.

[93] R. Greene-Roesel, M. C. Diógenes, D. R. Ragland, and L. A. Lindau, *Effectiveness of a Commercially Available Automated Pedestrian Counting Device in Urban Environments: Comparison with Manual Counts*, in proceding of *Transportation Research Board Annual Meeting* 2008: Washington

[94] B. Fisher, S. Perkins, A. Walker, and E. Wolfart. *Hough Transform*. 1994 [cited 2006 19 June]; Available from: http://www.cee.hw.ac.uk/hipr/html/hough.html.

10 Appendix A - Software developed

A significant software system has been developed to read and interpret the data available from the IRISYS in house software. This appendix provides an introduction to the software system developed to help find patterns in the data.

In order to achieve the above goals the software performed several different tasks. Firstly it provides a mechanism for reading the file format produced by the IRISYS in-house recording software used for data capture. Secondly it provided a mechanism for editing the files to remove measured trajectories from the data files. This was added to allow the removal of data originating from passers by not taking part in the experiments. The software saves the edited reads file produced by IRISYS in-house testing tool and process the data into a collection of trajectories. It is possible to save (and re-open) these in xml. Thirdly, it provided a graphical display of the trajectories and left to right swing data to help visualise any useful data.

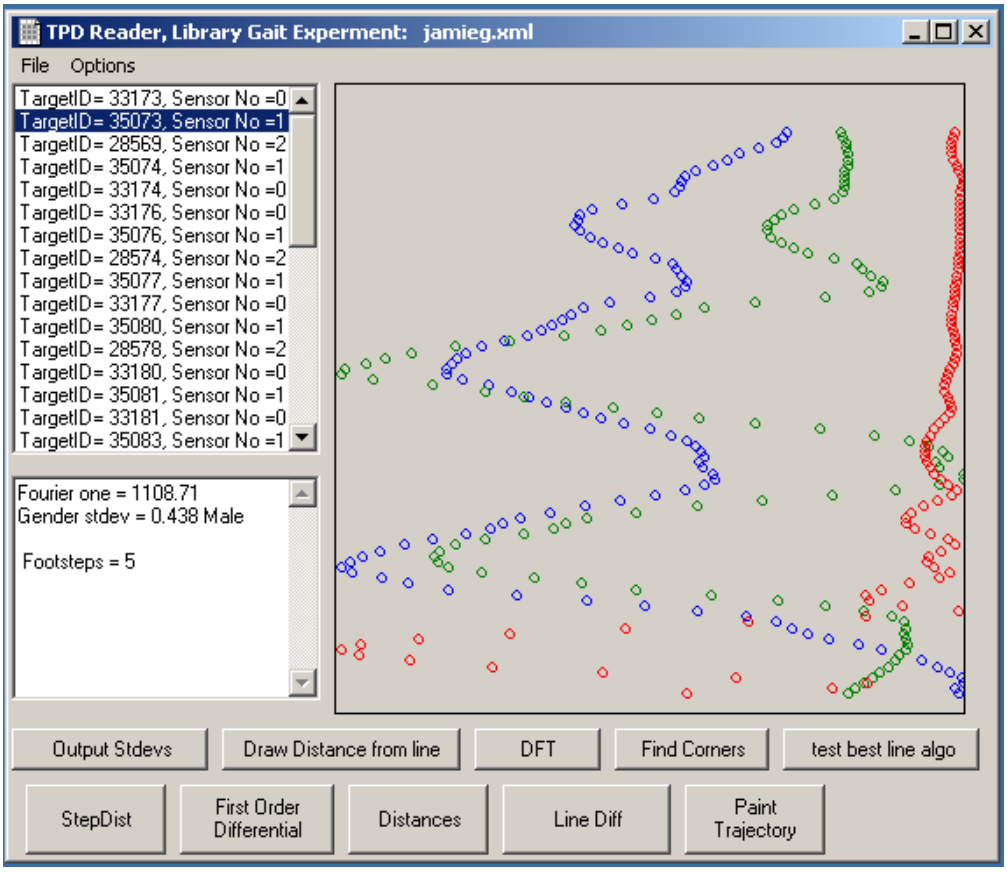

Figure 10-1: Screen shot, main screen

Figure 10-1 shows a screen shot the application's main screen. The menu provides access to the application's open and save facilities. When files have been loaded each

target appears in the list box at the left of the application. Some information about the target is also displayed in the features text box below the list of targets. What information is displayed there depends on which of the analysis buttons have been pressed. Each of the buttons along the bottom performs two actions. First it processes the data in a prescribed way, second it displays the processed data in the gray display area and writes the data values to a comma separated values (csv) file.

In the example shown the blue data is the distance from the best fit line, when filtering is done only after fitting the line. The green data is the distance from the line when the data is filtered both before and after fitting the lines. The red data is after performing a discreet Fourier transform on the data.

Figure 10-2 shows a second screen used for deleting unwanted trajectory and stereo analysis. When a target is selected it is drawn in one of the three boxes (which one depends on which detector recorded it).

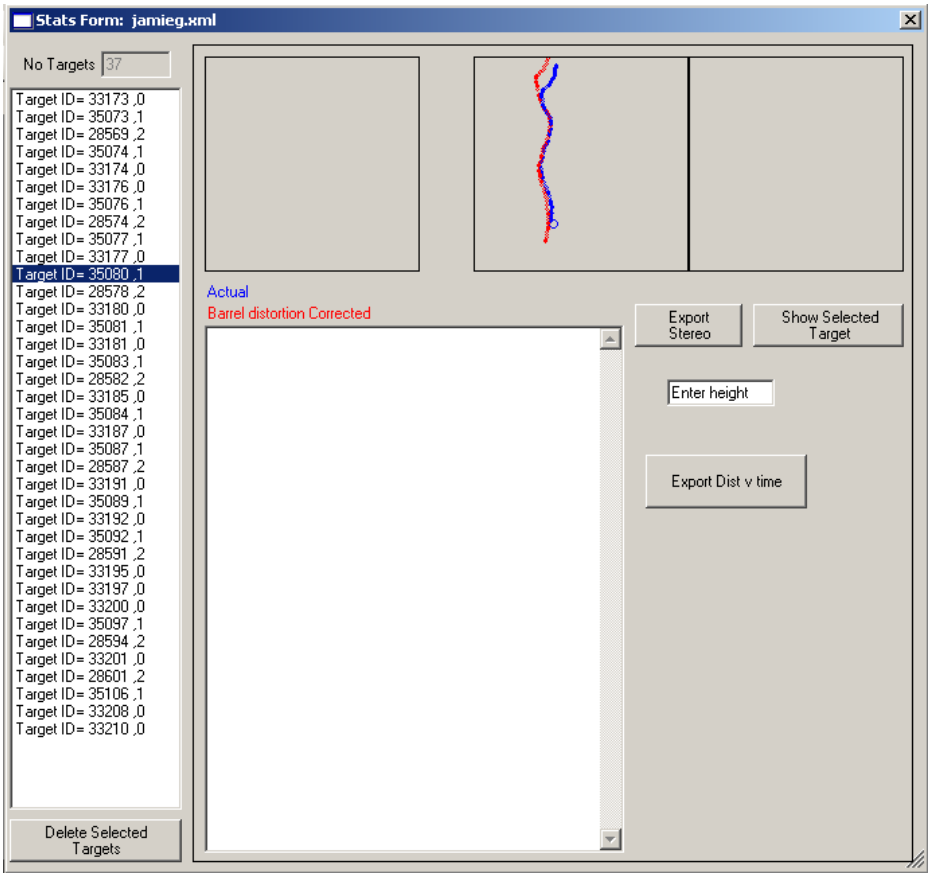

Figure 10-2: Second screen shot

11 Appendix B - Questionnaire used

Human gait/ signature analysis experiments

The purpose of this experiment is to establish if stereo pairs of the IRISYS people counters can be used to obtain a signature or indication of the people passing under them. The experiment will take approximately 10 min and will require you to walk as normally as possible under our sensors several times, and complete this form.

By filling out this form you are consenting to the information you provide being used for research purposes. Your personal information will be treated with confidentially.

I ask that you provide the following information, or if you are unsure of it that you allow me to measure it. All personal data will be stored in a secure location and anonymised before dissemination.

Name: _____

Gender: _____

Weight: (Kg <50[ ] 50-60[ ] 58-68[ ] 66-76[ ] 74-84[ ] 82-92[ ] >92[ ])

Height: _____

Age: (<18[ ] 16-26[ ] 24-34[ ] 32-42[ ] 40-50[ ] 48-58[ ] 56-66[ ] >66[ ])

Inside leg measurement: _____

Floor to hip measurement: _____

Do you have a physical condition that may affect your walk (e.g. a limp): (YES/NO)

Tick this box if you do not consent to me measuring your movement in the future without explicitly asking your consent. ☐

Thank you for your time helping with this research.

Tim Chamberlain
Research Student
School of Computing
Napier University

File Name & Path: _____

12 Appendix C - Linear regression used

This appendix details the linear regression method used for this project. It starts with the parametric description of a straight line (r, theta) and follows on to describe the regression technique.

12.1.1 The parametric description of a straight line

The standard mathematical technique of expressing a straight line is to use the equation y= ax + b where a and b respectively describe the slope and intersection with the y axis. This equation is theoretically able to represent any straight line except one with infinite gradient. Due to this exception it is more appropriate to use the parametric description of a line, which can describe any possible straight line. This consists of describing the line by the angle and length of its normal shown in Figure 12-1. The parametric description of a line is well explained by Fischer *at al* [94].

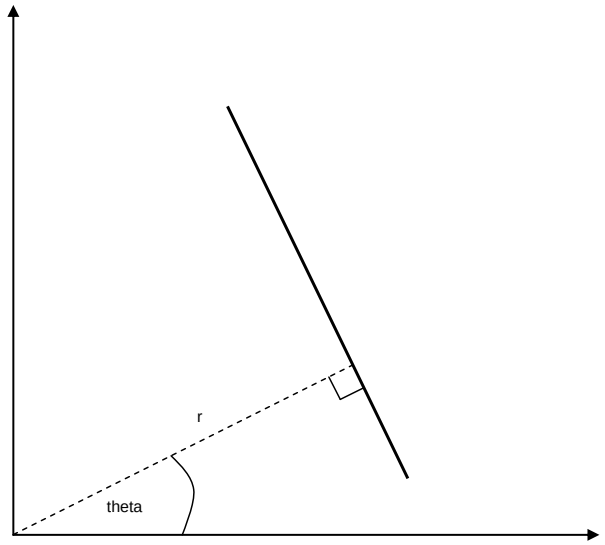

Figure 12-1: Parametric description of a straight line

12.1.2 Best fit linear regression

There are well established methods for finding best fit lines such as the Least Squares Method developed in the late 1700's. Sadly the least squares method is only appropriate for data where there is error in only one dimension. The data we have contains error in both the x and y dimensions, so the least squares method is not appropriate. Sequential regression must be performed to find the best fit line for the data.

The method used to establish how well the line fits the data is to sum the shortest distances from each point to the line. Equation 3-1 shows how the sum of shortest distances from an array of points (x, y) to the line (r, theta) is calculated. The smaller the value of *f*, the better the line fits the data.

$$f = \frac{\sum_{i=0}^{i=n-1} abs\left(\left(x_i.\cos(\theta) + y_i.\sin(\theta)\right) - r\right)}{n}$$

Equation 12-1: Line fit equation

If the value of theta is known, it is possible to calculate the best value of r for the corresponding data by summing the distance as shown in Equation 12-2.

$$r = \sum_{i=0}^{i=n-1} \left(x_i.\cos(\theta) + y_i.\sin(\theta)\right)$$

Equation 12-2: Value of r for known theta

The value of theta is unknown. It is therefore necessary to try a range of values of theta and find the one which provides the best fit. This provides an algorithm with a computation time linearly proportional to the number of data points multiplied by the number of different values of theta used.

13 Appendix D – Oscillation Magnitude Results

Person A (male)	Person B (male)	Person C (male)	Person D (male)	Person E (male)	Person F (male)	Person G (male)	Person H (male)	Person I (male)	Person J (female)	Person K (female)	Person L (female)	Person M (female)	Person N (female)	Person O (female)	Person P (female)	Person Q (female)	Person R (female)	Person S (female)
0.3399	0.0228	0.2739	0.0488	0.0535	0.2060	0.1915	0.0427	0.1400	0.0093	0.0434	0.0728	0.0131	0.0168	0.0468	0.0526	0.0545	0.1768	0.0453
0.0362	0.0350	0.0443	0.0466	0.0668	0.0600	0.1206	0.0176	0.0361	0.0099	0.0023	0.0048	0.0207	0.0402	0.0064	0.0046	0.0045	0.0123	0.0075
0.0958	0.0180	0.0631	0.3090	0.0535	0.0577	0.0373	0.1887	0.0968	0.0190	0.0186	0.0132	0.0611	0.0252	0.0130	0.0066	0.0188	0.0118	0.0293
0.0291	0.0223	0.0859	0.0234	0.0350	0.1099	0.8515	0.0290	0.1790	0.0269	0.1508	0.0354	0.0456	0.0813	0.0530	0.0543	0.1181	0.1134	0.2711
0.0854	0.0452	0.0455	0.0451	0.0576	0.2074	0.1265	0.0105	0.0689	0.0242	0.0697	0.1156	0.0499	0.0231	0.0110	0.0208	0.0080	0.0443	0.0565
0.0900	0.0591	0.0430	0.0193	0.1076	0.0509	0.1383	0.2729	0.0441	0.1002	0.0362	0.0023	0.0136	0.0240	0.0101	0.0040	0.0885	0.0296	0.0385
0.0320	0.0286	0.1073	0.0650	0.1942	0.0420	0.0776	0.0326	0.1065	0.0417	0.0431	0.0591	0.0222	0.0858	0.0268	0.0644	0.0183	0.0411	0.0303
0.1272	0.0614	0.0371	0.0388	0.1180	0.0347	0.0971	0.0157	0.2631	0.0202	0.0075	0.0097	0.0063	0.0534	0.0312	0.0171	0.1131	0.0579	0.0167
0.1439	0.0688	0.0231	0.0550	0.0220	0.1814	0.4138	0.0156	0.0539	0.0339	0.0037	0.0114	0.0338	0.0328	0.0470	0.0378	0.0098	0.0958	0.0062
0.0211	0.0444	0.0301	0.1587	0.0473	0.0267	0.1105	0.0609	0.2829	0.0232	0.1195	0.0300	0.0216	0.0063	0.0906	0.0137	0.0125	0.0130	0.3333
0.1545	0.1060	0.2012	0.1298	0.1279	0.0615	0.1631	0.0450	0.3577	0.1011	0.1130	0.0320	0.0529	0.0347	0.0086	0.0339	0.0060	0.0172	0.1415
0.0580	0.0787	0.0913	0.0686	0.1103	0.0275	0.1436	0.2156	0.0343	0.0423	0.0048	0.1893	0.1393	0.0427	0.0383	0.0870	0.0327	0.2422	0.0171
0.1288	0.5900	0.2017	0.0140	0.2220	0.2027	0.1194	0.0232	0.4061	0.0202	0.0406	0.0627	0.0746	0.0566	0.0236	0.0227	0.0545	0.1045	0.0374
0.0962	0.0306	0.0319	0.0173	0.2605	0.0675	0.2850	0.2470	0.2687	0.0339	0.0052	0.0469	0.0486	0.0207	0.0404	0.0063	0.0103	0.0115	0.0081

Table 13-1: Oscillation Magnitudes from choreographed data collected at Napier

Person A (male)	Person B (male)	Person C (male)	Person D (male)	Person E (male)	Person F (female)	Person G (female)	Person H (female)	Person I (female)	Person J (female)
0.0928	0.0324	0.0417	0.0428	0.0161	0.0211	0.0131	0.0049	0.0264	0.0056
0.0821	0.0200	0.0309	0.0187	0.0155	0.0247	0.0169	0.0070	0.0273	0.0068
0.0858	0.0174	0.0069	0.0358	0.0121	0.0402	0.0223	0.0083	0.0362	0.0045
0.0888	0.0164	0.0364	0.0961	0.0177	0.0103	0.0106	0.0148	0.0280	0.0038
0.0855	0.0332	0.0160	0.0563	0.0303	0.0386	0.0069	0.0126	0.0255	0.0085
0.0822	0.0307	0.0259	0.0141	0.0438	0.0205	0.0040	0.0258	0.0314	0.0108
0.0493	0.0406	0.0195	0.0203	0.0410	0.0347	0.0150	0.0164	0.0531	0.0150
0.0906	0.0395	0.0270	0.0235	0.0842	0.0110	0.0262	0.0046	0.0385	0.0101
0.0518	0.0486	0.0236	0.0073	0.0106	0.0206	0.0062	0.0056	0.0525	0.0059
0.0519	0.0353	0.0395	0.0304	0.0200	0.0221	0.0086	0.0050	0.0209	0.0113

Table 13-2: Oscillation magnitudes from Choreographed data collected at IRISYS

Detector 0	Detector 1	Detector 2
0.3399	0.0362	0.0958
0.0900	0.0291	0.0854
0.1272	0.0320	0.1439
0.0580	0.0211	0.0962
0.1288	0.0135	0.0269
0.2535	0.0298	0.0965

Table 13-3: Person A (male), Oscillation magnitude choreographed, Napier

Detector 0	Detector 1	Detector 2
0.2060	0.0600	0.0577
0.1099	0.0509	0.0420
0.2074	0.0267	0.0615
0.0347	0.0675	0.0362
0.1814	0.0334	0.0765
0.0275	0.0640	0.0400
0.2027	0.4055	0.0379
0.0722	0.0529	0.0280

Table 13-4: Person B (male), Oscillation magnitude choreographed, Napier

Detector 0	Detector 1	Detector 2
0.0180	0.0228	0.0350
0.0223	0.0591	0.0452
0.0614	0.0286	0.0688
0.0787	0.0444	0.1060
0.5900	0.0306	0.0582
0.1452	0.0354	0.0544

Table 13-5: Person C (male), Oscillation magnitude choreographed, Napier

Detector 0	Detector 1	Detector 2
0.0252	0.0168	0.0402
0.0240	0.0231	0.0813
0.0534	0.0328	0.0858
0.0347	0.0063	0.0427
0.0262	0.0207	0.0566
0.0524	0.0596	0.3602

Table 13-6: Person J (female), Oscillation magnitude choreographed, Napier

Detector 0	Detector 1	Detector 2
0.0131	0.0207	0.0611
0.0499	0.0136	0.0456
0.0222	0.0063	0.0338
0.0216	0.0529	0.1393
0.0098	0.0486	0.0746
0.0320	0.0300	0.1893
0.0228	0.0469	0.0627
0.0391	0.0853	0.1898
0.0083	0.0453	0.1316

Table 13-7: Person K (female), Oscillation magnitude choreographed, Napier

Detector 0	Detector 1	Detector 2
0.0453	0.0075	0.0293
0.0385	0.0565	0.2711
0.0303	0.0167	0.0062
0.0171	0.1415	0.3333
0.0374	0.0081	0.0067
0.0075	0.1150	0.2131

Table 13-8: Person R (female), Oscillation magnitude choreographed, Napier

0.944	0.057	0.050	0.043	0.027	0.032	0.122	0.086	0.047	0.045	0.216														
0.042	0.138	0.030	0.026	0.093	0.027	0.075	0.041	0.030	0.046	0.264														
0.085	0.426	0.050	0.019	1.371	0.112	0.087	0.052	0.839	0.066	0.086														
0.271	0.034	0.210	0.103	0.584	0.028	0.040	0.174	0.034	0.066	0.081														
0.238	0.019	0.135	0.048	0.061	0.046	0.356	0.069	0.044	0.077	0.153														
0.135	0.063	0.099	0.055	0.168	0.025	0.029	0.078	0.062	0.082	0.109														
0.122	0.072	0.048	0.091	0.070	0.059	0.059	0.064	1.259	0.097															
0.043	0.225	0.691	0.091	0.141	0.046	0.086	0.416	0.033	0.126															
0.069	0.055	0.044	0.075	0.153	0.033	0.095	0.044	0.034	0.175															
0.031	0.078	0.344	0.023	0.109	0.033	0.042	0.020	0.035	0.183															

Table 13-9: Gender conformation data

14 Appendix D (cont) - Cadence Results

Person A	Person B	Person C	Person D	Person E	Person F	Person G	Person H	Person I	Person J	Person K	Person L	Person M	Person N	Person O	Person P	Person Q
525	570	495	565	860	572	694	440	705	652	405	720	804	550	604	814	790
348	942	473	594	480	456	414	617	626	454	270	622	585	450	420	381	517
366	493	260	645	770	497	728	500	727	810	866	260	280	880	847	480	570
312	450	577	520	720	586	754	882	822	980	840	696	607	472	594	682	737
365	520	364	640	520	498	368	788	720	566	705	558	750	531	805	984	566
323	942	438	572	396	805	402	470	634	520	480	585	474	590	771	637	592
409	550	466	518	615	471	506	630	1080	908	465	950	697	665	318	800	637
685	500	480	860	516	490	444	424	891	220	490	797	645	523	420	922	694
440	506	390	540	447	300	441	622	278	540	712	570	468	256	345	518	383
453	475	430	616	382	445	920	454	700	510	900	550	507	617	555	950	574
453	503	615	515	531	762	685	452	797	582	813	994	650	574	450	293	562
420	496	312	535	540	352	365	232	496	378	890	900	485	412	977	440	840
526	900	591	762	385	489	228	668	501	574	660	545	684	630	433	592	660
608	684	613	516	356	525	860	760	572	997	810	507	643	810	754	436	600

Table 14-1: Cadence results Napier dataset (ms)

Measure	Person A	Person B	Person C	Person D	Person E	Person F	Person G	Person H	Person I	Person J	Person K	Person L	Person M	Person N	Person O	Person P	Person Q
Average cadence measure (ms)	445.2143	609.3571	464.5714	599.8571	537	517.7143	557.7857	567.0714	682.0714	620.7857	664.7143	661	591.3571	568.5714	592.3571	637.7857	623
Height (cm)	186	165	183	185	178	183	173	180	179	174	178	167	168	168	155	160	173
Inside Leg Length (cm)	92	86	82	90	83	83	75	79	92	76	90	82	77	83	73	81	80
Out Side leg length (cm)	111	94	109	100	120	106	97	102	99	90	104	96	94	104	91	96	97
Hip Size (outside-inside) (cm)	19	8	27	10	37	23	22	23	7	14	14	14	17	21	18	15	17

Table 14-2: Cadence v height and leg length

Person A	Person B	Person C	Person D	Person E	Person F	Person G	Person H	Person I	Person J	Person K	Person L	Person M	Person N	Person O	Person P	Person Q
616	604	629	605	617	601	543	564	631	632	608	597	589	626	556	602	621
464	589	589	623	530	549	553	571	638	530	542	631	678	612	541	573	554
602	567	634	645	616	615	584	657	675	637	611	539	667	596	721	644	668
587	570	533	648	578	576	625	664	547	676	604	701	637	643	600	572	670
523	610	764	618	687	546	574	579	584	577	633	636	691	573	623	528	712
632	603	595	712	623	569	671	605	645	525	724	586	559	610	528	553	574
586	601	613	598	644	596	625	666	616	610	622	575	605	650	629	691	637
590	564	613	638	551	523	598	633	605	634	612	670	727	661	608	628	569
486	593	611	596	580	610	601	609	577	663	593	647	551	569	598	601	639
569	576	498	643	635	566	611	531	597	613	554	623	549	611	633	605	580
536	611	616	631	674	561	669	660	582	557	693	626	625	637	627	591	691
541	611	589	567	569	605	624	549	682	712	612	583	615	560	646	641	629
575	574	576	605	625	538	670	599	602	625	604	617	622	600	619	590	559
608	582	635	620	554	628	583	649	677	665	580	661	612	519	726	612	632

Table 14-3: Filtered Fourier cadence results (ms)

Person A	Person B	Person C	Person D	Person E	Person F	Person G	Person H	Person I	Person J	Person K	Person L	Person M	Person N	Person O	Person P	Person Q
345	303	274	306	278	284	256	282	276	259	246	410	265	291	282	286	257
229	281	231	301	226	312	274	302	310	222	165	331	262	180	238	237	210
264	275	311	353	278	281	297	264	395	303	270	263	234	235	328	203	295
256	290	209	335	239	258	278	221	254	343	304	370	319	288	296	235	252
233	328	287	307	299	321	201	262	263	258	329	286	244	266	292	219	269
360	300	248	310	261	269	208	244	337	265	321	272	281	234	208	215	308
250	293	289	273	307	266	313	274	355	288	296	210	296	256	276	247	236
282	327	299	381	237	308	263	340	313	391	304	348	298	281	320	284	230
190	346	214	354	314	317	277	357	241	281	224	189	286	303	297	291	307
253	315	200	244	297	261	296	299	362	295	248	304	287	347	239	236	234
222	287	249	303	359	258	340	305	287	251	321	254	308	253	256	240	216
243	275	231	309	291	319	371	296	280	313	311	280	254	290	303	376	310
296	309	261	307	274	296	287	279	276	282	282	283	271	237	279	260	239
216	261	273	328	238	355	283	284	269	339	263	411	286	190	297	270	329

Table 14-4 Weighted Fourier cadence results (ms)

15 Appendix E –Published Work

This appendix contains copy of publications and presentations produced from research presented in this thesis.

15.1 Peer reviewed papers

15.1.1 "PED 2005" (2007), book chapter

J. Kerridge, S. Keller, T. Chamberlain and N. Sumpter (2007), *Collecting pedestrian trajectory data in real-time*, Pedestrian evacuation and dynamics 2005, pages 27-39, Springer, Berlin Heidelberg, ISBN 978-3-540-47062-5

15.1.2 ITS World congress (2006), conference paper

T. Chamberlain, A. Armitage, M. Rutter, T.D. Binnie (2006), *Pedestrian sensing with feature extraction*: Proceedings of the ITS world congress cd-rom, London, October 10th 2006

15.1.3 TRB annual meeting (2005), conference paper

J. Kerridge, S. Keller, T. Chamberlain, N. Sumpter, (2005), *Collecting processing and calculating pedestrian flow data in real-time*, Proceedings of 84th Annual Meeting of Transportation Research Board, Washington D.C.

15.2 Conference presentations & papers

15.2.1 CMPS(2007), workshop presentation

T. Chamberlain, S. Clayton, Prof J. Kerridge, Dr A. Armitage, Dr M. Rutter, Dr T. D. Binnie, Dr N. Urquhart, (2007), *Using low cost Infrared Sensors for data capture*, Workshop on calibration of microscopic pedestrian movement simulations, Dec 13-14th,Arsenal Research, Vienna

15.2.2 UTSG (2006), conference paper

T. Chamberlain, A. Armitage, M. Rutter, T.D. Binnie (2006), *Working towards identifiable feature extraction from pedestrians' gait*, Proceedings of 38th Annual UTSG Conference, Trinity College, Dublin

15.2.3 Napier Faculty of Computing & Engineering conference (2005), conference paper

T. Chamberlain, A. Armitage, M. Rutter, T.D. Binnie (2005), *The use of thermal detectors in establishing ground truth in the evaluation of video pedestrian tracking algorithms*, Faculty of Engineering & Computing Postgraduate Research Conference, Napier University

15.2.4 UTSG (2005), conference paper

A. Armitage, D. Binnie, T. Chamberlain, M. Nilsson and M. Rutter (2005), *Tracking pedestrians using visible & infrared systems*, Proceedings of 37th Annual UTSG Conference, University of the West of England, Bristol

15.2.5 PREP (2004), conference paper

T. Chamberlain, A. Armitage, M. Rutter, T. D. Binnie, (2004) *Using Low-Resolution Thermal Sensors in Stereo To Measure Pedestrian Movement*, PREP, University of Hertfordshire, poster proceedings p251